Beam Instrumentation & Diagnostics Part 2

CAS Introduction to Accelerator Physics

Kaunas, 23rd of September 2022

Peter Forck

Gesellschaft für Schwerionenforschung (GSI)

p.forck@gsi.de

2nd part of this lecture covers:

- **Transverse profile techniques**
- **Emittance determination at transfer lines**
- **Diagnostics for bunch shape determination**

For peace and freedom

Copyright statement and speaker's release for video publishing

Measurement of Beam Profile

The beam width can be changed by focusing via quadruples.

Transverse matching between ascending accelerators is done by focusing.

→ Profiles have to be controlled at many locations.

Synchrotrons: Lattice functions ***β(s)*** and ***D(s)*** are fixed ⇒ width ***σ*** and emittance ***ε*** are:

$$\sigma_x^2(s) = \varepsilon_x \beta_x(s) + \left(D(s) \frac{\Delta p}{p} \right)^2 \quad \text{and} \quad \sigma_y^2(s) = \varepsilon_y \beta_y(s) \quad \text{(no vertical bend)}$$

Transfer lines: Lattice functions are 'smoothly' defined due to variable input emittance.

Typical beam sizes:

e⁻-beam: typically Ø 0.01 to 3 mm, **protons:** typically Ø 1 to 30 mm

A great variety of devices are used:

- ***Optical techniques:*** Scintillating screens (all beams), synchrotron light monitors (e⁻), optical transition radiation (e⁻, high-energetic p), ionization profile monitors (protons)
- ***Electronics techniques:*** Secondary electron emission SEM grids, wire scanners (all)

Outline:

- **Scintillation screens:**

  emission of light, universal usage, limited dynamic range

- **Optical Transition Radiation**
- **SEM-Grid**
- **Wire scanner**
- **Ionization Profile Monitor**
- **Synchrotron Light Monitors**
- **Summary**

Scintillation Screen

Scintillation: Particle's energy loss in matter causes emission of light

→ the most direct way of profile observation as used from the early days on!

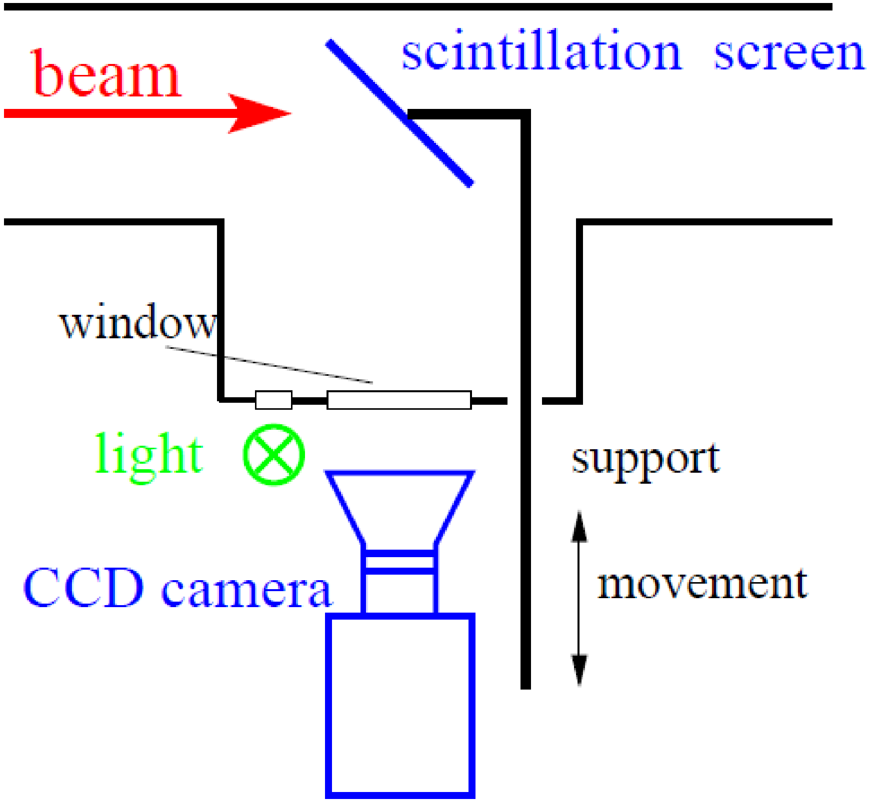

Pneumatic drive with Ø70 mm screen:

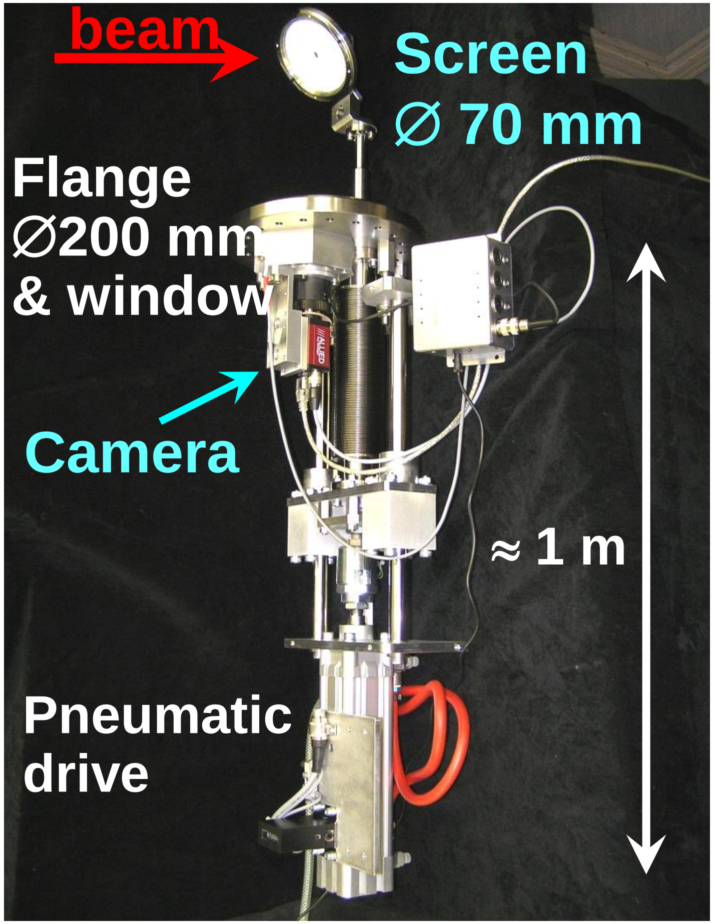

Example of Screen based Beam Profile Measurement

Advantage of screens:

- ➢Direct 2-dim measurement
- ➢High spatial resolution
- ➢Cheap realization

⇒ widely used at transfer lines

Disadvantage of screens:

- ➢ Intercepting device
- ➢ Some material might be brittle
- ➢ Possible low dynamic range
- ➢Might be destroyed by the beam (radiation demage)

Observation with CMOS camera

Example: GSI LINAC, 4 MeV/u, low current, YAG:Ce screen

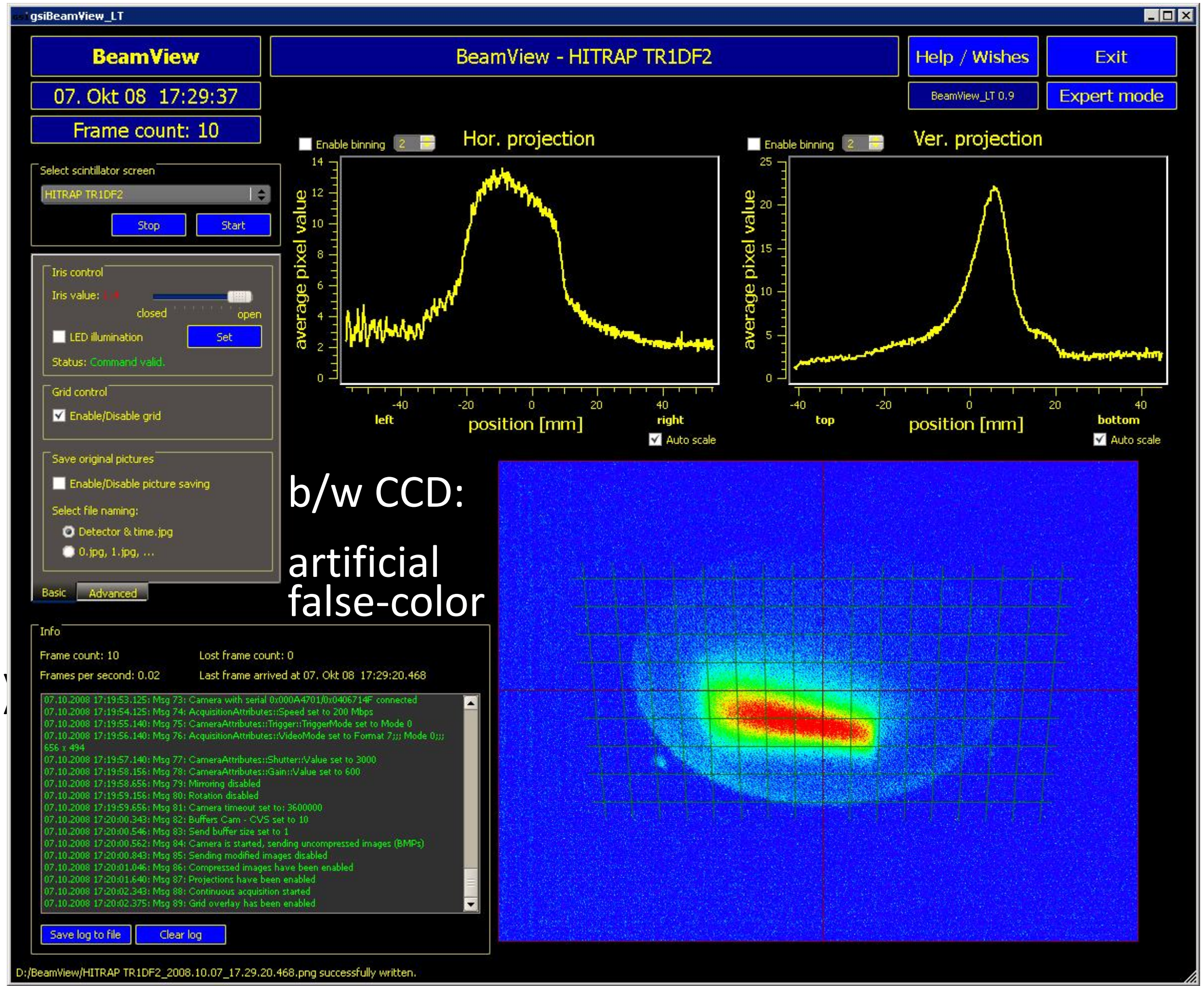

Scintillation Screen (beam stopped)

Light output from various Scintillating Screens

Example: *Color CCD camera: Images at different particle intensities determined for U at 300 MeV/u*

Alumina: Al_2O_3

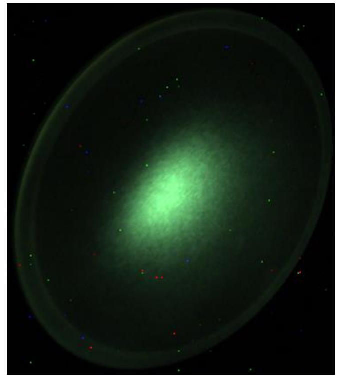

CsI:Tl

Chromox: Al_2O_3:Cr

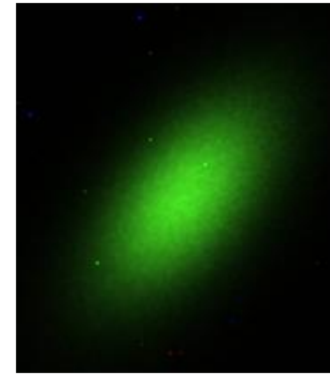

P43

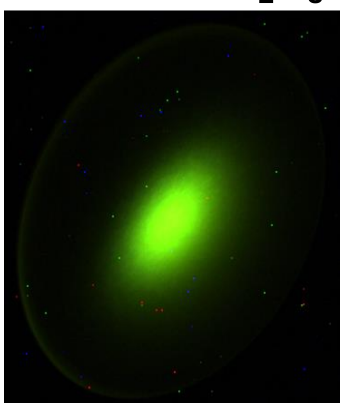

YAG:Ce

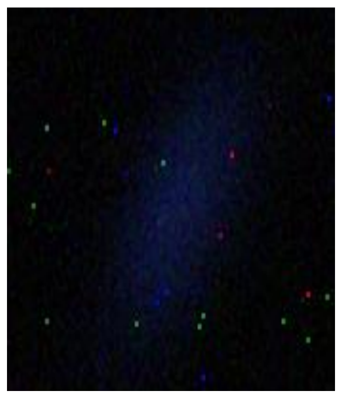

Quartz

Quartz:Ce

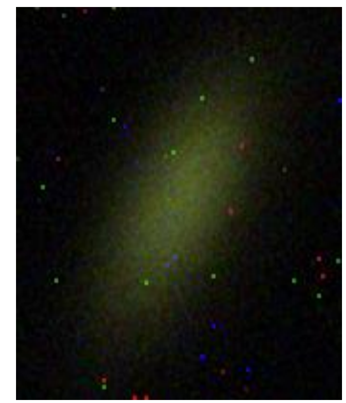

ZrO_2:Mg

- Very different light yield i.e. photons per ion‘s energy loss
- Different wavelength of emitted light

Material Properties for Scintillating Screens

Some materials and their basic properties:

Name	Type	Material	Activ.	Max. λ	Decay
Chromox	Cera-mics	Al_2O_3	Cr	700nm	≈ 10ms
Alumina		Al_2O_3	Non	380nm	≈ 10ns
YAG:Ce	Crystal	$Y_3Al_5O_{12}$	Ce	550nm	200ns
LYSO		$Lu_{1.8}Y_{.2}SiO_5$	Ce	420nm	40ns
P43	Powder of gains Ø≈10µm on glass	Gd_2O_3S	Tb	545nm	1ms
P46		$Y_3Al_5O_{12}$	Ce	530nm	300ns
P47		Y_2SiO_5	Ce&Tb	400nm	100ns

Standard drive with P43 screen

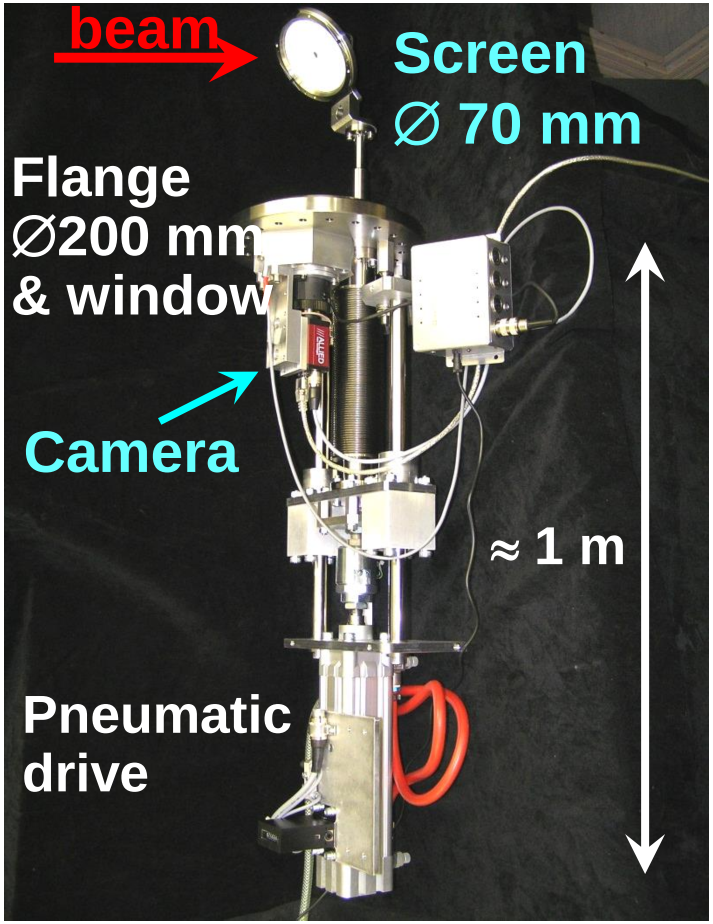

Properties of a good scintillator:

- Large light output at optical wavelength
  → standard CCD camera can be used
- Large dynamic range → usable for different currents
- Short decay time → observation of variations
- Radiation hardness → long lifetime
- Good mechanical properties → typ. size up to Ø 10 cm

(Phosphor Pxx grains of Ø ≈ 10 µm on glass or metal).

Outline:

- Scintillation screens:
  emission of light, universal usage, limited dynamic range
- Optical Transition Radiation:
  light emission due to crossing material boundary, mainly for relativistic beams
- SEM-Grid
- Wire scanner
- Ionization Profile Monitor
- Synchrotron Light Monitors
- Summary

Optical Transition Radiation: Depictive Description

Optical Transition Radiation OTR for a single charge *e*:

Assuming a charge ***e*** approaches an ideal conducting boundary e.g. metal foil

- image charge is created by electric field
- dipole type field pattern
- field distribution depends on velocity β and Lorentz factor γ due to relativistic trans. field increase
- penetration of charge through surface within t < 10 fs: sudden change of source distribution
- emission of radiation with dipole characteristic

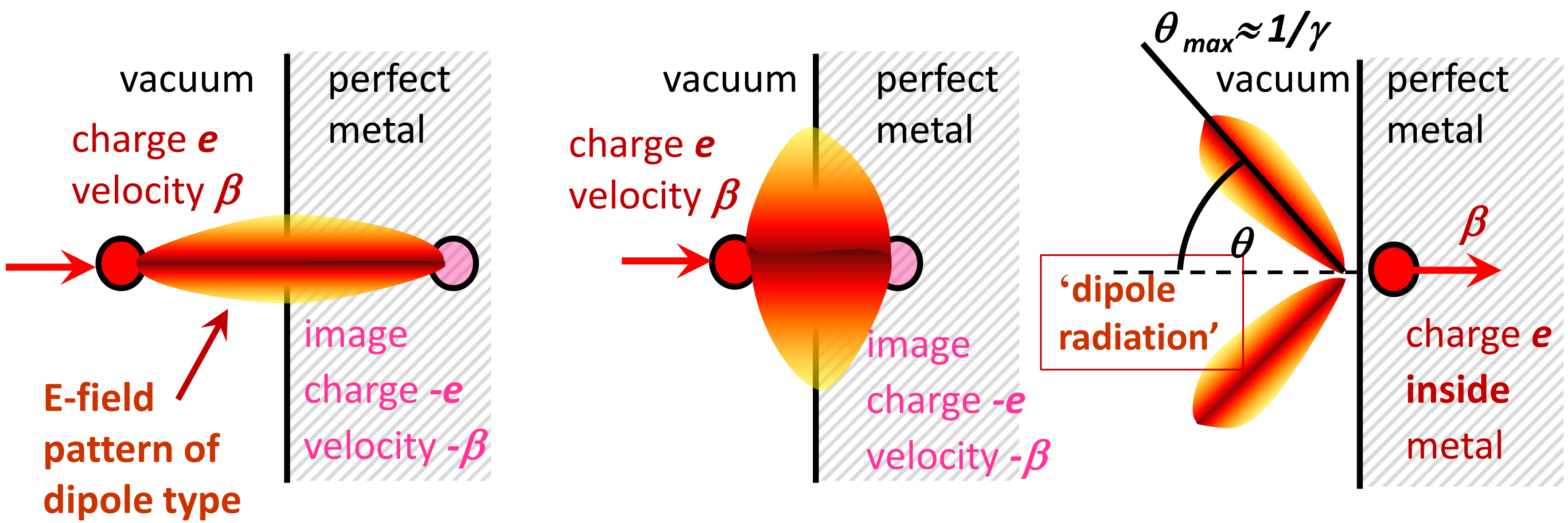

sudden change charge distribution
rearrangement of sources ⇔ radiation

Other physical interpretation: Impedance mismatch at boundary leads to radiation

Optical Transition Radiation: Depictive Description

Optical Transition Radiation OTR can be described in classical physics:

approximated formula for normal incidence & in-plane polarization:

$$\frac{d^2W}{d\theta\, d\omega} \approx \frac{2e^2\beta^2}{\pi c} \cdot \frac{\sin^2\theta \cdot \cos^2\theta}{\left(1-\beta^2\cos^2\theta\right)^2}$$

W: radiated energy

ω: frequency of wave

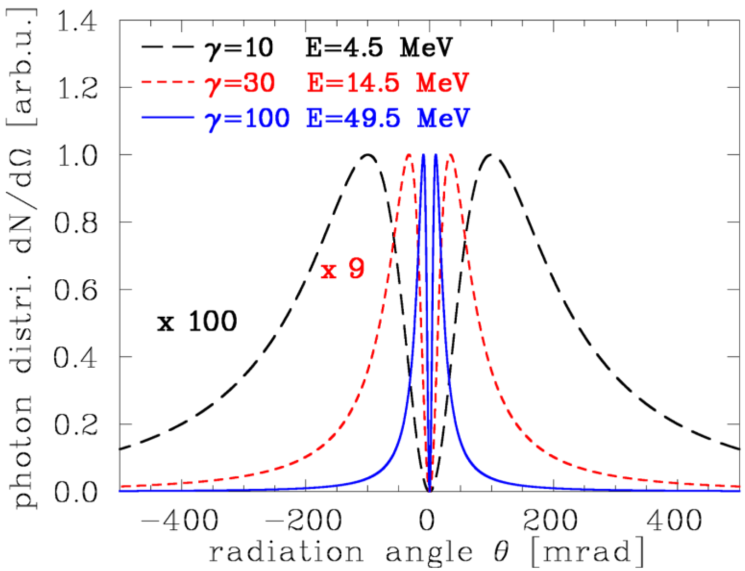

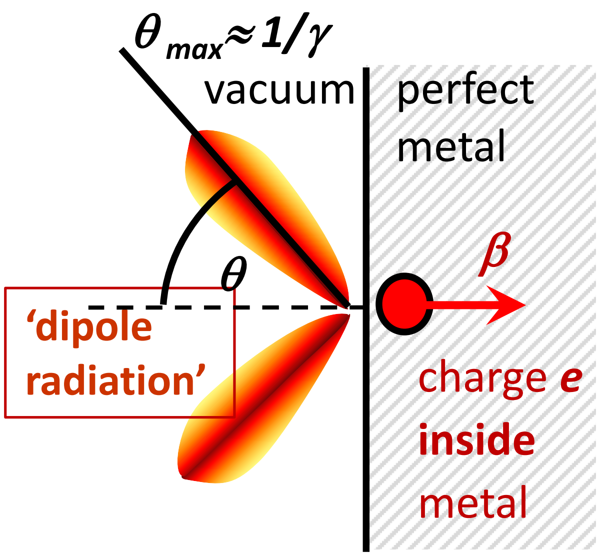

Angular distribution of radiation in optical spectrum:

- lope emission pattern depends on velocity or Lorentz factor γ
- peak at angle $\theta \approx 1/\gamma$
- emitted energy i.e. amount of photons scales with $W \propto \beta^2$
- broad wave length spectrum (i.e. no dependence on ω)

→ suited for high energy electrons

sudden change charge distribution
rearrangement of sources ⇔ radiation

Technical Realization of Optical Transition Radiation OTR

OTR is emitted by charged particle passage through a material boundary.

Photon distribution:

within a solid angle $d\Omega$ and

Wavelength interval λ_{begin} to λ_{end}

$$\frac{dN_{photon}}{d\Omega} = N_{beam} \cdot \frac{2e^2\beta^2}{\pi c} \cdot \log\left(\frac{\lambda_{begin}}{\lambda_{end}}\right) \cdot \frac{\theta^2}{\left(\gamma^{-2} + \theta^2\right)^2}$$

- Detection: Optical 400 nm < λ < 800 nm

  using image intensified CCD

- Larger signal for relativistic beam $\gamma \gg 1$
- Low divergence for $\gamma \gg 1 \Rightarrow$ large signal

$\Rightarrow$ **well suited for e⁻ beams**

$\Rightarrow$ **p-beam used for $E_{kin} \gtrsim$ 10 GeV $\Leftrightarrow \gamma \gtrsim 10$**

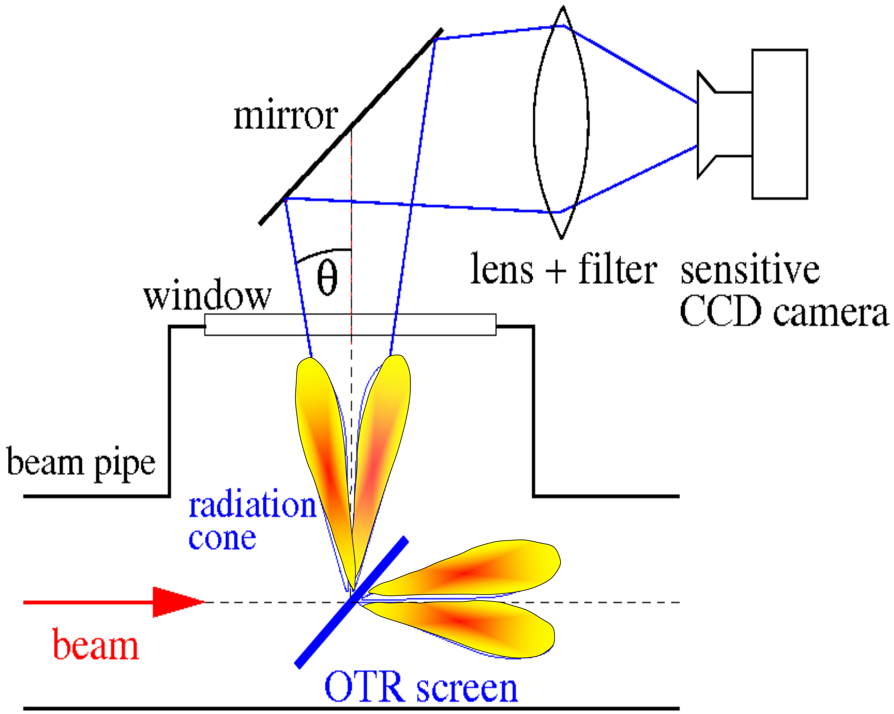

- Insertion of thin Al-foil under 45°
- Observation of low light by CCD.

Example of realization at TERATRON:

➢ Insertion of foil
e.g. 5 μm Kapton coated with 0.1μm Al

Advantage: thin foil ⇒ low heating & straggling
2-dim image visible

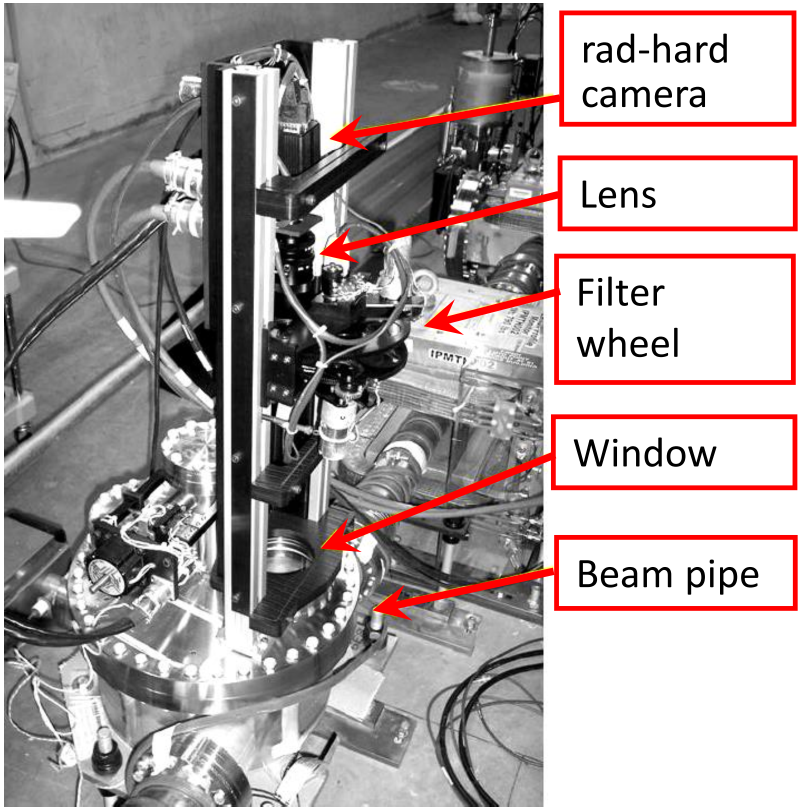

Results at FNAL-TEVATRON synchrotron

with 150 GeV proton

Using fast camera: Turn-by-turn measurement

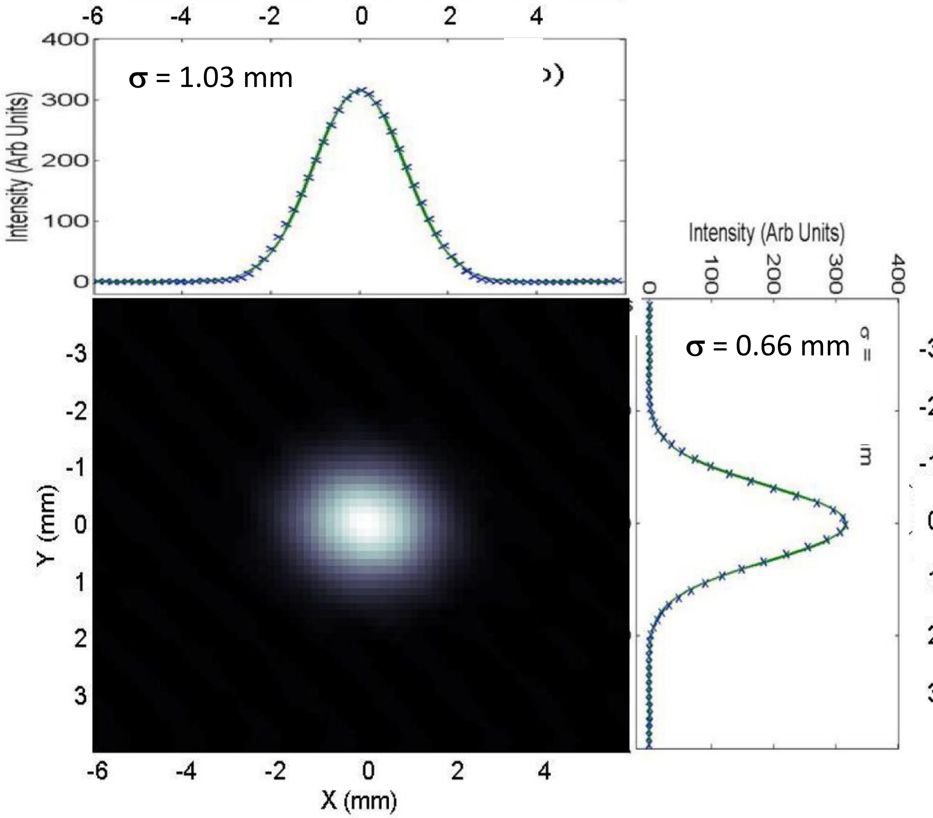

Courtesy V.E. Scarpine (FNAL) et al., BIW'06

Installation of OTR and scintillation screens on same drive:

Example: ALBA LINAC 100 MeV

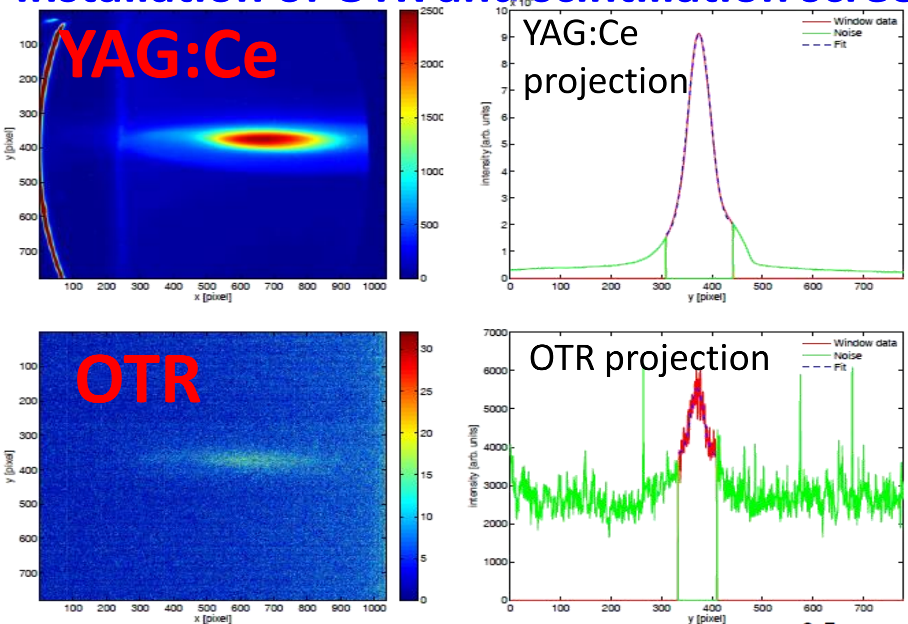

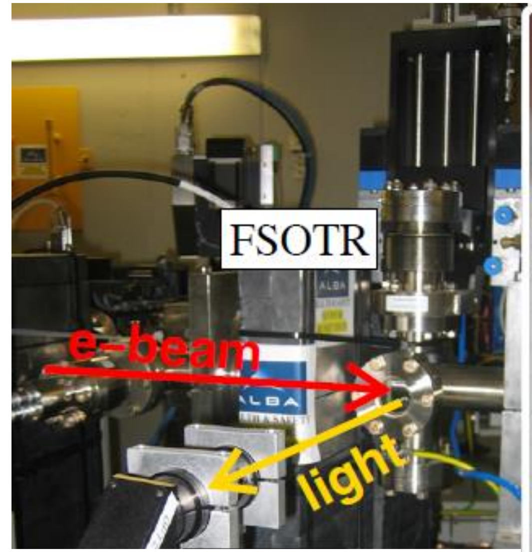

Results:

- Much more light from YAG:Ce for 100 MeV (γ=200) electrons light output $I_{YAG} \approx 10^5 I_{OTR}$
- Broader image from YAG:Ce due to finite YAG:Ce thickness

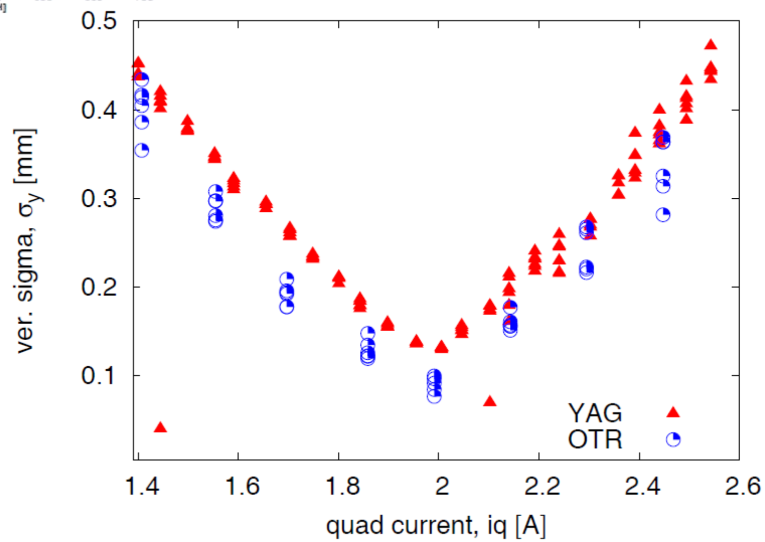

Courtesy of U. Iriso et al., DIPAC'09

Comparison between Scintillation Screens and OTR

OTR: electrodynamic process → beam intensity linear to # photons, high radiation hardness

Scint. Screen: complex atomic process → saturation possible, for some low radiation hardness

---

OTR: thin foil Al or Al on Mylar, down to 0.25 µm thickness

→ minimization of beam scattering (Al is low Z-material e.g. plastics like Mylar)

Scint. Screen: thickness ≈ 1 mm inorganic, fragile material, not always radiation hard

---

OTR: low number of photons → expensive image intensified CCD

Scint. Screen: large number of photons → simple CCD sufficient

---

OTR: complex angular photon distribution → resolution limited

Scint. Screen: isotropic photon distribution → simple interpretation

---

OTR: large γ needed → e^--beam with E_{kin} > 100 MeV, proton-beam with E_{kin} > 100 GeV

Scint. Screen: for all beams

Remark:

1. OTR: beam angular distribution measurable → beam emittance

2. OTR not suited for LINAC-FEL due to **coherent** light emission (not covered here)
but scintillation screens can be used.

Outline:

- Scintillation screens:

  emission of light, universal usage, limited dynamic range

- Optical Transition Radiation:

  light emission due to crossing material boundary, mainly for relativistic beams

- SEM-Grid:

  emission of electrons, workhorse, limited resolution

- Wire scanner
- Ionization Profile Monitor
- Synchrotron Light Monitors
- Summary

Secondary Electron Emission by Ion Impact

Energy loss of ions in metals close to a surface:

Closed collision with large energy transfer: → fast e⁻ with E_{kin} >> 100 eV

Distant collision with low energy transfer : → slow e⁻ with $E_{kin} \leq$ 10 eV

→ 'diffusion' & scattering with other e⁻: scattering length $L_s \approx$ 1 - 10 nm

→ at surface ≈ 90 % probability for escape

Secondary **electron yield** and energy distribution comparable for all metals!

⇒ ***Y = const. * dE/dx*** (Sternglass formula)

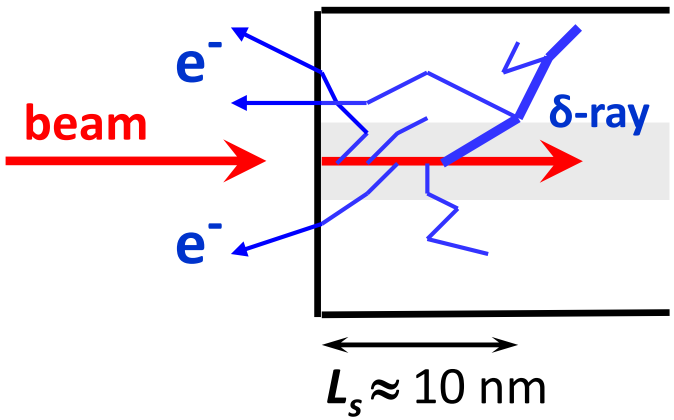

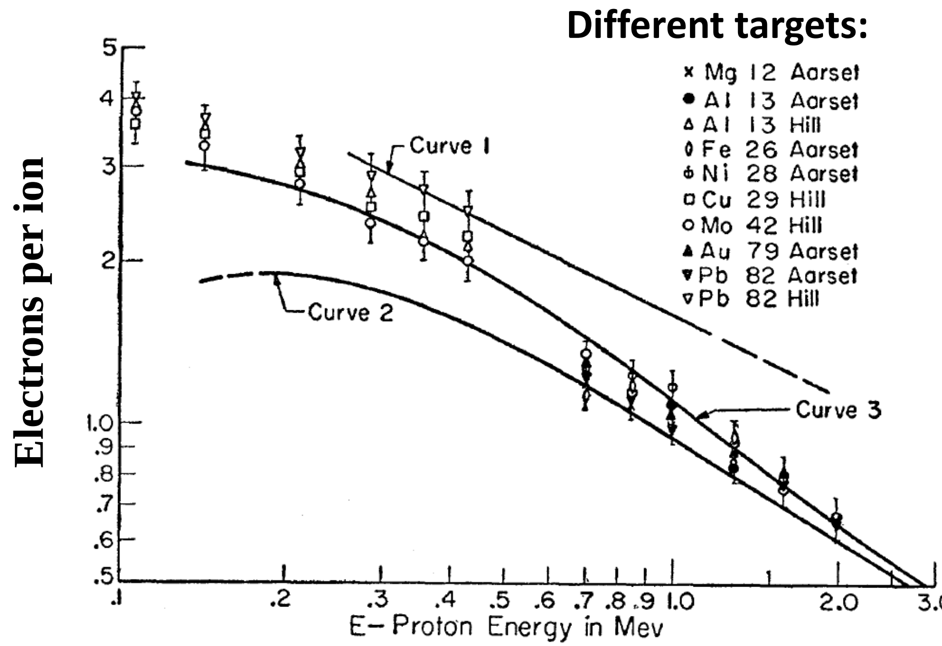

From E.J. Sternglass, Phys. Rev. 108, 1 (1957)

Secondary Electron Emission Grids = SEM-Grid

Beam surface interaction: e⁻ emission → measurement of current.

Example: 15 wire spaced by 1.5 mm:

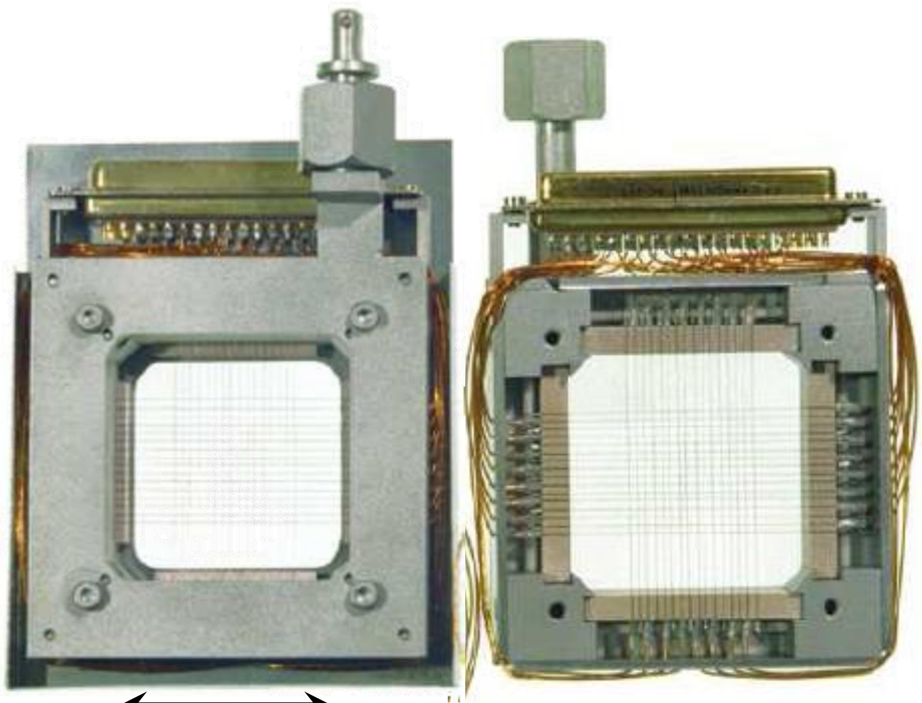

SEM-Grid drive on ∅200 mm flange:

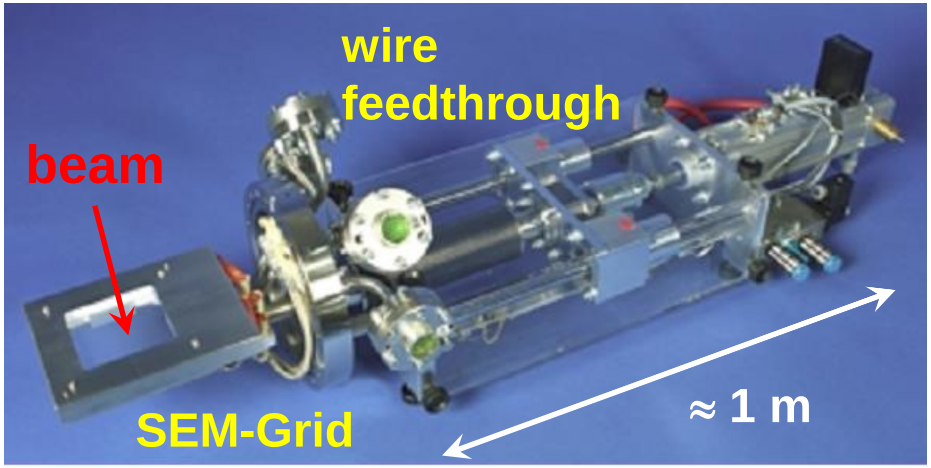

Parameter	Typ. value
# wires per plane	10 ...100
Active area	$(5...20\ cm)^2$
Wire ∅	25....100 μm
Spacing	0.3...2 mm
Material	e.g. W or Carbon
Max. beam power	1 W/mm

Secondary Electron Emission Grids = SEM-Grid

Beam surface interaction: e⁻ emission → measurement of current.

Example: 15 wire spaced by 1.5 mm:

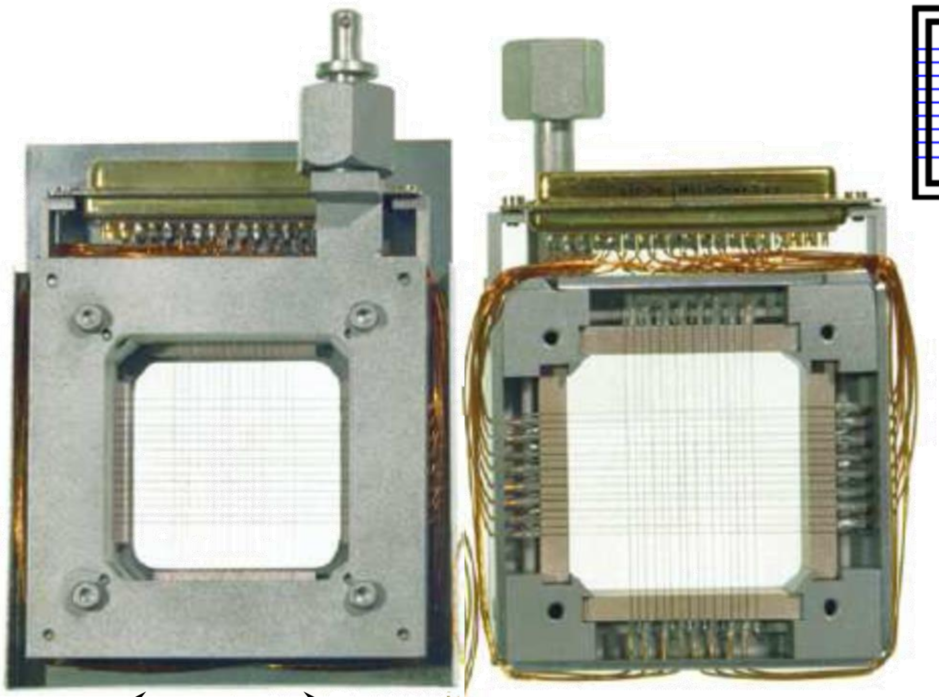

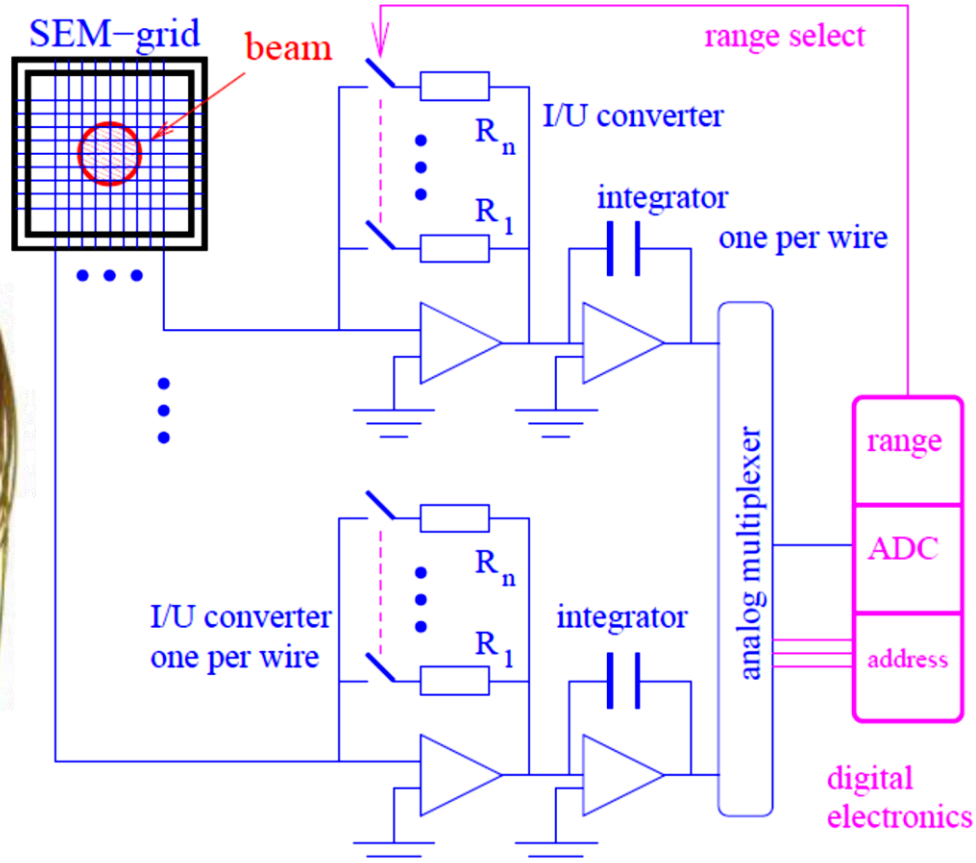

Each wire is equipped with one I/U converter

different ranges settings by R_i

→ very large dynamic range up to 10^6.

Example of Profile Measurement with SEM-Grids

Even for low energies, several SEM-Grid can be used due to the ≈ 80 % transmission

⇒ frequently used instrument beam optimization: setting of quadrupoles, energy….

Example: C^{6+} beam of 11.4 MeV/u at different locations at GSI-LINAC

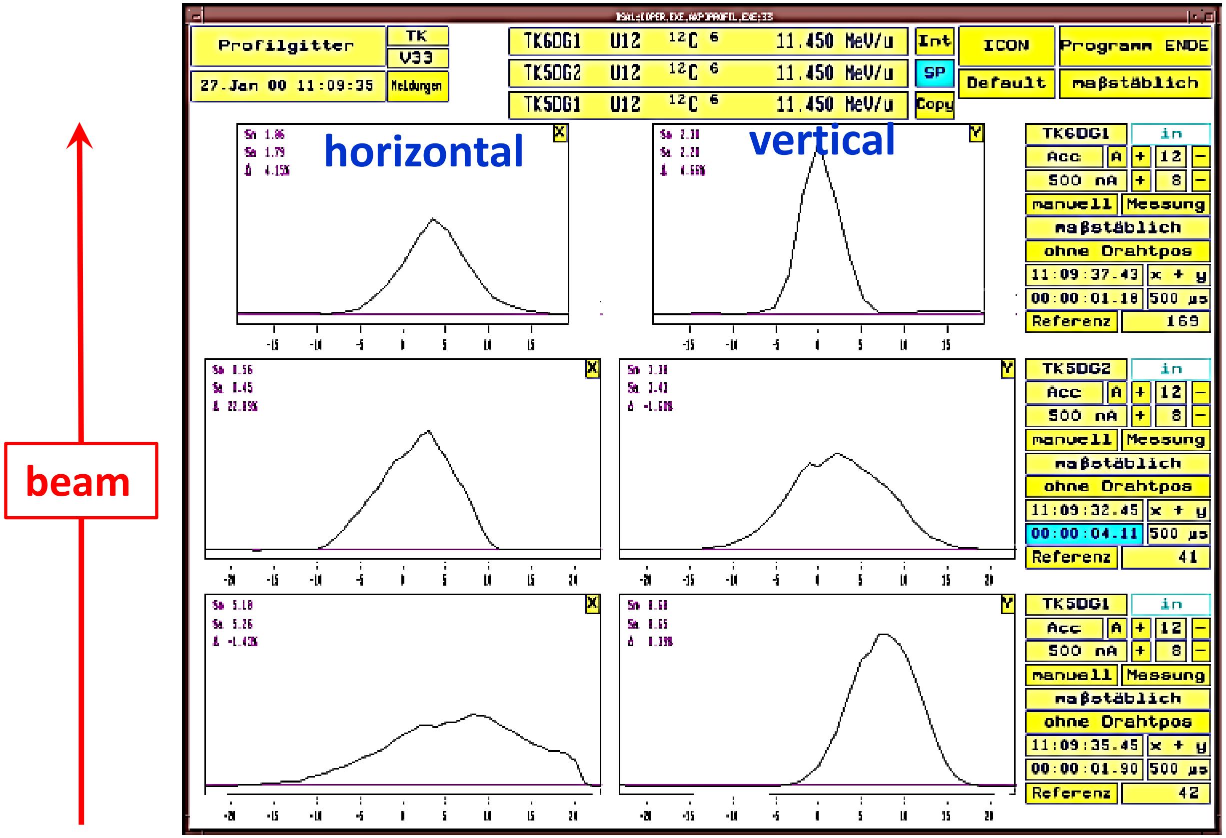

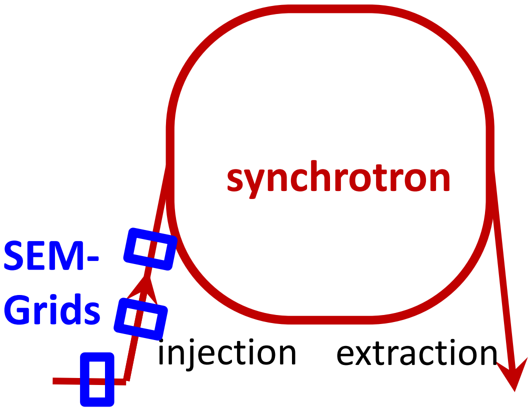

The Artist view of a SEM-Grid = Harp

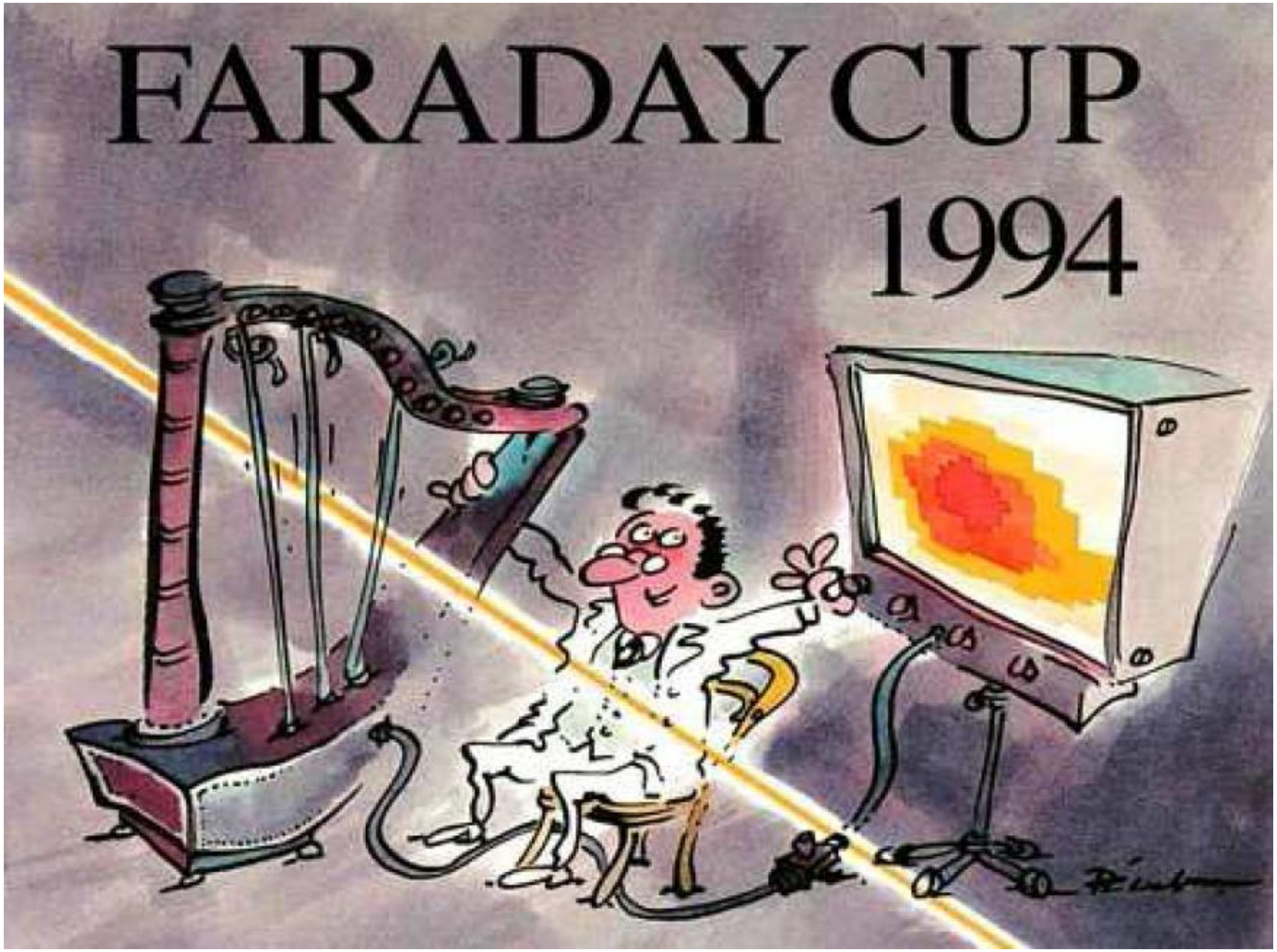

Outline:

- Scintillation screens:

  emission of light, universal usage, limited dynamic range
- Optical Transition Radiation:

  light emission due to crossing material boundary, mainly for relativistic beams
- SEM-Grid:

  emission of electrons, workhorse, limited resolution
- **Wire scanner:**

  emission of electrons, workhorse, scanning method
- **Ionization Profile Monitor**
- **Synchrotron Light Monitors**
- **Summary**

Slow, linear Wire Scanner

Idea: One wire is scanned through the beam!

Wire diameter 100 µm < d_{wire} < 10 µm

Slow, linear scanner are used for:

- Low energy protons
- High resolution measurements for e⁻ beam
  by de-convolution $\sigma^2_{beam}=\sigma^2_{meas}-d^2_{wire}$
  ⇒ resolution down to 1 µm range can be reached
- Detection of beam halo

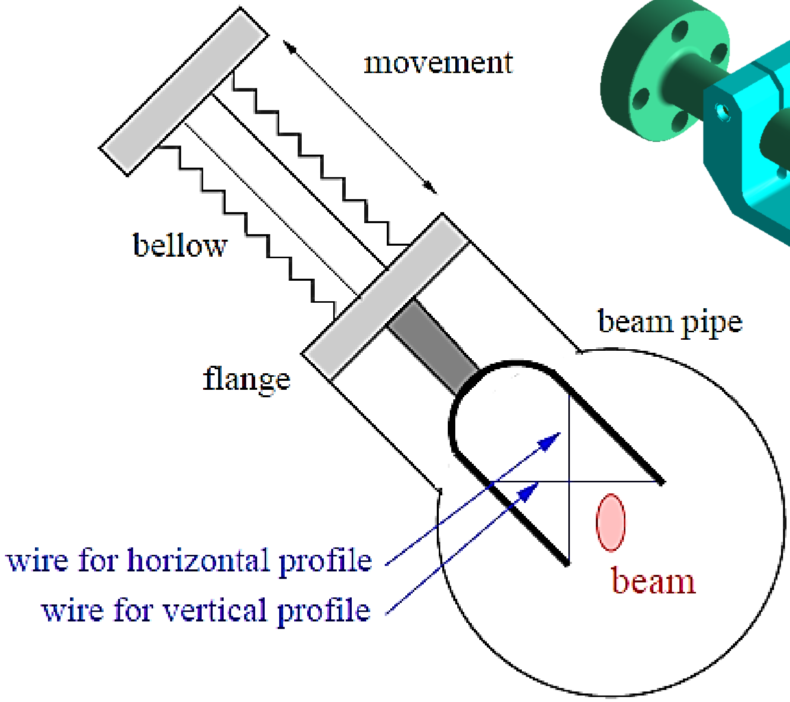

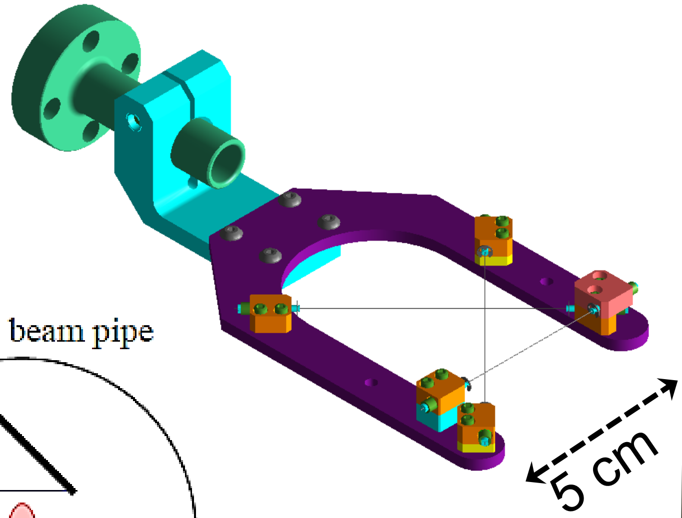

Example: Wires scanner at CERB LINAC4

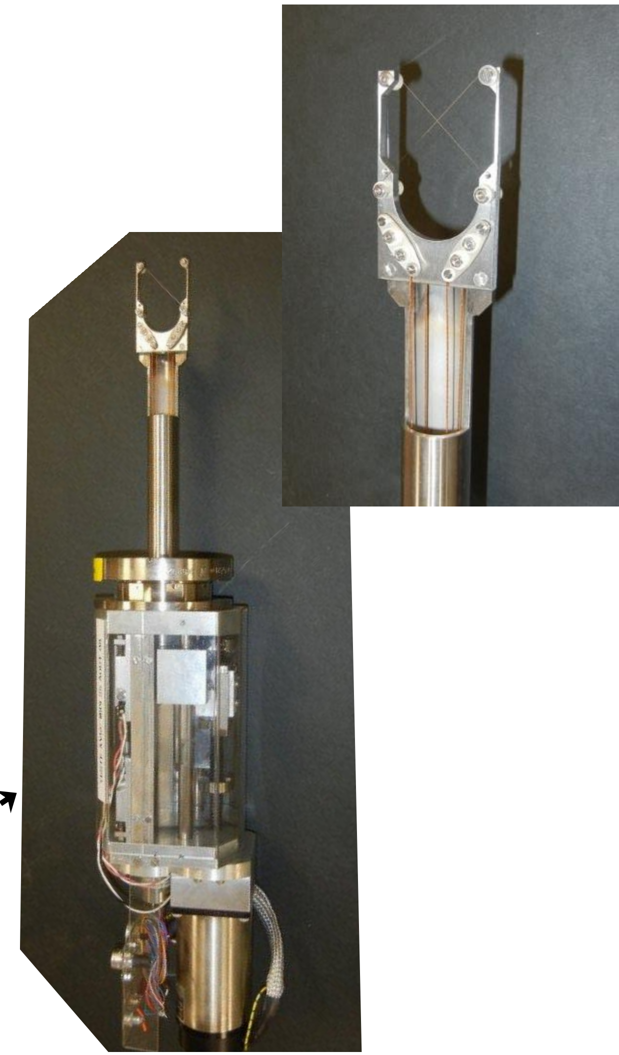

The Artist view of a Beam Scraper or Scanner

Fast, Flying Wire Scanner

In a synchrotron ***one*** wire is scanned though the beam as fast as possible.

Fast pendulum scanner for synchrotrons; sometimes it is called ***'flying wire'***:

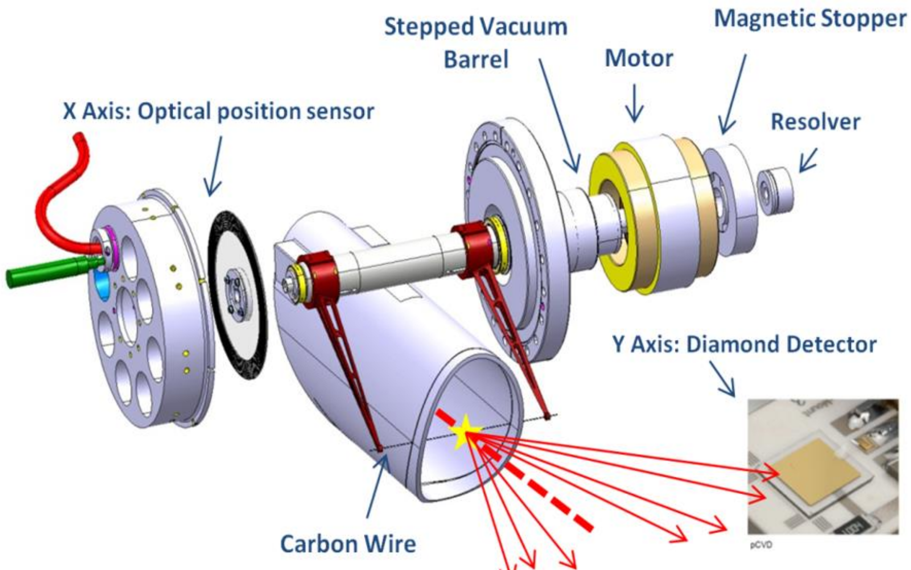

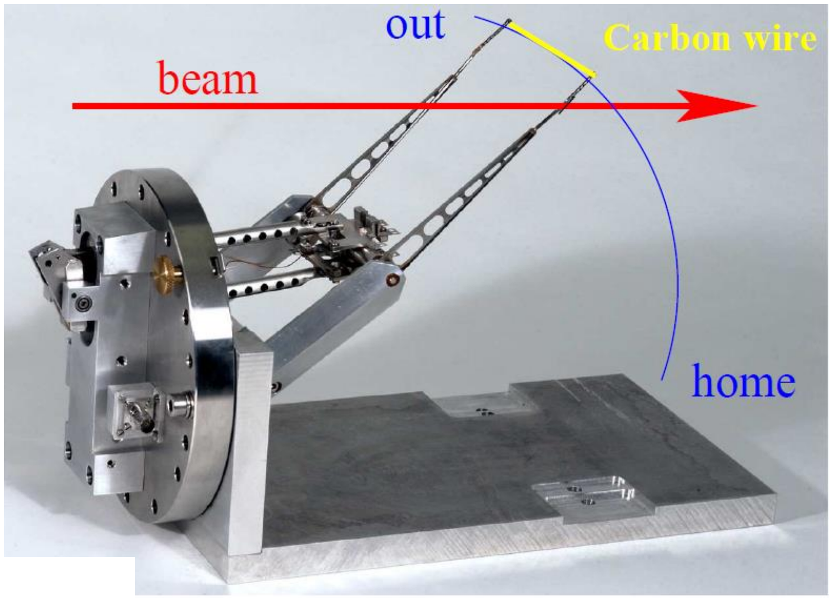

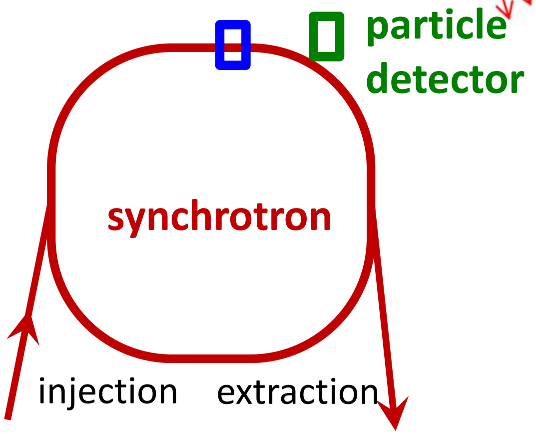

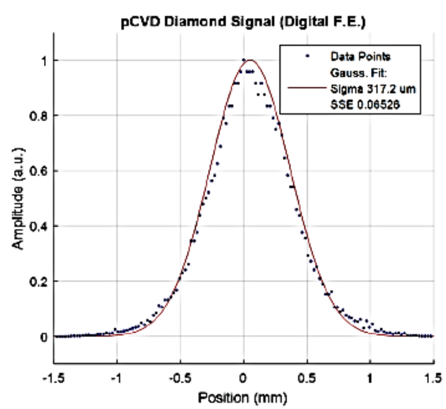

From https://twiki.cern.ch/twiki/bin/viewauth/BWSUpgrade/

Usage of Flying Wire Scanners

Material: carbon or SiC → low Z-material for low energy loss and high temperature.

Thickness: down to 10 μm → high resolution.

Detection: High energy **secondary particles** with a detector like a beam loss monitor

Secondary particles:

Proton beam → hadrons shower (π, n, p...)

Electron beam → Bremsstrahlung photons.

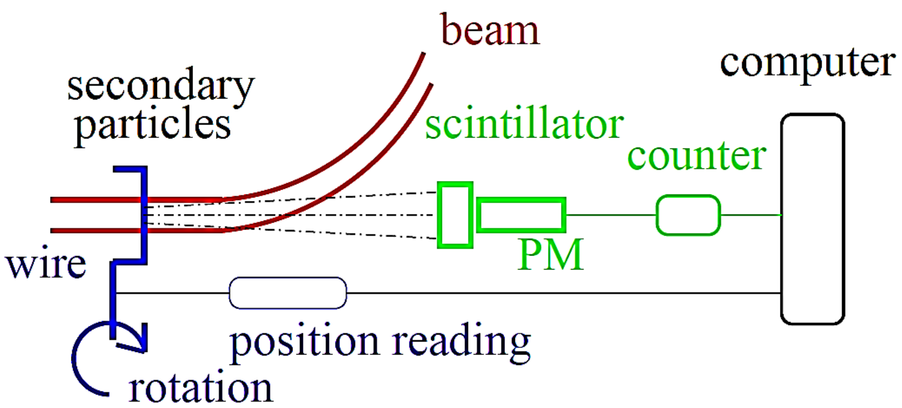

Proton impact on scanner at CERN-PS Booster:

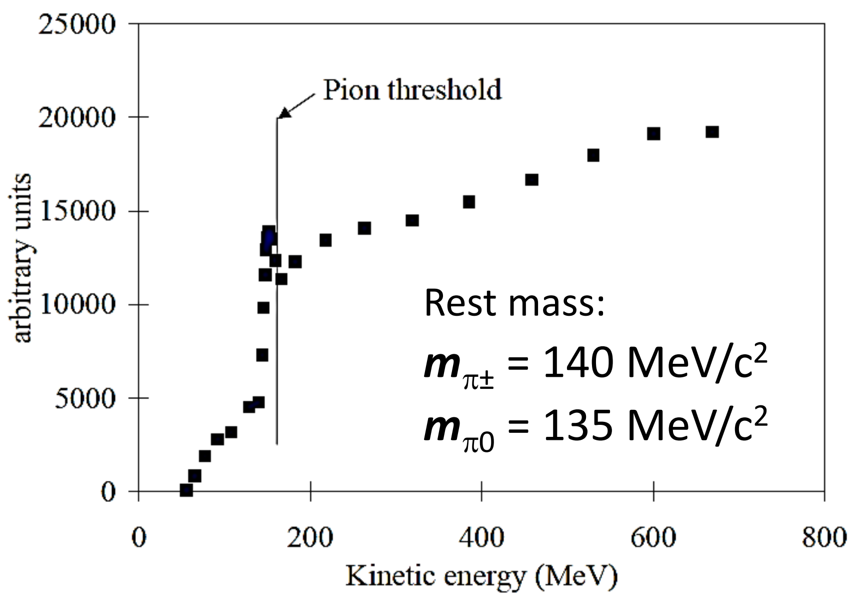

U. Raich et al., DIPAC 2005

Kinematics of flying wire:

Velocity during passage typically 10 m/s = 36 km/h and typical beam size ∅ 10 mm ⇒ time for traversing the beam $t \approx 1$ ms

Challenges: Wire stability for fast movement with high acceleration

The Artist View of a Wire Scanner

Comparison between SEM-Grid and slow linear Wire Scanners

Grid: Measurement at a single moment in time

Scanner: Fast variations can not be monitored

→ for pulsed LINACs precise synchronization is needed

Grid: Resolution of a grid is fixed by the wire distance (typically 1 mm)

Scanner: For slow scanners the resolution is about the wire thickness (down to 10 µm)

→ used for e−-beams having small sizes (down to 10 µm)

Grid: Needs one electronics channel per wire

→ expensive electronics and data acquisition

Scanner: Needs a precise movable feed-through → expensive mechanics.

Flying wire:

Grid: **Not** adequate at synchrotrons for stored beam parameters

Scanner: **At high energy synchrotrons:** flying wire scanners are nearly non-destructive

Measurement of Beam Profile

Outline:

- Scintillation screens:

  emission of light, universal usage, limited dynamic range
- Optical Transition Radiation:

  light emission due to crossing material boundary, mainly for relativistic beams
- SEM-Grid:

  emission of electrons, workhorse, limited resolution
- Wire scanner:

  emission of electrons, workhorse, scanning method
- **Ionization Profile Monitor:**

  secondary particle detection from interaction beam-residual gas
- **Synchrotron Light Monitors**
- **Summary**

Ionization Profile Monitor at GSI Synchrotron

Non-destructive device for proton synchrotron:

- Beam ionizes the residual gas by electronic stopping
- Gas ions or e⁻ accelerated by E -field ≈1 kV/cm
- Spatial resolved single particle detection

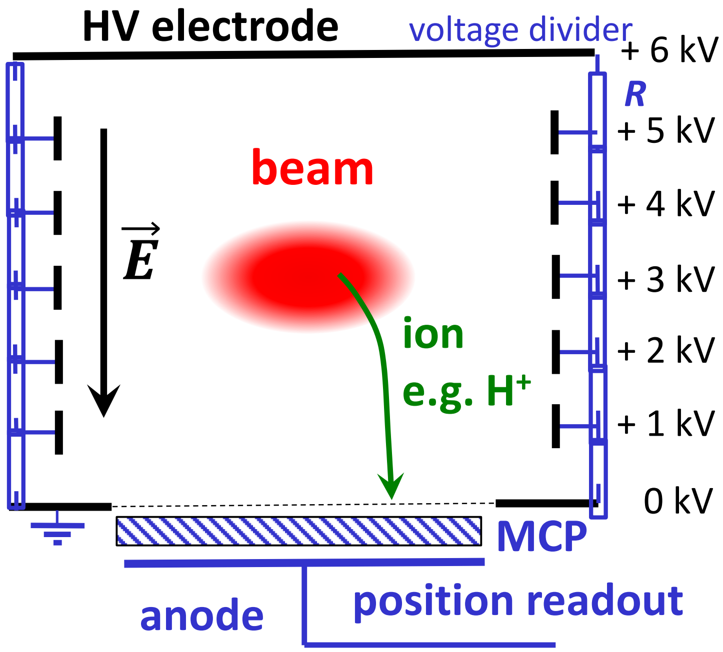

Typical vacuum pressure:

Transfer line: N_2 $10^{-8}...10^{-6}$ mbar $\cong$ $3\cdot10^{8}...3\cdot10^{10}cm^{-3}$

Synchrotron: H_2 $10^{-11}...10^{-9}$ mbar $\cong$ $3\cdot10^{5}...3\cdot10^{7}cm^{-3}$

Realization at GSI synchrotron:
One monitor per plane

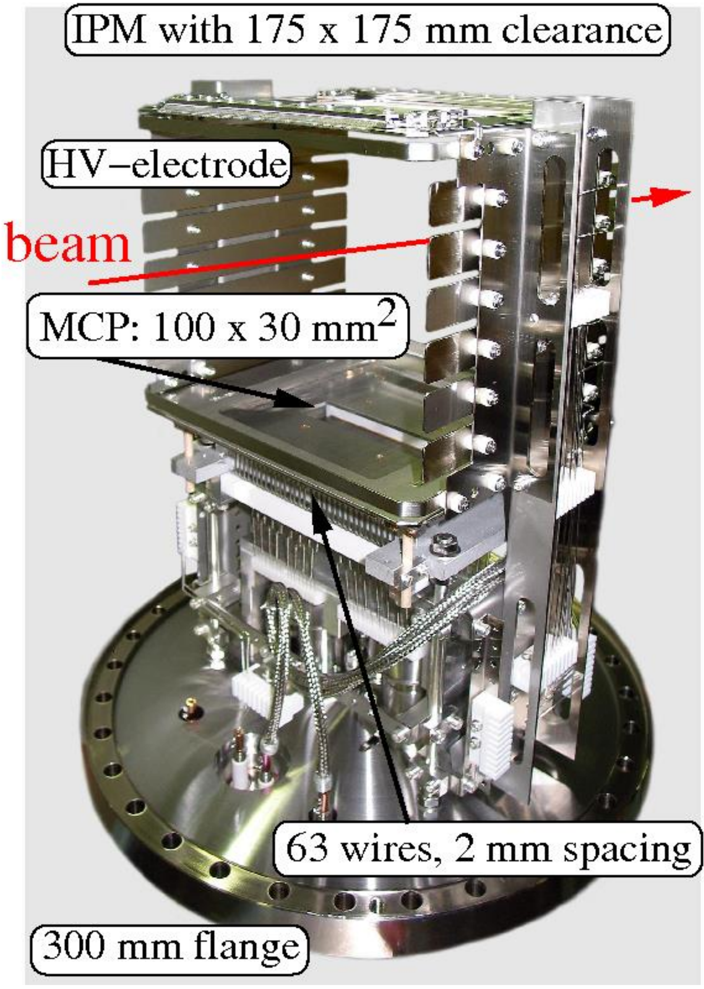

Ionization Profile Monitor Realization

The realization for the heavy ion storage ring ESR at GSI:

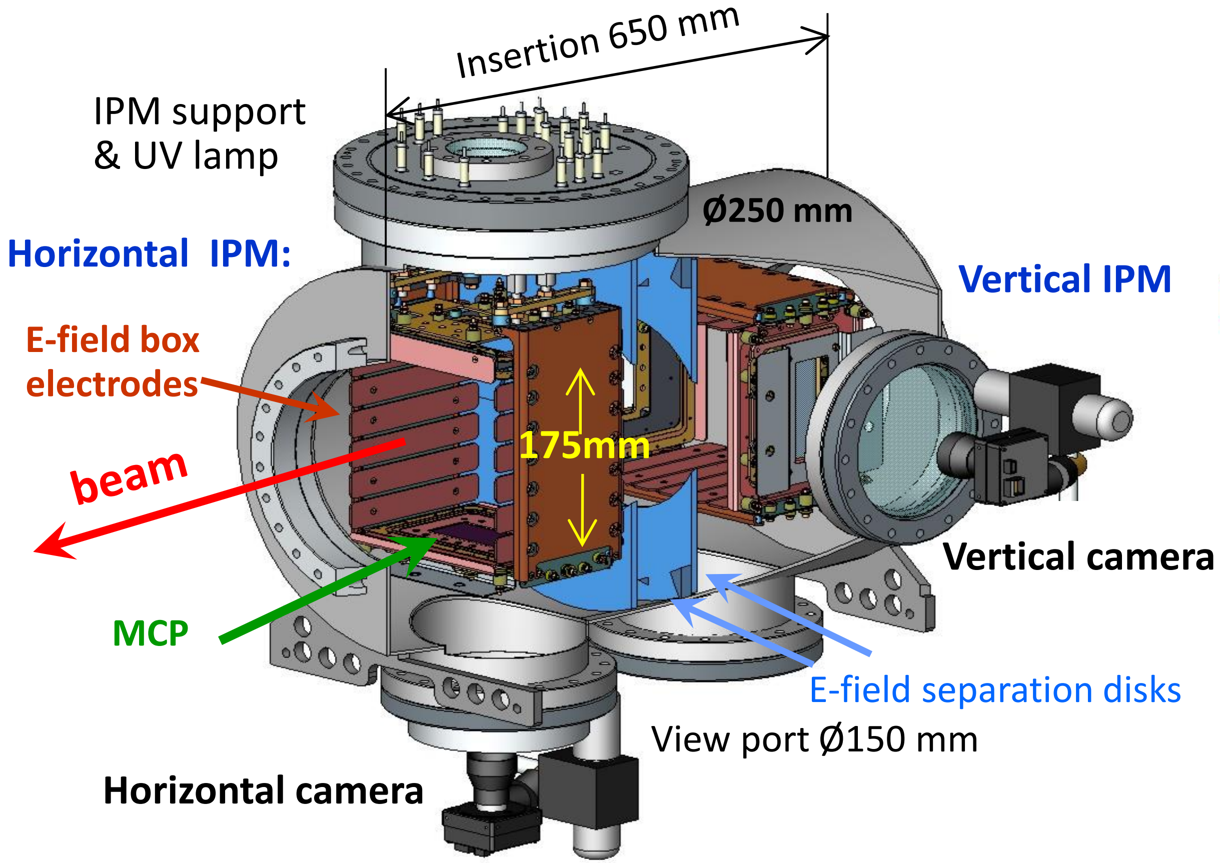

Realization at GSI synchrotron:
One monitor per plane

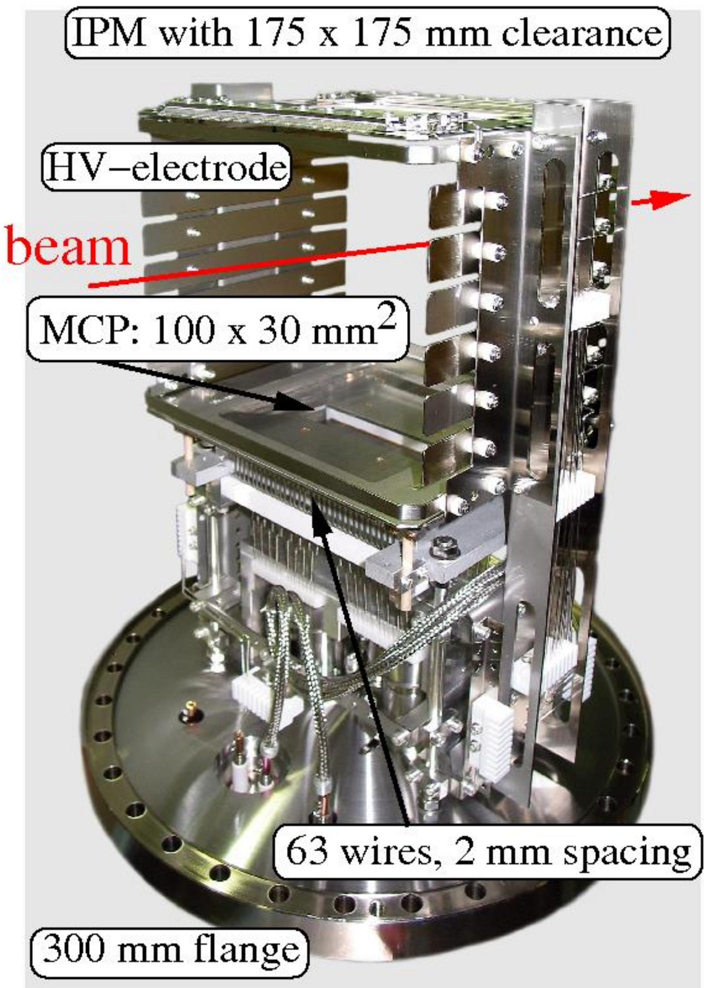

Typical vacuum pressure:

Transfer line: N_2 $10^{-8}...10^{-6}$ mbar $\cong$ $3\cdot10^{8}...3\cdot10^{10}$ cm^{-3}

Synchrotron: H_2 $10^{-11}...10^{-9}$ mbar $\cong$ $3\cdot10^{5}...3\cdot10^{7}$ cm^{-3}

Ionization Profile Monitor Realization

The realization for the heavy ion storage ring ESR at GSI:

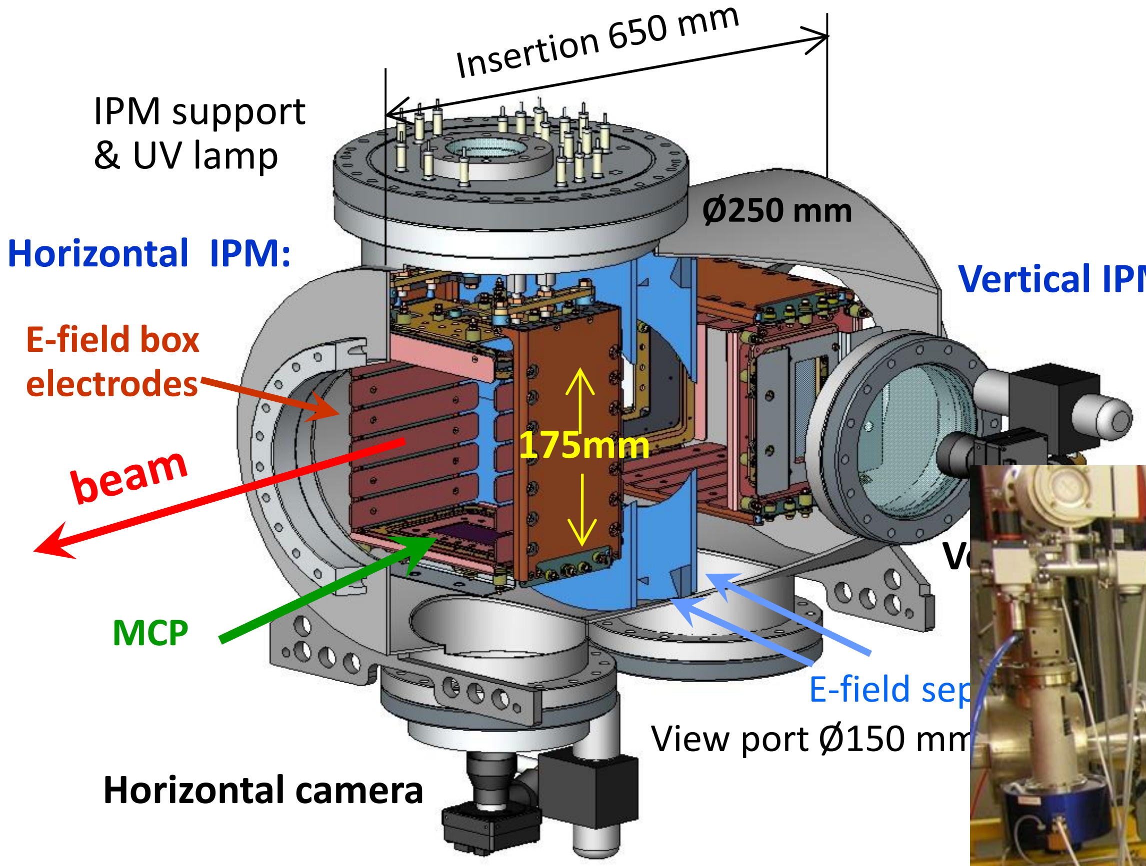

Realization at COSY synchrotron for one plane:

‘Adiabatic’ Damping during Acceleration

The emittance $\varepsilon = \int dx dx'$ is defined via the position deviation and angle in **lab-frame**

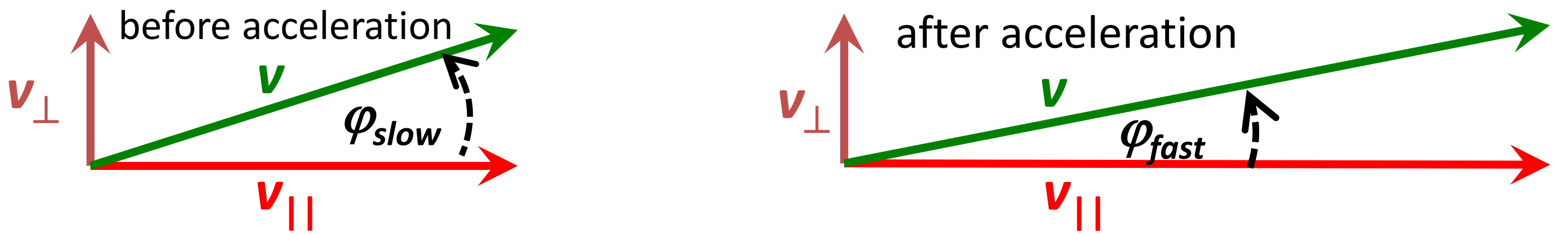

After acceleration the longitudinal velocity is increased $\Rightarrow$ angle φ is smaller

The angle is expressed in momenta: $x' = p_\perp / p_{||}$ the emittance is $\langle xx' \rangle = 0$: $\varepsilon = x \cdot x' = x \cdot p_\perp / p_{||}$

$\Rightarrow$ under ideal conditions the emittance can be normalized to the momentum $p_{||} = \gamma \cdot m \cdot \beta c$

$\Rightarrow$ normalized emittance $\varepsilon_{norm} = \beta\gamma \cdot \varepsilon$ is preserved with the Lorentz factor γ and velocity $\beta = v/c$

Example: Acceleration in GSI-synchrotron for C^{6+} from 6.7 $\rightarrow$ 600 MeV/u (β = 12 $\rightarrow$ 79 %) observed by IPM

theoretical width: $\langle x \rangle_f = \sqrt{\frac{\beta_i \cdot \gamma_i}{\beta_f \cdot \gamma_f}} \cdot \langle x \rangle_i$

$= 0.33 \cdot \langle x \rangle_i$

measured width: $\langle x \rangle_f \approx 0.37 \cdot \langle x \rangle_i$

IPM is well suited
for long time observations
without beam disturbance
$\rightarrow$ mainly used at proton synchrotrons.

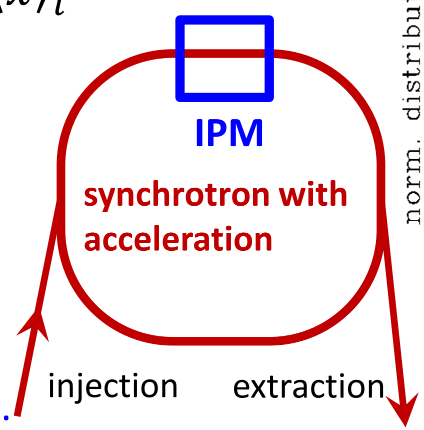

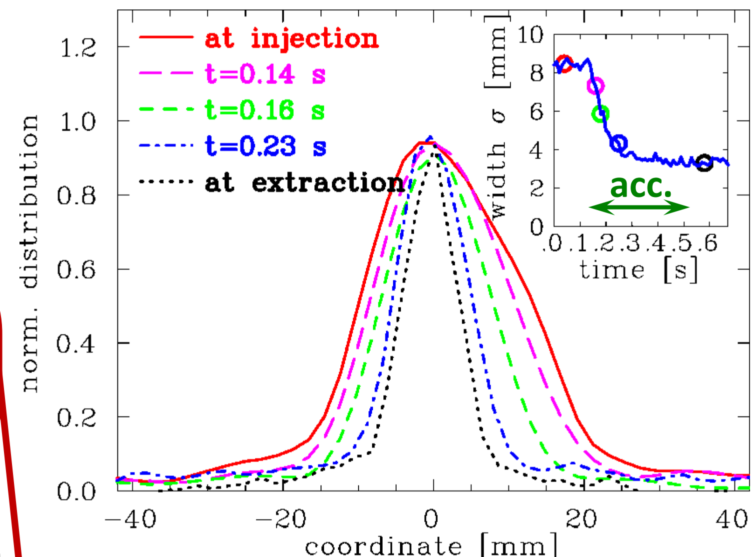

Outline:

- Scintillation screens:
  emission of light, universal usage, limited dynamic range
- Optical Transition Radiation:
  light emission due to crossing material boundary, mainly for relativistic beams
- SEM-Grid:
  emission of electrons, workhorse, limited resolution
- Wire scanner:
  emission of electrons, workhorse, scanning method
- Ionization Profile Monitor:
  secondary particle detection from interaction beam-residual gas
- **Synchrotron Light Monitors:**
  photon detection of emitted synchrotron light in optical and X-ray range
- **Summary**

An electron bent (i.e. accelerated) by a dipole magnet emit synchrotron light

see lecture 'Electron Beam Dynamics' by Lenny Rivkin

This light is emitted

into a cone of

opening 2/γ in lab-frame.

$\Rightarrow$Well suited for rel. e^-

For protons:

Only for energies E_{kin} > 100 GeV

Rest frame of electron: **Laboratory frame:**

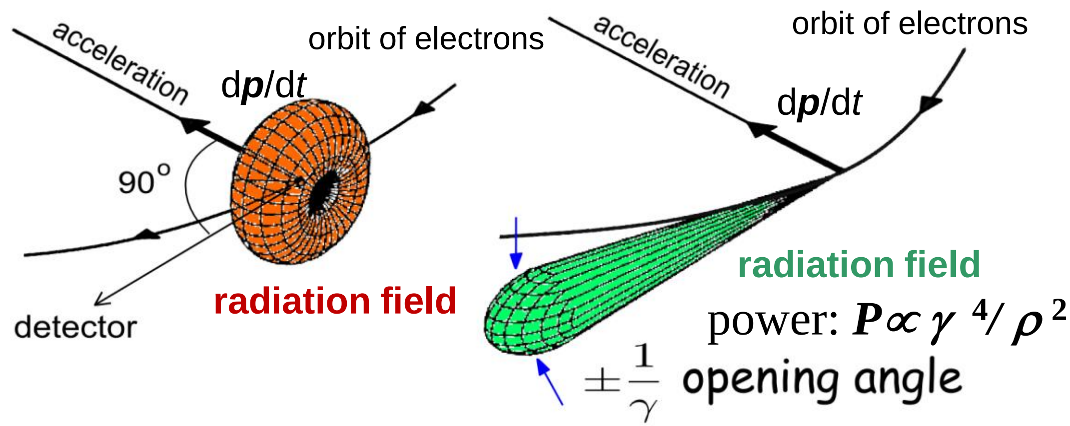

The light is focused to a intensified CCD.

Advantage:

Signal anyhow available!

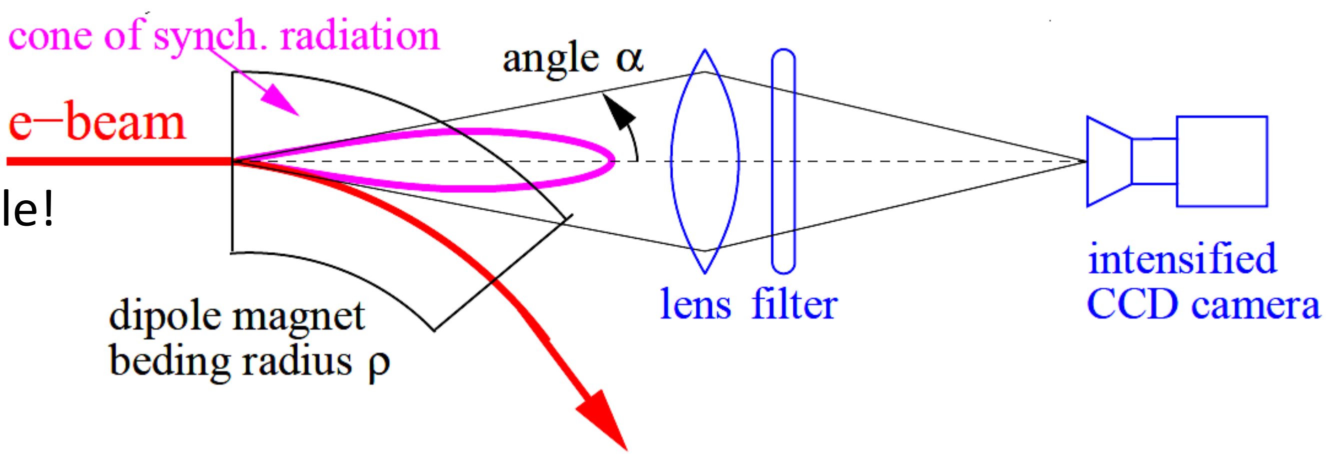

Realization of a Synchrotron Radiation Monitor

Extracting out of the beam's plane by a (cooled) mirror

→ Focus to a slit + wavelength filter for optical wavelength

→ Image intensified CCD camera

Example: ESRF monitor from dipole with bending radius 22 m (blue or near UV)

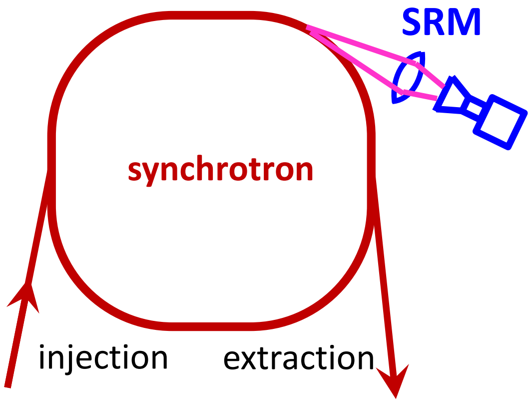

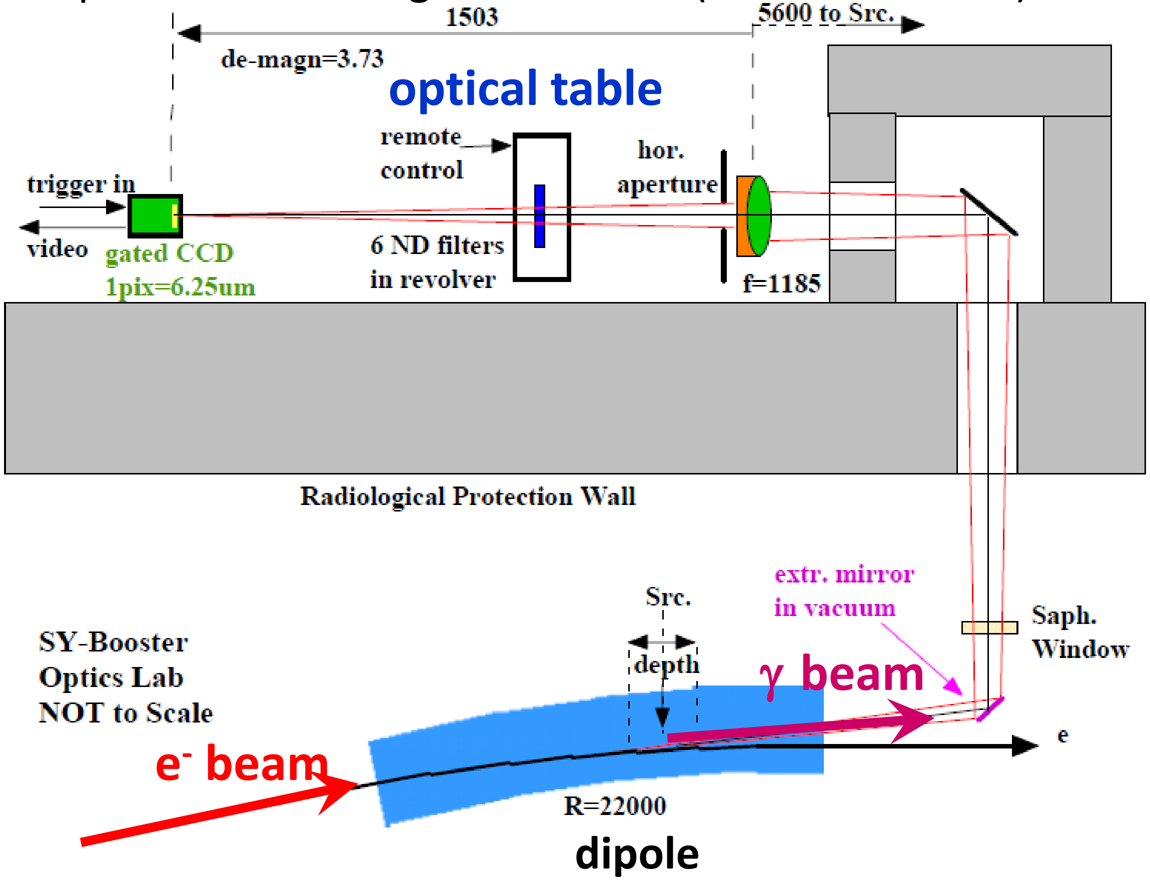

Courtesy K. Scheidt et al., DIPAC 2005

Result from a Synchrotron Light Monitor

Example: Synchrotron radiation facility APS accumulator ring and blue wavelength:

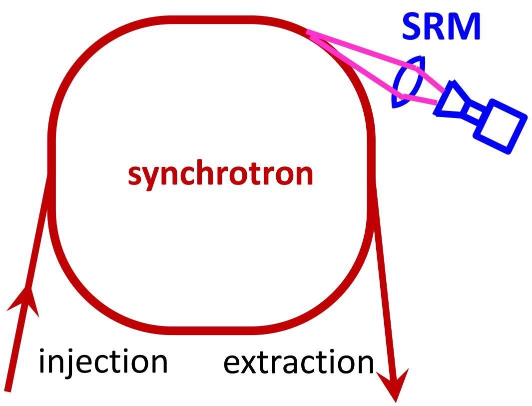

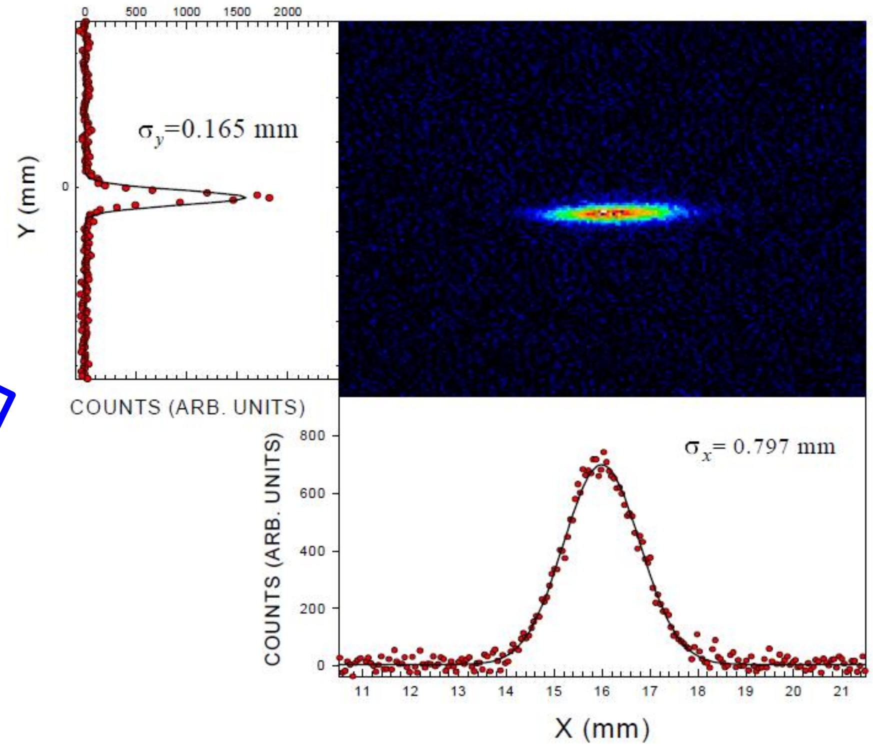

B.X. Yang (ANL) et al. PAC'97

Advantage: Direct measurement of 2-dim distribution, good optics for visible light

Realization: Optics outside of vacuum pipe

Disadvantage: Resolution limited by the diffraction due to finite apertures in the optics.

'Adiabatic Damping' for an Electron Beam

***Example*:** Booster at the light source ALBA acceleration from 0.1 → 3 GeV within 130 ms

Profile measure by synchrotron radiation monitor:

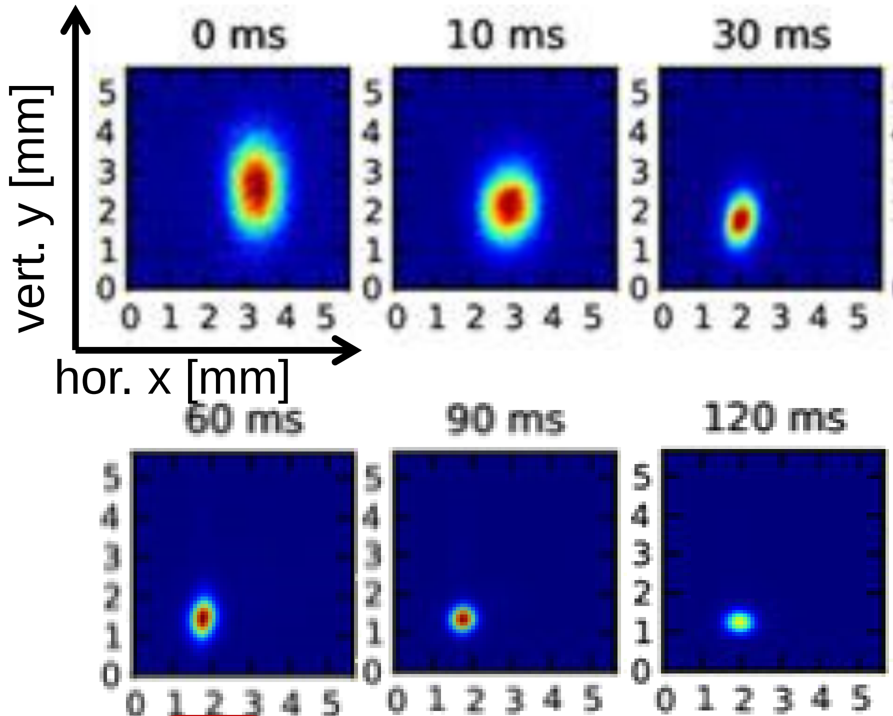

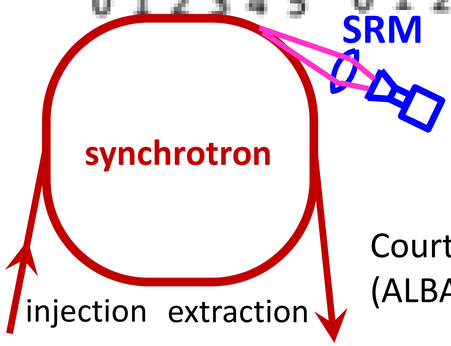

Courtesy U. Iriso & M. Pont (ALBA) et al. IPAC 2011

The beam emittance in influenced by:

- Adiabatic damping
- Longitudinal momentum contribution

  via dispersion $\Delta x_D(s) = D(s) \cdot \frac{\Delta p}{p}$

  total width $\Delta x_{tot}(s) = \sqrt{\varepsilon\beta(s) + D(s) \cdot \frac{\Delta p}{p}}$
- Quantum fluctuation due to light emission

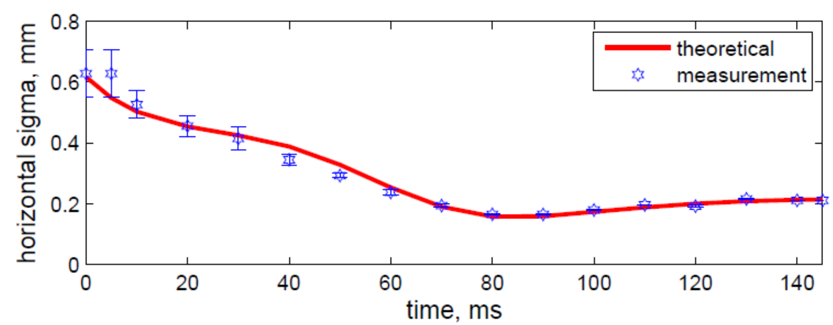

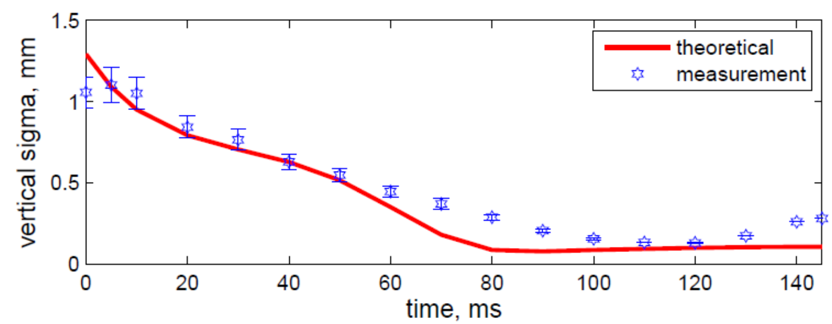

The Artist View of a Synchrotron Light Monitor

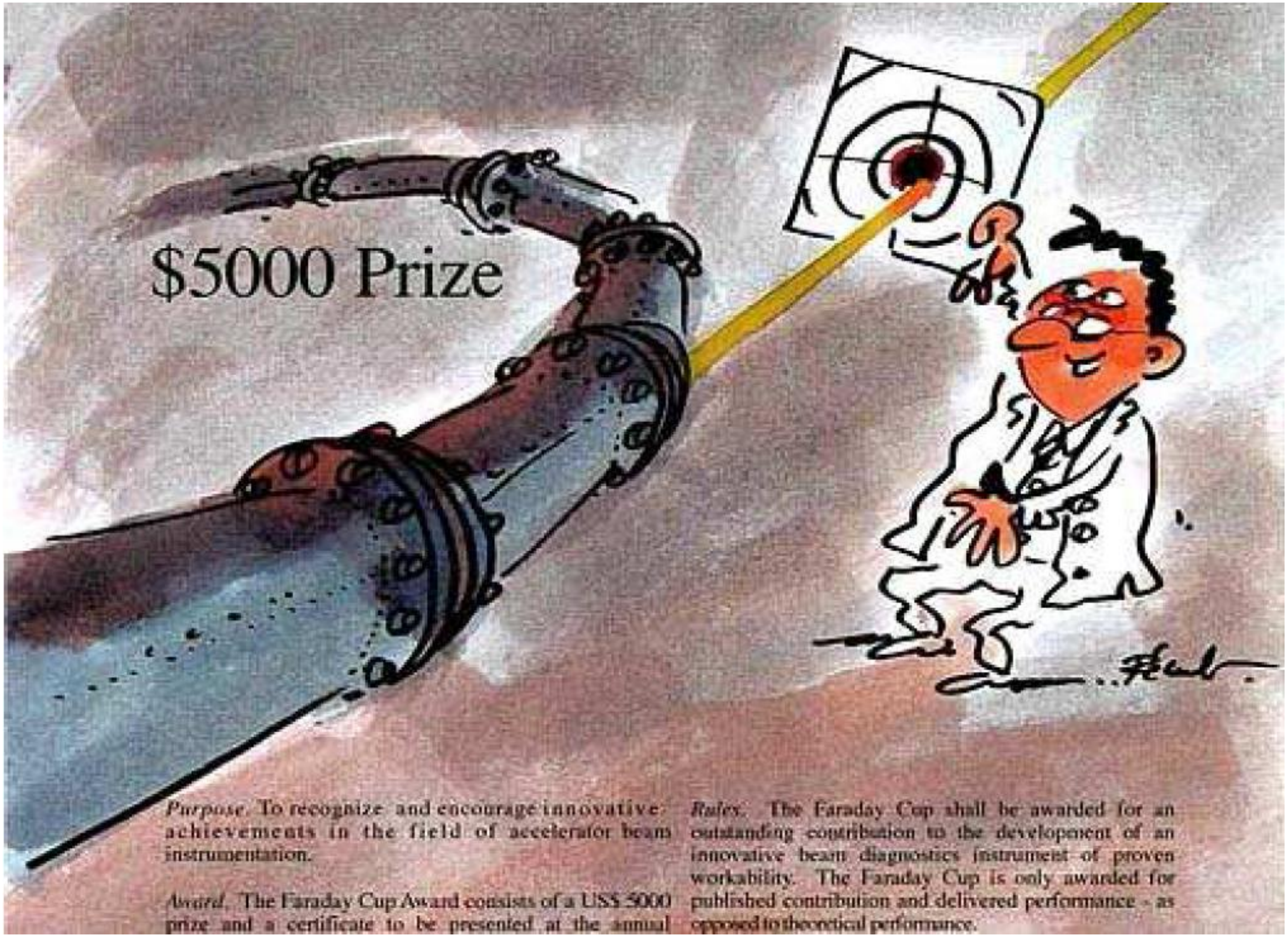

Diffraction Limit of Synchrotron Light Monitor

Limitations:

Diffraction limits the resolution due to Fraunhofer diffraction

Pattern width for 1:1 image:

$$\sigma \simeq \frac{\lambda}{2D/L} \simeq 0.6 \cdot \left(\frac{\lambda^2}{\varrho}\right)^{1/3}$$

$\Rightarrow \sigma \simeq 100$ µm for typical cases

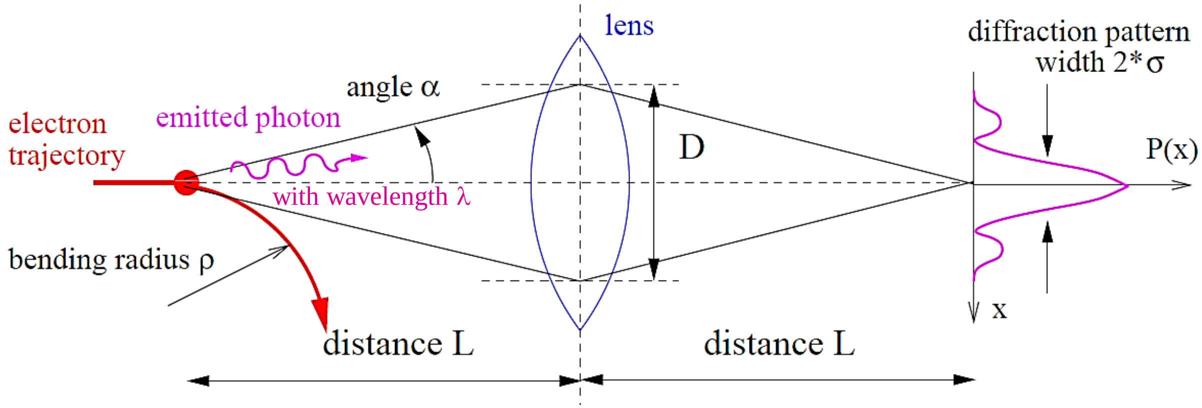

Improvements:

- ***Shorter wavelength:***

  Using X-rays and an aperture of Ø 1mm
  → 'X-ray pin hole camera',
  achievable resolution $\boldsymbol{\sigma} \simeq 10$ µm

- ***Interference technique:***

  At optical wavelength using a double slit
  → interference fringe blurring
  compared to point source
  achievable resolution $\boldsymbol{\sigma} \simeq 1$ µm.

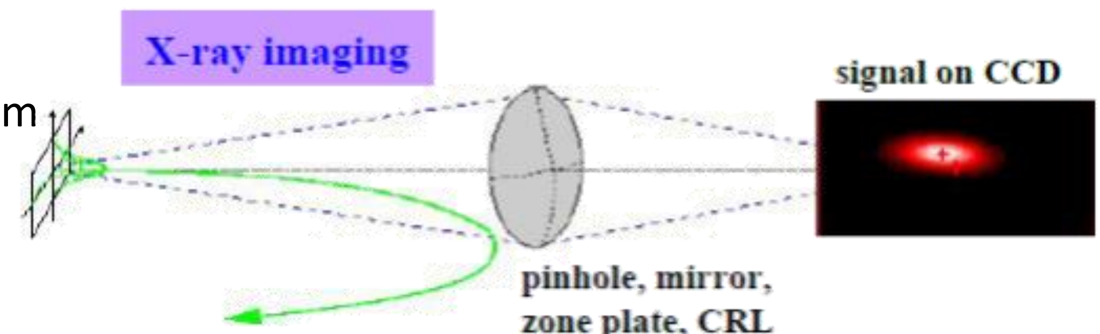

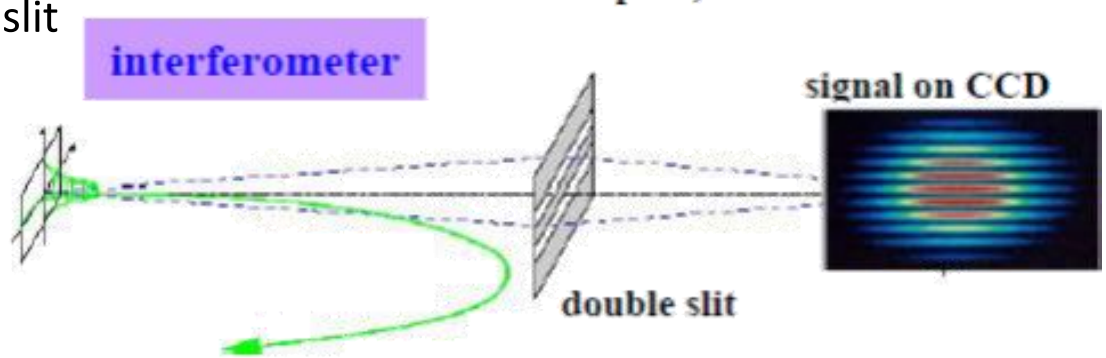

Summary for Beam Profile Measurement

Different techniques are suited for different beam parameters:

e^--beam: typically Ø 0.01 to 3 mm, **protons:** typically Ø 1 to 30 mm

Intercepting ↔ non-intercepting methods

Direct observation of electrodynamics processes:

- Optical synchrotron radiation monitor: non-destructive, for e^--beams, complex, limited res.
- X-ray synchrotron radiation monitor: non-destructive, for e^--beams, very complex
- OTR screen: nearly non-destructive, large relativistic γ needed, e^--beams mainly

Detection of secondary photons, electrons or ions:

- Scintillation screen: destructive, large signal, simple setup, all beams
- Ionization profile monitor: non-destructive, expensive, limited resolution, for protons

Wire based electronic methods:

- SEM-grid: partly destructive, large signal and dynamic range, limited resolution
- Wire scanner: partly destructive, large signal and dynamics, high resolution, slow scan.

Measurement of transverse Emittance

The emittance characterizes the whole beam quality, assuming linear behavior as described by second order differential equation.

It is defined within the phase space as: $\varepsilon_x = \frac{1}{\pi} \int_A dx dx'$

The measurement is based on determination of:

Either profile width $\boldsymbol{\sigma_x}$ and angular width $\boldsymbol{\sigma_x'}$ at one location
Or profile width $\boldsymbol{\sigma_x}$ at different locations and linear transformations.

Different devices are used at transfer lines:

- Lower energies E_{kin} < 100 MeV/u: slit-grid device, pepper-pot (suited in case of non-linear forces).
- All beams: Quadrupole variation method using linear transformations (**not** well suited in the presence of non-linear forces)

Synchrotron: lattice functions results in stability criterion

$\Rightarrow$ beam width delivers emittance: $\varepsilon_x = \frac{1}{\beta_x(s)}\left[\sigma_x^2 - \left(D(s)\frac{\Delta p}{p}\right)\right]$ and $\varepsilon_y = \frac{\sigma_y^2}{\beta_y(s)}$

Trajectory and Characterization of many Particles

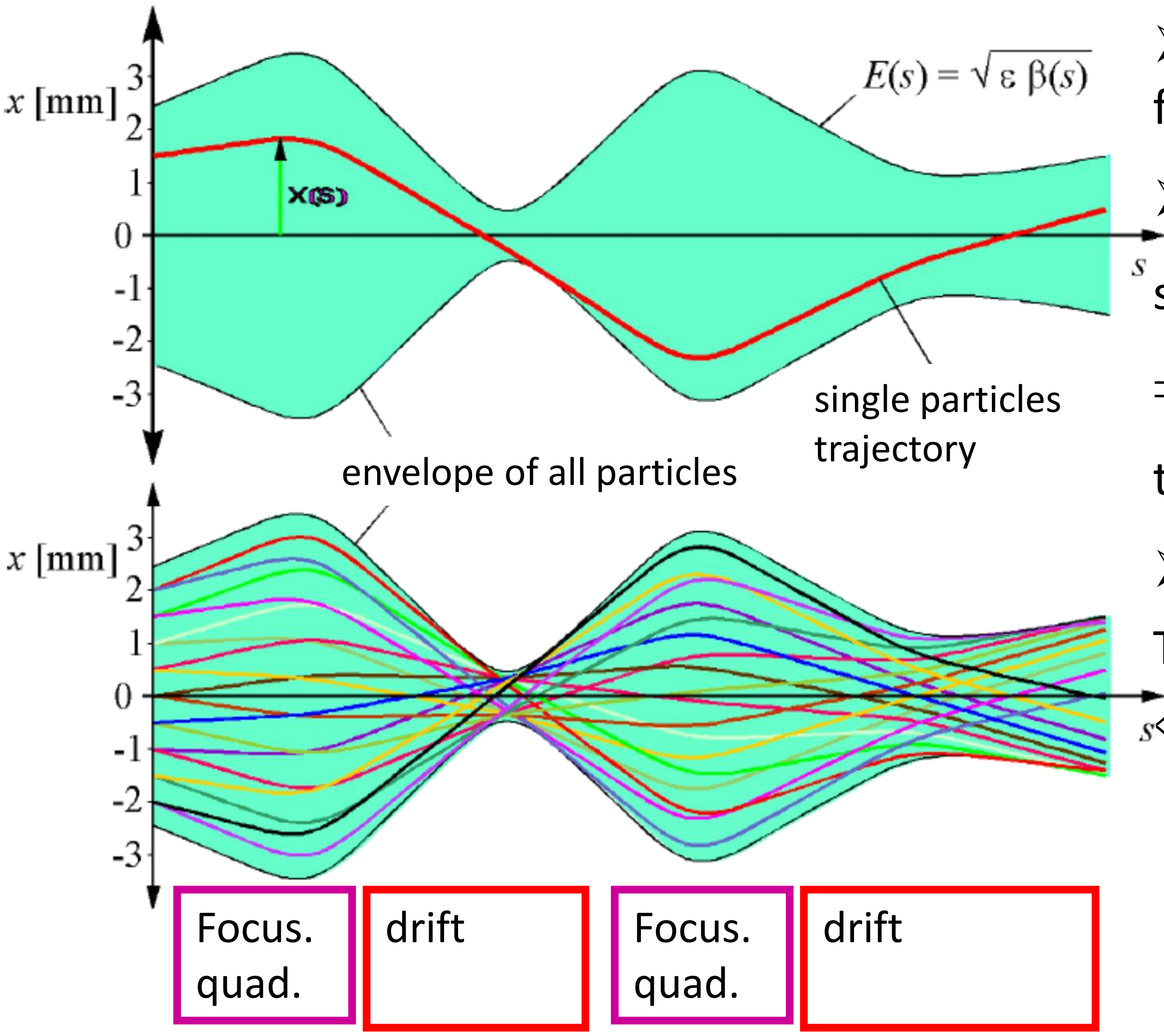

Courtesy K.Wille

- Single particle trajectories are forming a beam
- They have a distribution of start positions and angles

$\Rightarrow$ Characteristic quantity is the **beam envelope**

- **Goal:**

Transformation of envelope
$\Leftrightarrow$ behavior of whole ensemble

see lecture
'Transverse linear Beam Dynamics'
by Wolfgang Hillert

Definition of Coordinates and basic Equations

The basic vector is 6 dimensional:

$$\vec{x} = \begin{pmatrix} x \\ x' \\ y \\ y' \\ l \\ \delta \end{pmatrix} = \begin{pmatrix} \text{hori. spatial deviation} \\ \text{horizontal divergence} \\ \text{vert. spatial deviation} \\ \text{vertical divergence} \\ \text{long. deviation} \\ \text{momentum deviation} \end{pmatrix} = \begin{pmatrix} [mm] \\ [mrad] \\ [mm] \\ [mrad] \\ [mm] \\ [10^{-3}] \end{pmatrix}$$

The transformation of a single particle from a location s_0 to s_1 is given by the Transfer Matrix R:

$$\vec{x}(s_1) = \mathbf{R}(s) \cdot \vec{x}(s_0)$$

The transformation of a the envelope from a location s_0 to s_1 is given by the Beam Matrix σ :

$$\boldsymbol{\sigma}(s_1) = \mathbf{R}(s) \cdot \boldsymbol{\sigma}(s_0) \cdot \mathbf{R}^{\mathrm{T}}(s)$$

6-dim Beam Matrix with *decoupled* hor., vert. and long. plane:

$$\boldsymbol{\sigma} = \begin{pmatrix} \sigma_{11} & \sigma_{12} & 0 & 0 & 0 & 0 \\ \sigma_{12} & \sigma_{22} & 0 & 0 & 0 & 0 \\ 0 & 0 & \sigma_{33} & \sigma_{34} & 0 & 0 \\ 0 & 0 & \sigma_{34} & \sigma_{44} & 0 & 0 \\ 0 & 0 & 0 & 0 & \sigma_{55} & \sigma_{56} \\ 0 & 0 & 0 & 0 & \sigma_{56} & \sigma_{66} \end{pmatrix}$$

horizontal
vertical
longitudinal
hor.-long. coupling
→ 9 values

Beam width for the three coordinates:

$$x_{rms} = \sqrt{\sigma_{11}}$$
$$y_{rms} = \sqrt{\sigma_{33}}$$
$$l_{rms} = \sqrt{\sigma_{55}}$$

Horizontal beam matrix:

$$\sigma_{11} = \langle x^2 \rangle$$
$$\sigma_{12} = \langle x\, x' \rangle$$
$$\sigma_{22} = \langle x'^2 \rangle$$

The Emittance for Gaussian and non-Gaussian Beams

The beam distribution can be non-Gaussian, e.g. at:

- Beams behind ion source
- Space charged dominated beams at LINAC & synchrotron
- Cooled beams in storage rings

General description of emittance using terms of 2-dim distribution:

$$\varepsilon_{rms} = \sqrt{\underbrace{\langle x^2 \rangle \langle x'^2 \rangle}_{\text{Variances}} - \underbrace{\langle xx' \rangle^2}_{\text{Covariance i.e. correlation}}}$$

It describes the value for 1 standard derivation

Variances

Covariance i.e. correlation

For Gaussian beams only: ε_{rms} $\leftrightarrow$ interpreted as area containing a fraction ***f*** of ions:

$$\varepsilon(f) = -2\pi\varepsilon_{rms} \cdot \ln(1 - f)$$

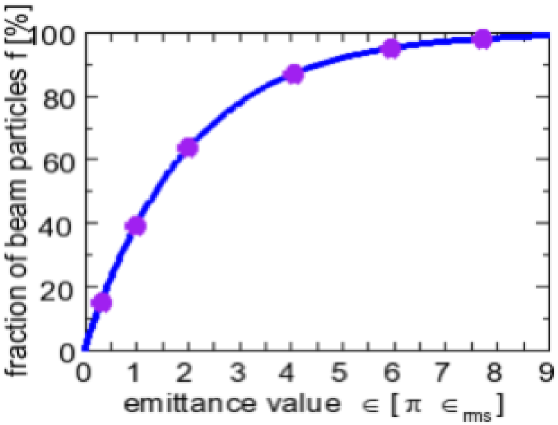

Emittance ε (*f*)	Fraction *f*
$1 \cdot \varepsilon_{rms}$	15 %
$\pi \cdot \varepsilon_{rms}$	39 %
$2\pi \cdot \varepsilon_{rms}$	63 %
$4\pi \cdot \varepsilon_{rms}$	86 %
$8\pi \cdot \varepsilon_{rms}$	98 %

Care:

No common definition of emittance concerning the fraction ***f***

The Slit-Grid Measurement Device

Slit-Grid: Direct determination of position and angle distribution.

Used for protons with E_{kin} < 100 MeV/u ⇒ range R < 1 cm.

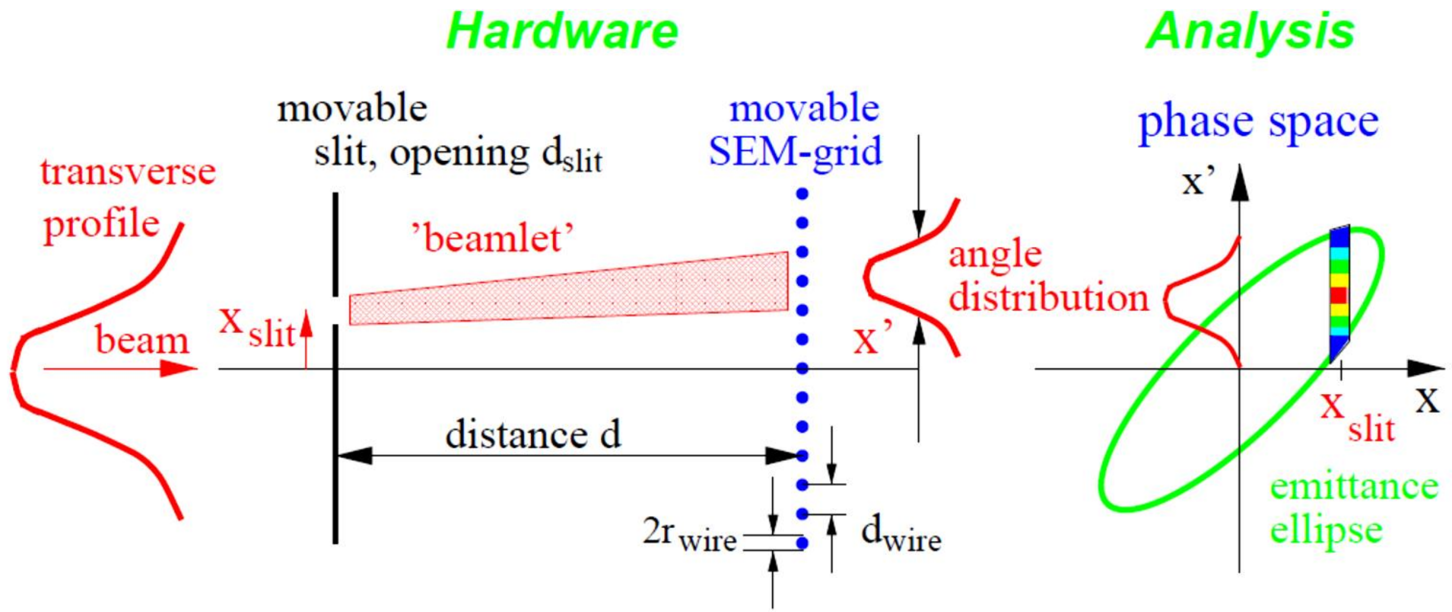

Slit: position ***P(x)*** with typical width: 0.1 to 0.5 mm

Distance: typ. 0.5 to 5 m (depending on beam energy 0. 1 ... 100 MeV)

SEM-Grid: angle distribution ***P(x')***

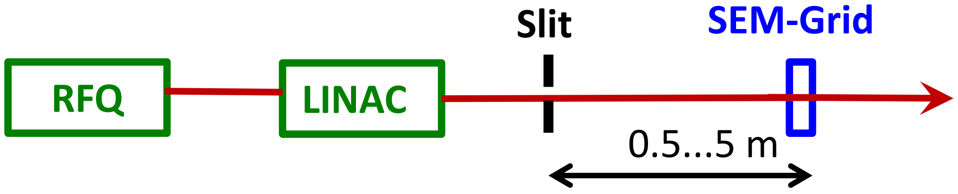

Display of Measurement Results

The distribution is depicted as a function of position [mm] & angle [mrad]

The distribution can be visualized by

- Mountain plot
- Contour plot

Calc. of 2nd moments $\langle x^2 \rangle$, $\langle x'^2 \rangle$ & $\langle xx' \rangle$

Emittance value ε_{rms} from

$$\varepsilon_{rms} = \sqrt{\langle x^2 \rangle \langle x'^2 \rangle - \langle xx' \rangle^2}$$

$\Rightarrow$ **Problems:**

- Finite **binning** results in limited resolution
- **Background** $\rightarrow$ large influence on $\langle x^2 \rangle$, $\langle x'^2 \rangle$ and $\langle xx' \rangle$

Or fit of distribution with an ellipse

$\Rightarrow$ **Effective emittance only**

Remark: Behind a ion source the beam might very non-Gaussian due to plasma density and aberration at quadrupoles

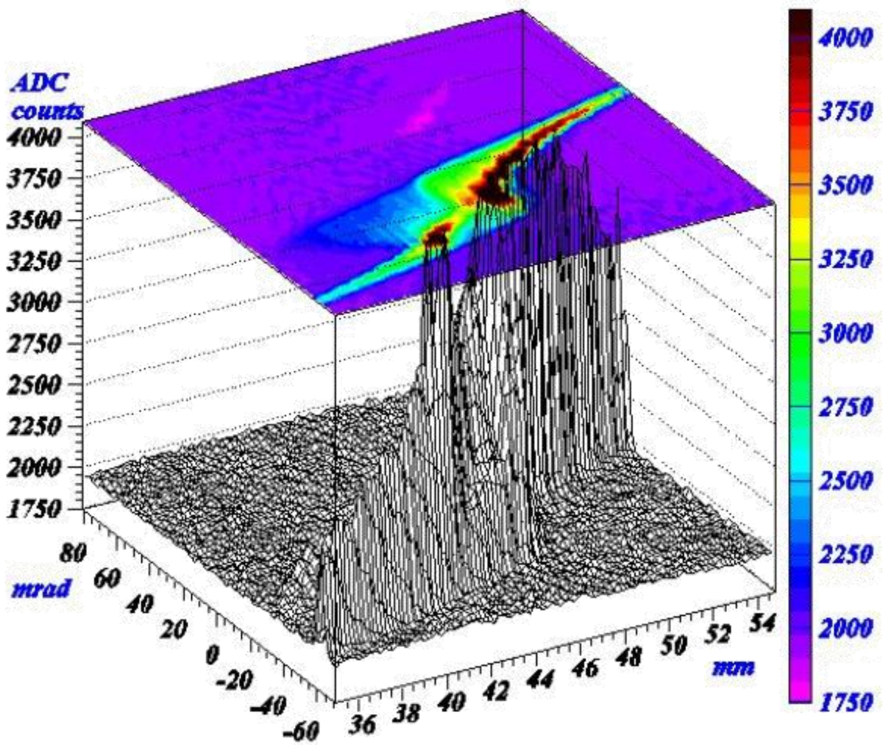

Beam: Ar^{4+}, 60 keV, 15 µA

at Spiral2 Phoenix ECR source.

P. Ausset, DIPAC 2009

Measurement of transverse Emittance

Outline:

- Definition and some properties of transverse emittance
- Slit-Grid device: scanning method

  scanning slit $\rightarrow$ beam position & grid $\rightarrow$ angular distribution
- **Quadrupole strength variation and position measurement**

  emittance from several profile measurement and beam optical calculation

Emittance Measurement by Quadrupole Variation

From a profile determination, the emittance can be calculated via linear transformation, if a well known and constant distribution (e.g. Gaussian) is assumed.

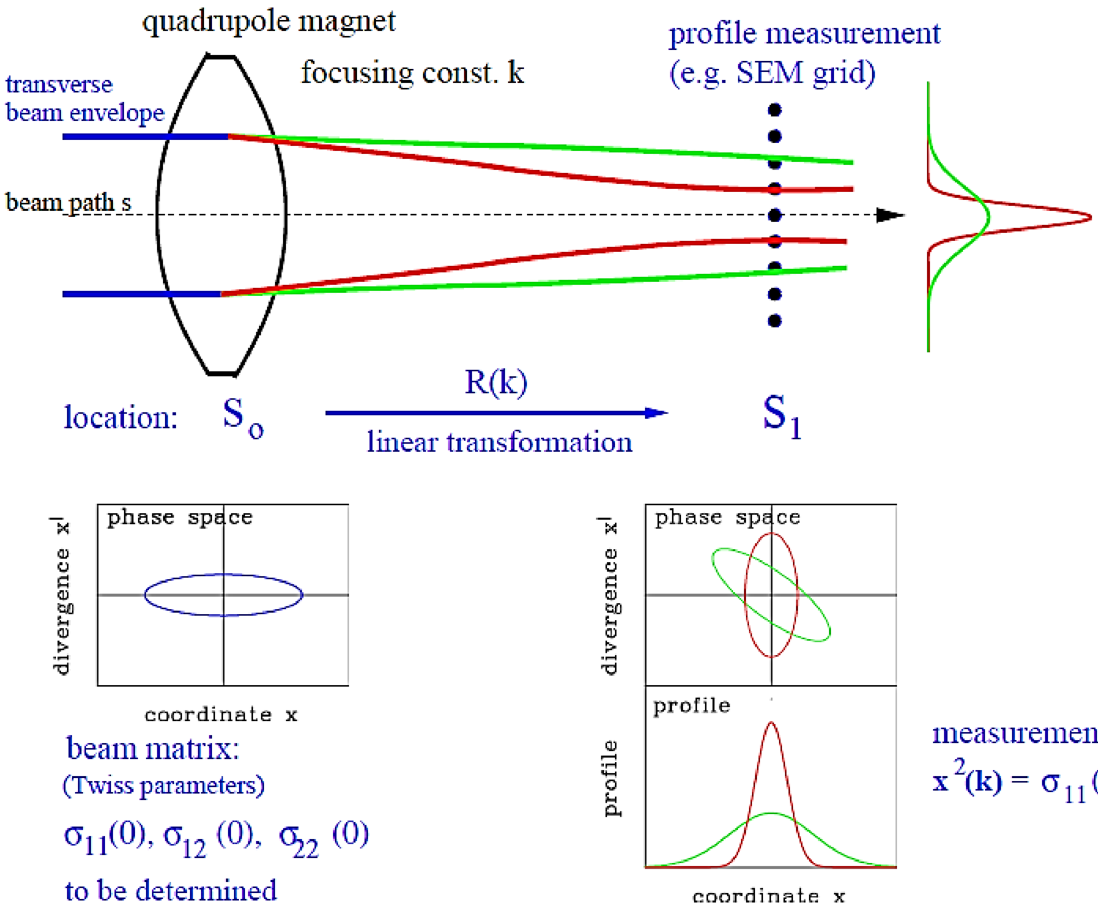

beam matrix:
(Twiss parameters)
$\sigma_{11}(0)$, $\sigma_{12}(0)$, $\sigma_{22}(0)$
to be determined

measurement:
$x^2(k) = \sigma_{11}(1,k)$

- Measurement of beam width

  $x^2_{max} = \sigma_{11}(s_1, k)$

  matrix **R(*k*)** describes the focusing.

- With the drift matrix the transfer is

  $\mathbf{R}(k_i) = \mathbf{R}_{drift} \cdot \mathbf{R}_{focus}(k_i)$

- Transformation of the beam matrix

  $\sigma(s_1,k_i) = \mathbf{R}(k_i) \cdot \sigma(s_0) \cdot \mathbf{R}^T(k_i)$

Task: Calculation of $\sigma(0)$

at entrance s_0 i.e. all three elements

Measurement of transverse Emittance

Using the 'thin lens approximation' i.e. the quadrupole has a focal length of ***f***:

$$\mathrm{R}_{focus}(\boldsymbol{K}) = \begin{pmatrix} \mathbf{1} & \mathbf{0} \\ -\mathbf{1}/\boldsymbol{f} & \mathbf{1} \end{pmatrix} \equiv \begin{pmatrix} \mathbf{1} & \mathbf{0} \\ \boldsymbol{K} & \mathbf{1} \end{pmatrix} \Rightarrow \mathrm{R}(\boldsymbol{L},\boldsymbol{K}) = \mathrm{R}_{drift}(\boldsymbol{L}) \cdot \mathrm{R}_{focus}(\boldsymbol{K}) = \begin{pmatrix} \mathbf{1}+\boldsymbol{LK} & \boldsymbol{L} \\ \boldsymbol{K} & \mathbf{1} \end{pmatrix}$$

Measurement of matrix-element $\boldsymbol{\sigma}_{\mathbf{11}}(s_1, K)$ from matrices $\boldsymbol{\sigma}(s_1,K_i) = \mathbf{R}(K_i) \cdot \boldsymbol{\sigma}(s_0) \cdot \mathbf{R}^{\mathbf{T}}(K_i)$

Example: Square of the beam width at ELETTRA 100 MeV e$^-$ Linac, YAG:Ce:

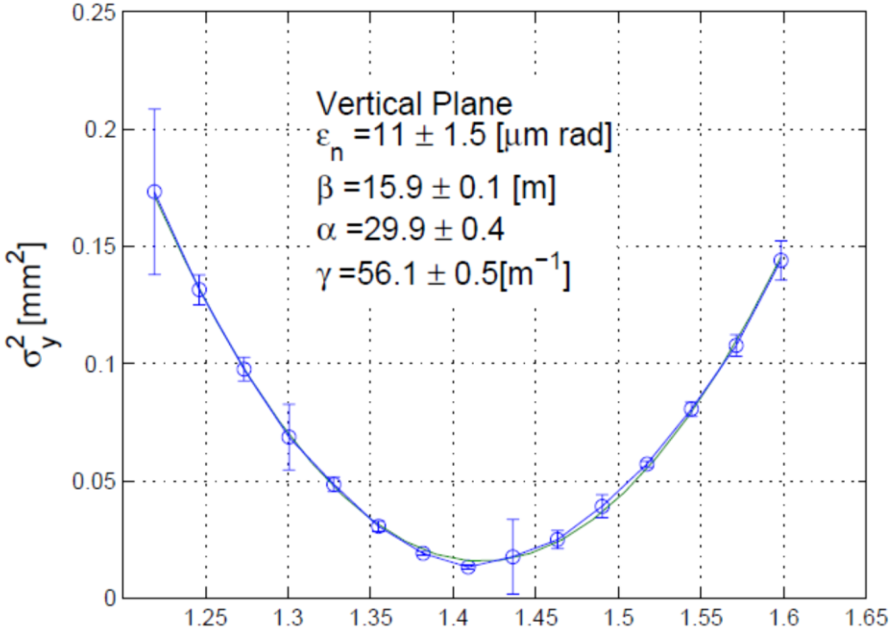

Focusing strength K [m^{-1}]

G. Penco (ELETTRA) et al., EPAC'08

For completeness: The relevant formulas

$$\begin{aligned} \sigma_{11}(1,K) = {} & L^2\sigma_{11}(0)\cdot K^2 \\ & + 2\cdot(\ L\sigma_{11}(0) + L^2\sigma_{12}(0)\ )\cdot K \\ & + L^2\sigma_{22}(0) + \sigma_{11}(0) \\ \equiv {} & a\cdot K^2 \ - \ 2ab\cdot K \ + \ ab^2 + c \end{aligned}$$

The three matrix elements at the quadrupole:

$$\boldsymbol{\sigma}_{11}(\mathbf{0}) = \frac{\boldsymbol{a}}{\boldsymbol{L}^2}$$

$$\boldsymbol{\sigma}_{12}(\mathbf{0}) = -\frac{\boldsymbol{a}}{\boldsymbol{L}^2}\left(\frac{\mathbf{1}}{\boldsymbol{L}} + \boldsymbol{b}\right)$$

$$\boldsymbol{\sigma}_{22}(\mathbf{0}) = \frac{\mathbf{1}}{\boldsymbol{L}^2}\left(\boldsymbol{ab}^2 + \boldsymbol{c} + \frac{\mathbf{2ab}}{\boldsymbol{L}} + \frac{\boldsymbol{a}}{\boldsymbol{L}^2}\right)$$

$$\boldsymbol{\varepsilon}_{rms} \equiv \sqrt{\det \boldsymbol{\sigma}(\mathbf{0})} = \sqrt{\boldsymbol{\sigma}_{11}(\mathbf{0})\cdot\boldsymbol{\sigma}_{22}(\mathbf{0}) - \boldsymbol{\sigma}_{12}^2(\mathbf{0})} = \sqrt{\boldsymbol{ac}}\,/\,\boldsymbol{L}^2$$

Summary for transverse Emittance Measurement

Emittance is the important quantity for comparison to theory.

It includes absolute value (value of $\boldsymbol{\varepsilon}$) & orientation in phase space ($\boldsymbol{\sigma_{ij}}$ or $\boldsymbol{\alpha}$, $\boldsymbol{\beta}$ and $\boldsymbol{\gamma}$)

three independent values $\varepsilon_{rms} = \sqrt{\sigma_{11} \cdot \sigma_{22} - \sigma_{12}} \equiv \sqrt{\langle x^2 \rangle \langle x'^2 \rangle - \langle xx' \rangle^2}$

assuming no coupling between horizontal, vertical and longitudinal planes

Transfer line, low energy beams → direct measurement of x- and x'-distribution:

- ***Slit-grid:*** movable slit → ***x***-profile, grid → ***x'***-profile

Transfer line, all beams → profile measurement + linear transformation:

- ***Quadrupole variation:*** one location, different setting of a quadrupole

Assumptions:
- well aligned beam, no steering
- no emittance blow-up due to space charge

Remark: Non-linear transformation possible via tomographic reconstruction

Important remark: For a synchrotron with a *stable beam storage*,

width measurement is sufficient using $x_{rms} = \sqrt{\varepsilon_{rms} \cdot \beta}$

Measurement of longitudinal parameter:

Bunch length measurement at

- **Synchrotron light sources**
- **Linear light sources**
- **Summary**

Longitudinal ↔ transverse correspondences:

- position relative to rf ↔ transverse center-of-mass
- bunch structure in time ↔ transverse profile
- momentum or energy spread ↔ transverse divergence
- longitudinal emittance ↔ transverse emittance.

The Bunch Position measured by a Pick-Up

The ***bunch position*** is given relative to the accelerating rf.

e.g. φ_{ref}=-30° inside a rf cavity

must be well aligned for optimal acceleration

Transverse correspondence: Beam position

Example: Pick-up signal for f_{rf}=36 MHz rf at GSI-LINAC:

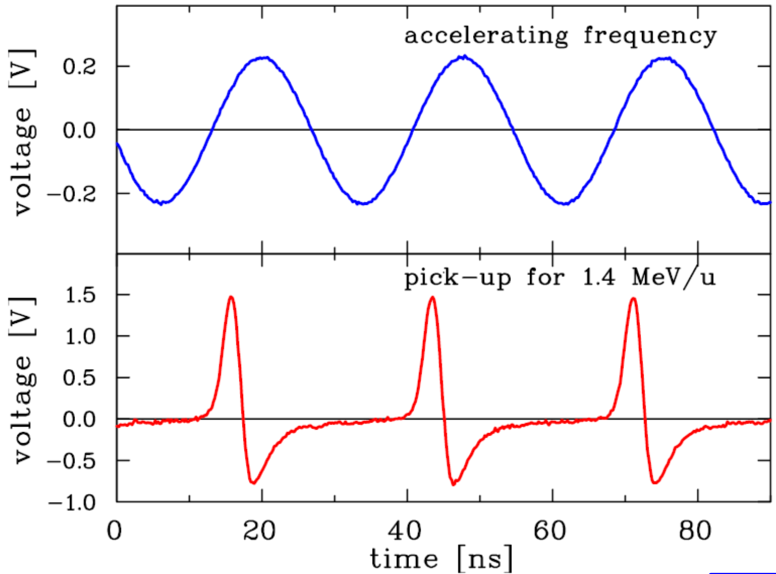

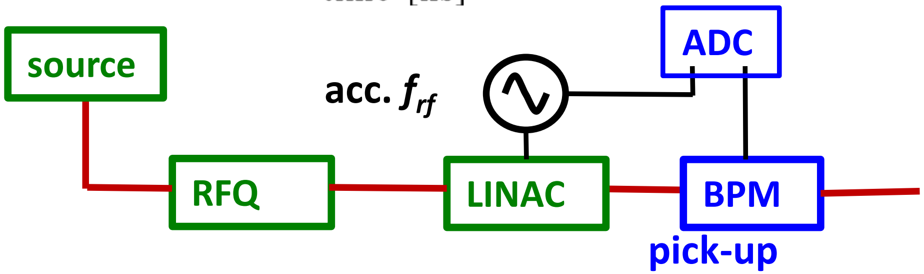

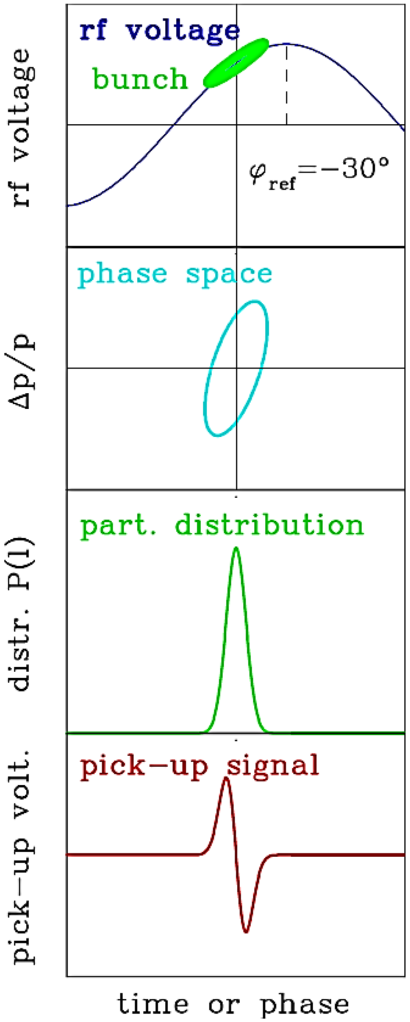

Bunch Length Measurement for relativistic Electrons

Electron bunches are too short (σ_t < 100 ps) to be covered by the bandwidth of pick-ups (f < 3 GHz ⇔ t_{rise} > 100 ps) for structure determination.

→ Time resolved observation of synchr. light with a streak camera: Resolution ≈ 1 ps.

Scheme of a streak camera

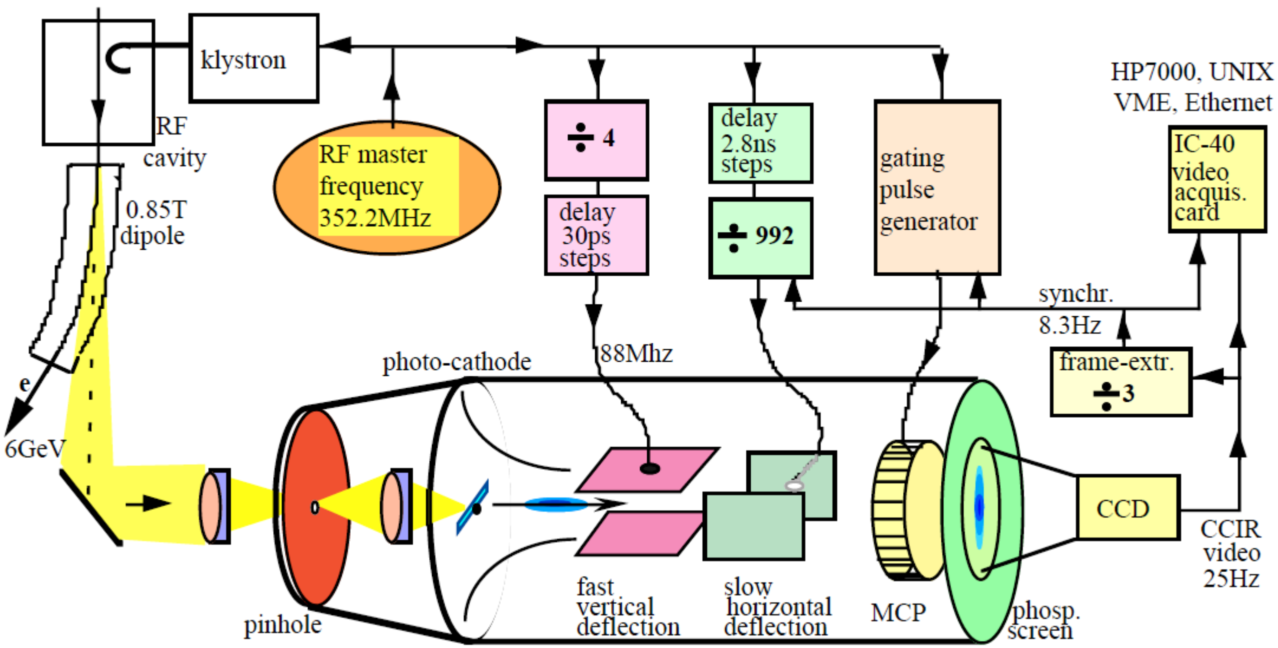

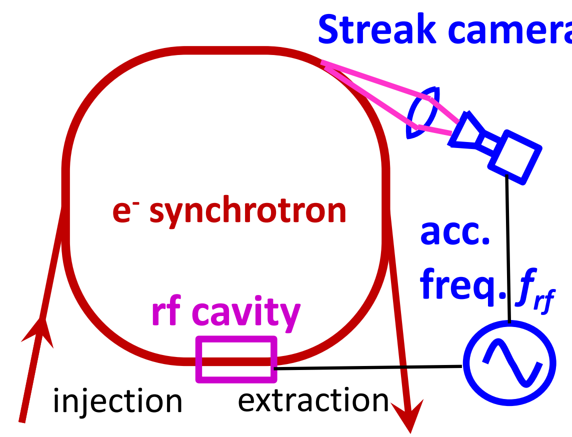

Technical Realization of a Streak Camera

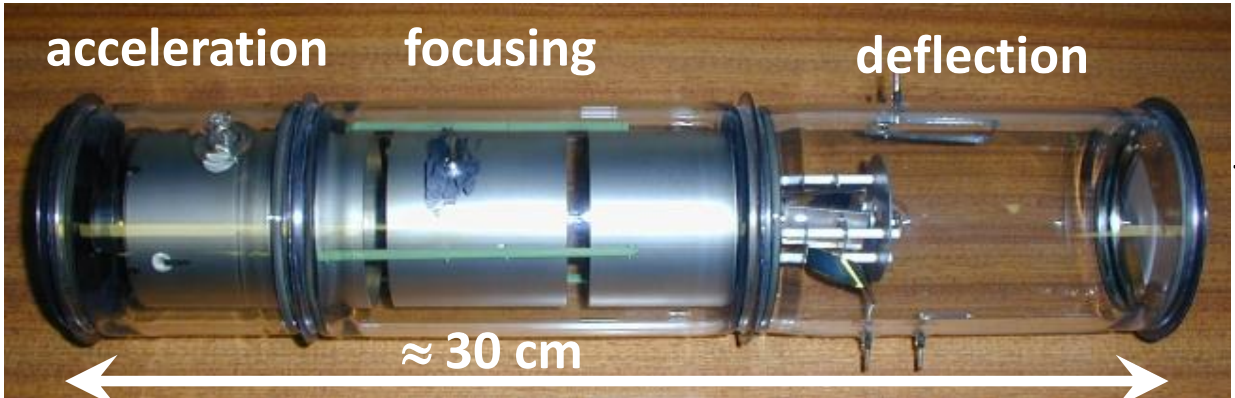

Hardware of a streak camera

Time resolution down to 0.5 ps:

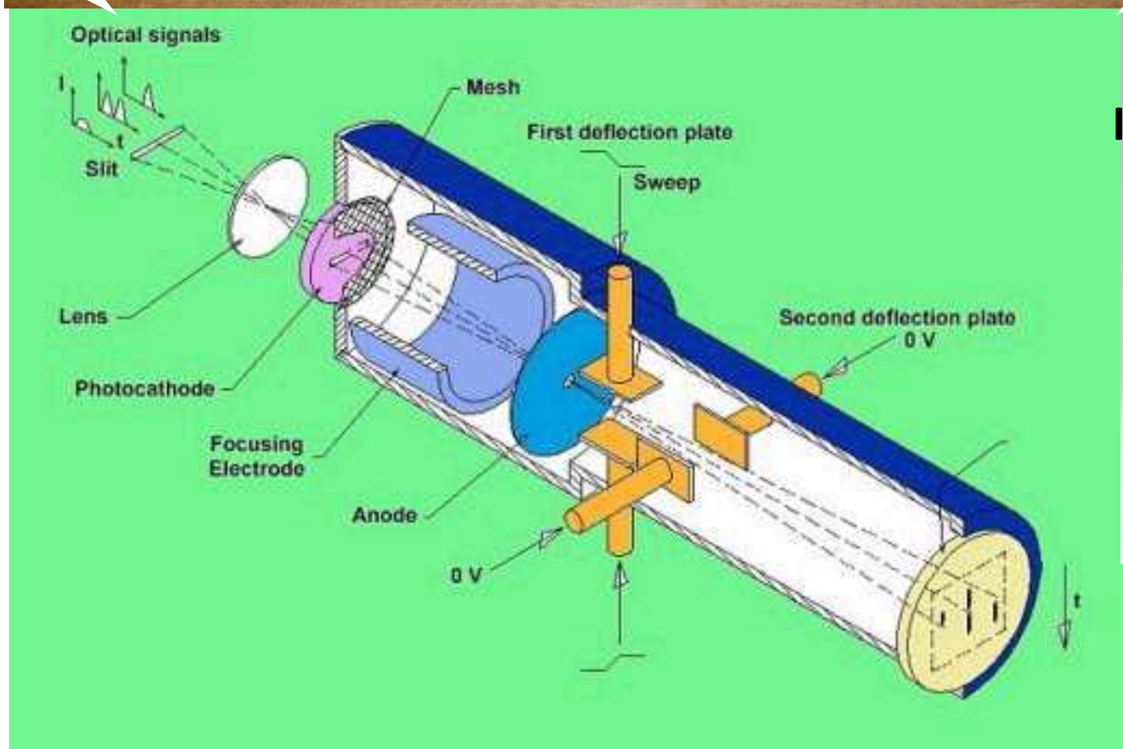

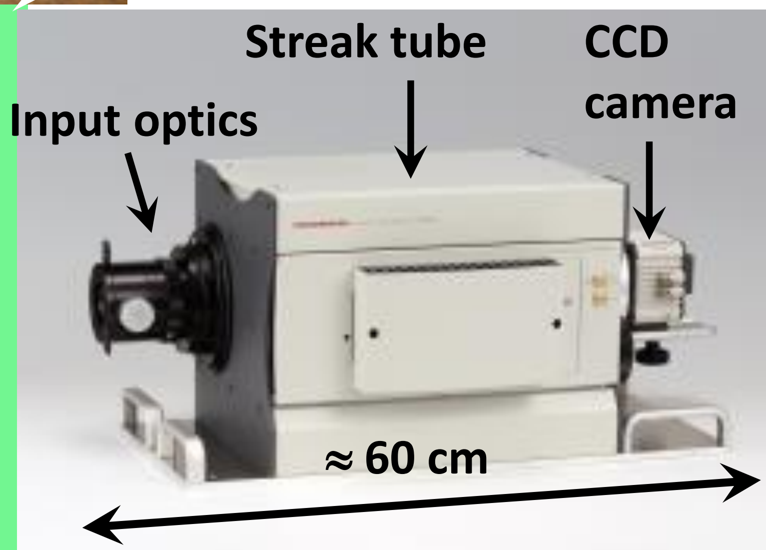

Technical Realization of a Streak Camera

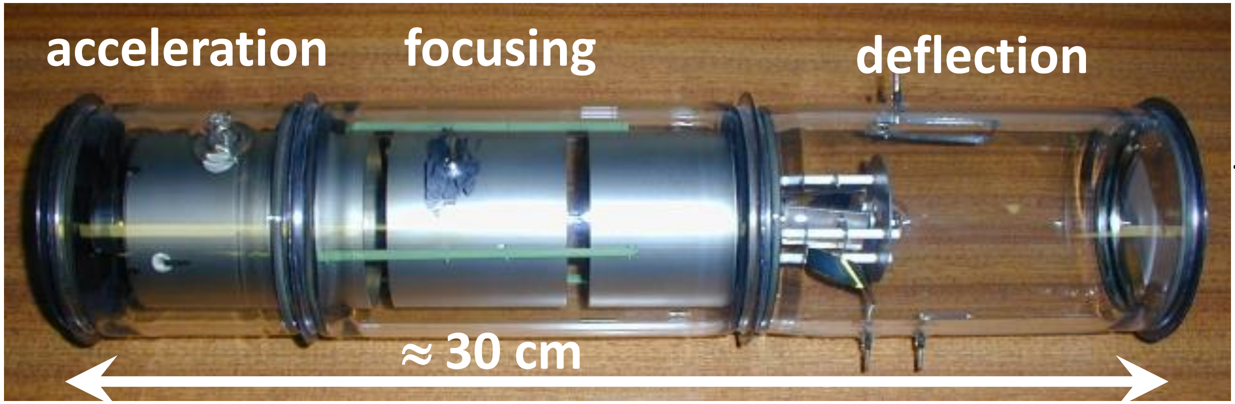

Hardware of a streak camera

Time resolution down to 0.5 ps:

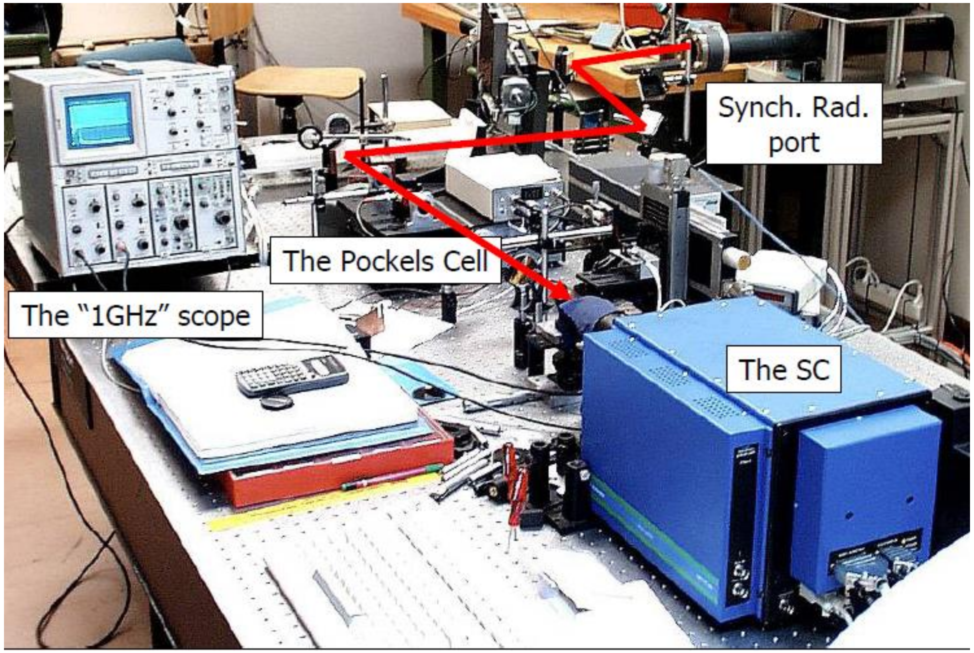

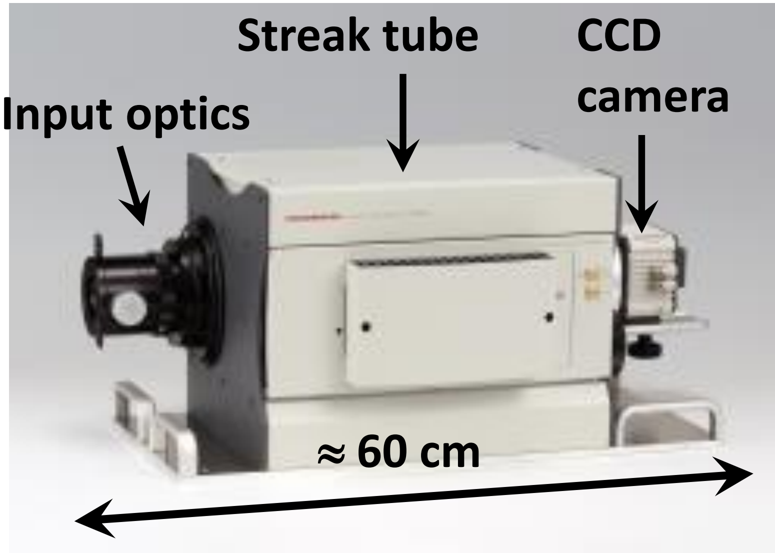

Results of Bunch Length Measurement by a Streak Camera

The streak camera delivers a fast scan in vertical direction (here 360 ps full scale)

and a slower scan in horizontal direction (24 µs).

Example: Bunch length at the synchrotron light source SOLEIL for $\boldsymbol{U_{rf}}$ = 2 MV

for slow direction 24 µs and scaling for fast scan 360 ps: measure $\boldsymbol{\sigma_t}$ = 35 ps.

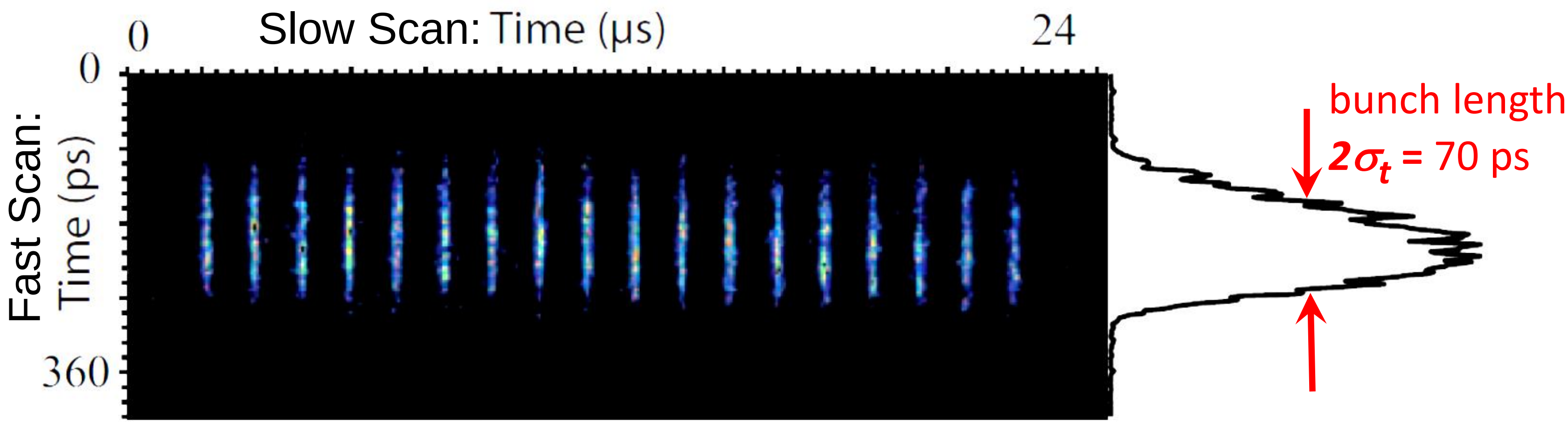

Short bunches are desired by the users

Example: Bunch length $\boldsymbol{\sigma_t}$ as a function of stored current (i.e. space charge de-focusing) at SOLEIL

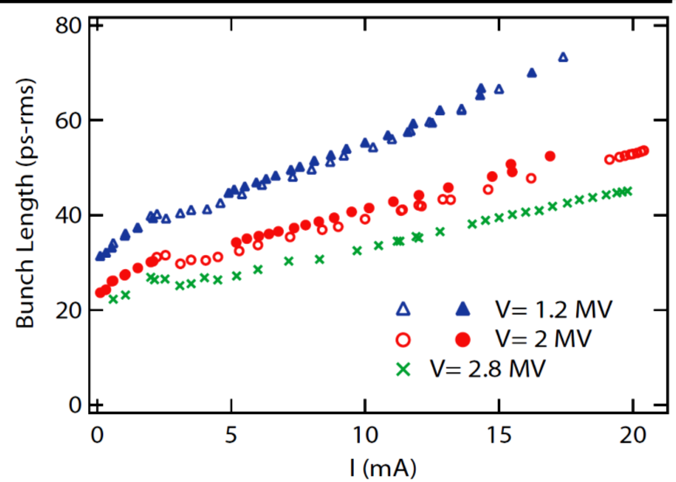

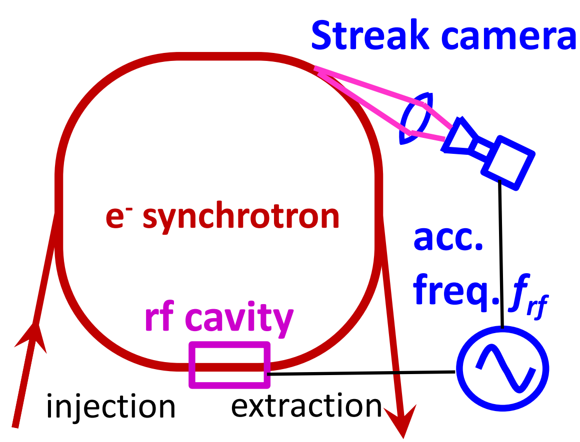

Courtesy of M. Labat et al., DIPAC'07

The Artist View of a Streak Camera

FARADAY CUP 1998

Purpose. To recognize and encourage innovative achievements in the field of accelerator beam instrumentation.

Award. The Faraday Cup Award consists of a US$ 5000 prize and a certificate to be presented at the next Beam Instrumentation Workshop. Winners participating in the BIW will be given a $1000 travel allowance.

Eligibility. Nominations are open to contributors of all nations regardless of the geographical location at which the work was done.
The Award goes normally to one person, but may be shared by recipients having contributed to the same accomplishment. It will normally be awarded to scientists in the early stage of their career. Nominations of candidates shall remain active for 2 competitions.

Establishment and support. The Award was established in 1991 with the support of the Beam Instrumentation Workshop Organizing Committee.

Rules. The Faraday Cup shall be awarded for an outstanding contribution to the development of an innovative beam diagnostics instrument of proven workability. The Faraday Cup is only awarded for published contribution and delivered performance -as opposed to theoretical performance. Rules are available on request.

Award Committee. The Beam Instrumentation Workshop Organizing Committee.

Nominations. The nomination package shall include the name of the candidate, relevant publications, a statement outlining his/her personal contribution and that of others, two letters from co-workers familiar with the candidate and his contribution. Two master copies suitable for photocopying of this package must be submitted not later than the 15th of November 1997 to Steven Smith c/o BIW'98 Secretariat, SLAC, Stanford University, Stanford CA 94305-4085, U.S.A..

Bunch Length Measurement by electro-optical Method

For Free Electron Lasers → bunch length below 1 ps is achieved

- Below the resolution of streak camera
- Short laser pulses with ***t*** **≈ 10 fs** and electro-optical modulator

Electro optical modulator: Birefringent, rotation angle depends on external electric field

Relativistic electron bunch: transverse ele. field $E_{\perp,lab} = \gamma E_{\perp,rest}$ carries the time information

Scanning of delay between bunch and laser → time profile after several pulses.

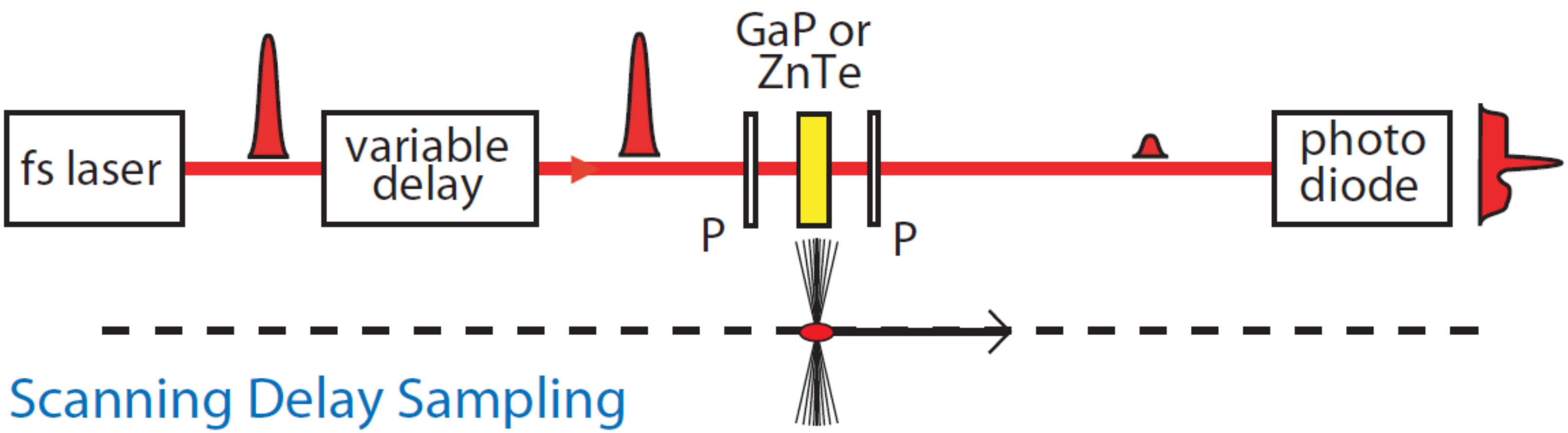

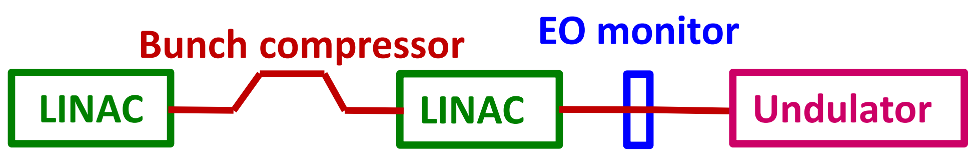

Courtesy S.P.Jamison et al., EPAC 2006

Bunch Length Measurement by electro-optical Method

For Free Electron Lasers → bunch length below 1 ps is achieved

Short laser pulse ⇔ broad frequency spectrum (property of Fourier Transformation)

Optical stretcher: Separation of colors by different path length

⇒ different colors at different time ⇒ **single-shot observation**

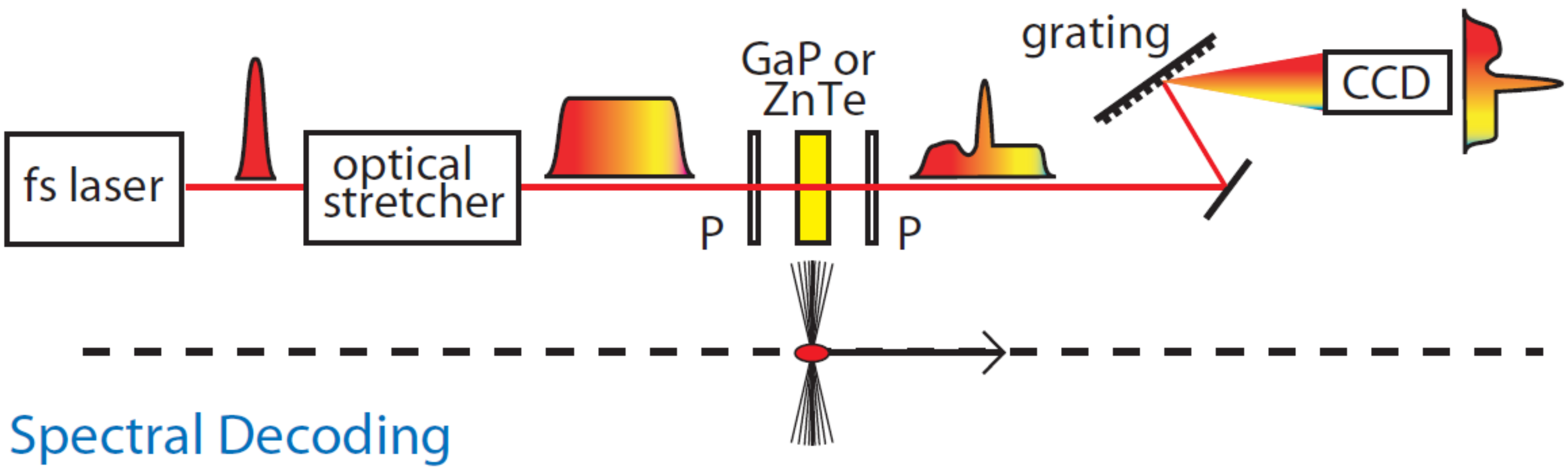

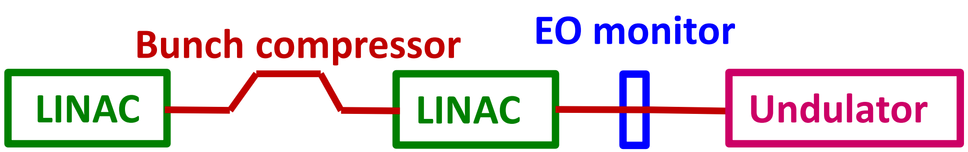

Courtesy S.P.Jamison et al., EPAC 2006

Hardware of a spectral-decoded EOSD Scanning Setup

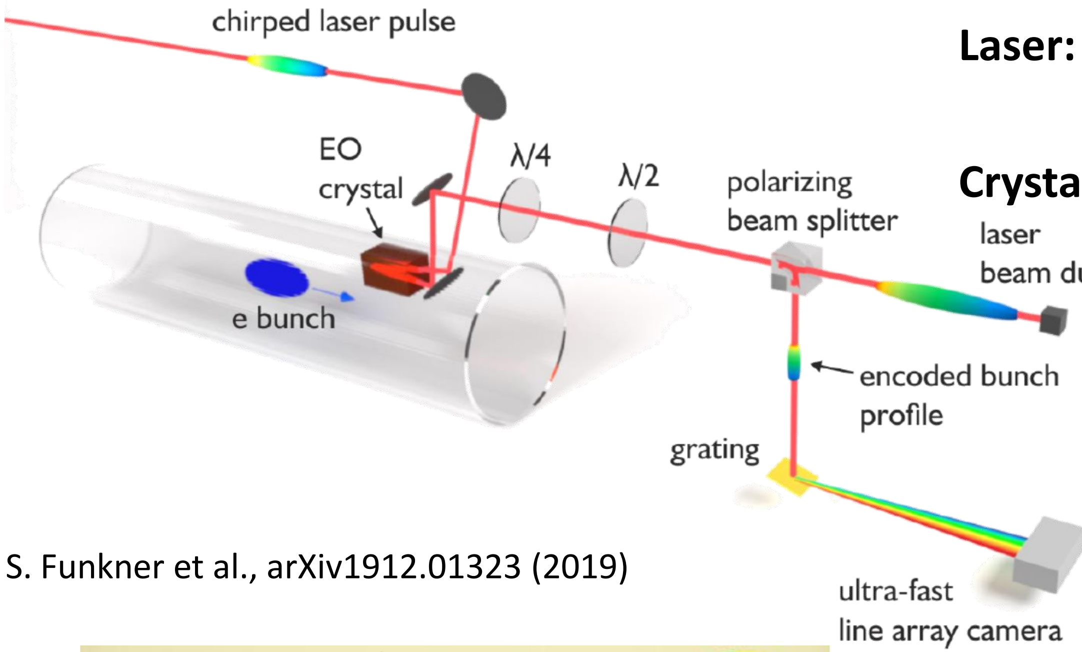

S. Funkner et al., arXiv1912.01323 (2019)

Laser: Commercial Ti:Sa or Yb-fibre,
10 fs duration, near IR,

Crystal: GaP or ZnTe, 100 μm thickness

Example: Bunch length at FLASH

100 fs bunch duration = 30 μm length !

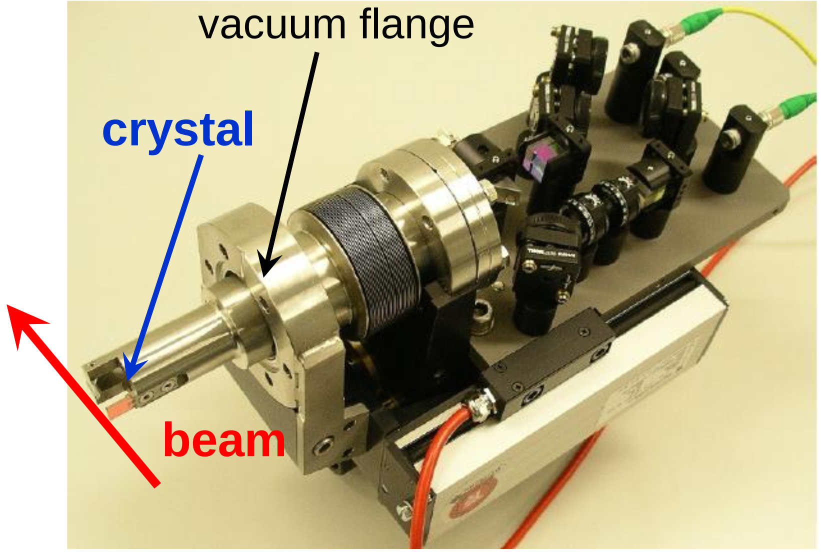

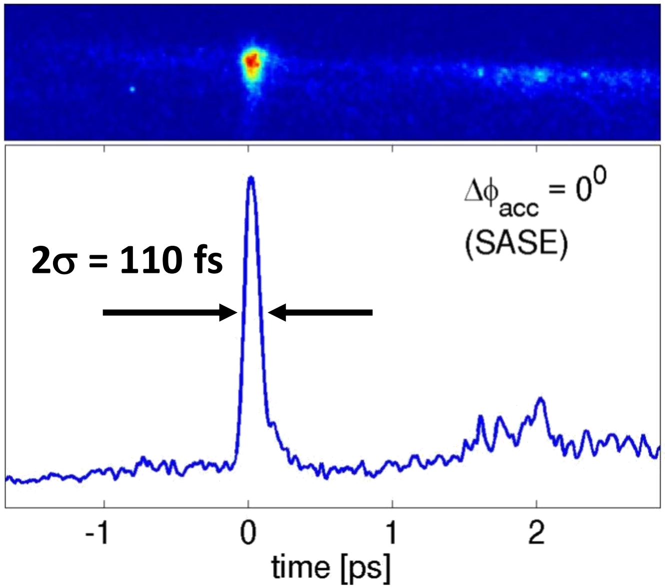

B. Steffen et al, DIPAC 2009

B. Steffen et al., Phys. Rev. AB 12, 032802 (2009)

Summary of longitudinal Measurements

Devices for bunch length at light sources:

Streak cameras:

- Time resolved monitoring of synchrotron radiation

  $\rightarrow$ for relativistic e^--beams, 10 ps < $\boldsymbol{t_{bunch}}$ < 1 ns

  Time resolution limit of streak camera ≈ 1 ps

Laser-based electro-optical modulation:

- Electro-optical modulation of short laser pulse

  $\rightarrow$ very high time resolution down to some fs time resolution

  Technical complex installation

Conclusion for Beam Diagnostics Course

Diagnostics is the 'sensory organ' for the beam.

It required for operation and development of accelerators

Several categories of demands leads to different installations:

- Quick, non-destructive measurements leading to a single number or simple plots
- Complex instrumentation used for hard malfunction and accelerator development
- Automated measurement and control of beam parameters i.e. feedback

The goal and a clear interpretation of the results is a important design criterion.

General comments:

- Quite different technologies are used, based on various physics processes
- Accelerator development goes parallel to diagnostics development

Thank you for your attention!

General Reading on Beam Instrumentation

- H. Schmickler (Ed.) *Beam Instrumentation*, Proc. CERN Accelerator School, Tuusula 2018 in prep.
- D. Brandt (Ed.), *Beam Diagnostics for Accelerators*, Proc. CERN Accelerator School, Dourdan, CERN-2009-005, 2009;
- Proceedings of several CERN Acc. Schools (introduction & advanced level, special topics).
- V. Smaluk, *Particle Beam Diagnostics for Accelerators: Instruments and Methods*, VDM Verlag Dr. Müller, Saarbrücken 2009.
- P. Strehl, *Beam Instrumentation and Diagnostics*, Springer-Verlag, Berlin 2006.
- M.G. Minty and F. Zimmermann, *Measurement and Control of Charged Particle Beams*, Springer-Verlag, Berlin 2003.
- S-I. Kurokawa, S.Y. Lee, E. Perevedentev, S. Turner (Eds.), *Proceeding of the School on Beam Measurement*, Proceedings Montreux, World Scientific Singapore (1999).
- P. Forck, *Lecture Notes on Beam Instrumentation and Diagnostics*, JUAS School, JUAS Indico web-site.
- Contributions to conferences, in particular to **I**nternational **B**eam **I**nstrumentation **C**onference IBIC.

Backup slides

Broadening due to the Beam's Space Charge: Ion Detection

Influence of the residual gas ion trajectory by :

- External electric field $\boldsymbol{E_{ex}}$
- Electric field of the beam's space charge $\boldsymbol{E_{space}}$

e.g. Gaussian density distribution for round beam: $E_{space}(r) = \frac{1}{2\pi\varepsilon_0} \cdot \frac{qeN}{l} \cdot \frac{1}{r} \cdot \left[1 - \exp\left(-\frac{r^2}{2\sigma^2}\right)\right]$

Estimation of correction: $\sigma^2_{corr} \approx \frac{e^2 \ln 2}{4\pi\varepsilon_0 \sqrt{m_p c^2}} \cdot \frac{qN}{l} \cdot d_{gap} \cdot \sqrt{\frac{1}{eU_{ex}}} \propto N \cdot d_{gap} \cdot \sqrt{\frac{1}{U_{ex}}}$

With the measured beam width is given by convolution: $\sigma^2_{meas} = \sigma^2_{true} + \sigma^2_{corr}$

Example: U^{73+}, 10^9 particles per 3 m bunch length, cooled beam with $\boldsymbol{\sigma_{true}}$ = 1 mm FWHM.

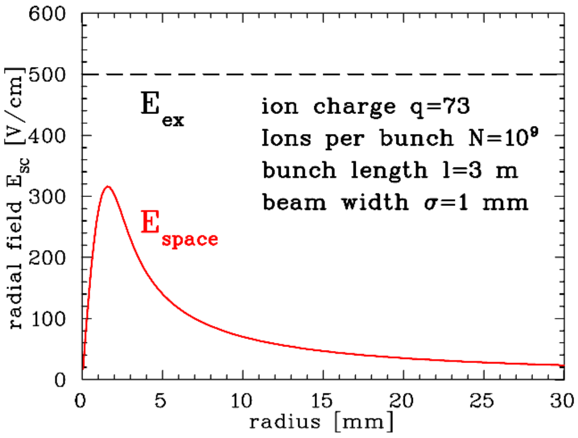

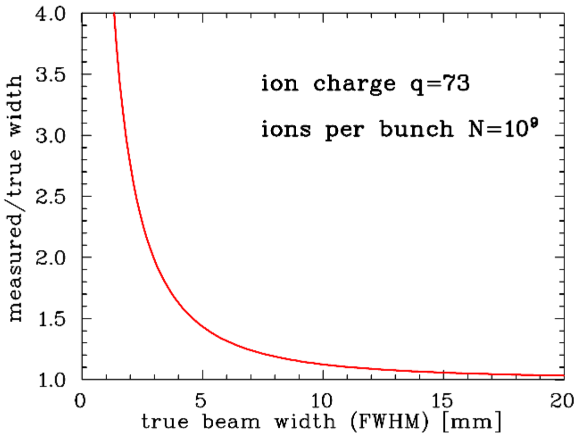

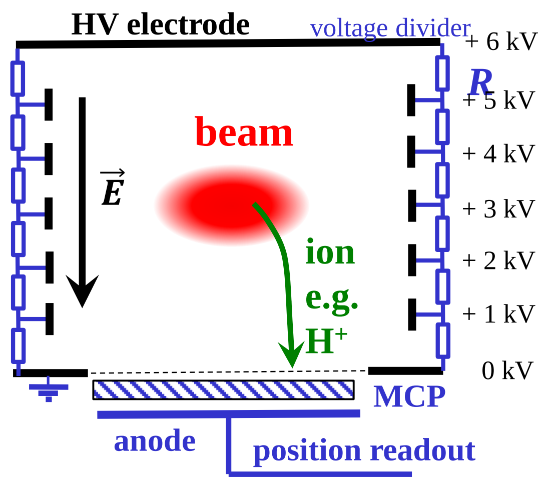

Electron Detection and Guidance by Magnetic Field

Ion detection mode:

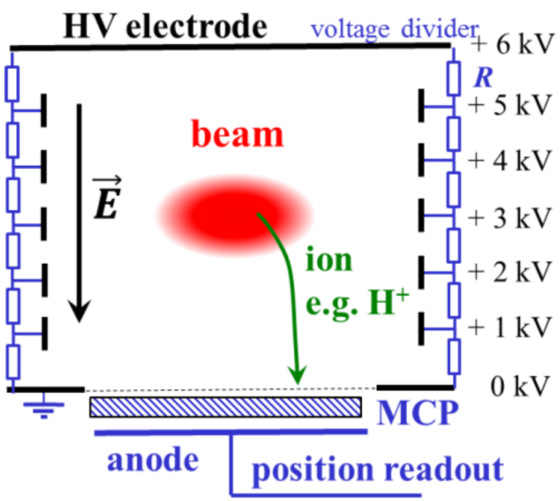

Electron detection mode:

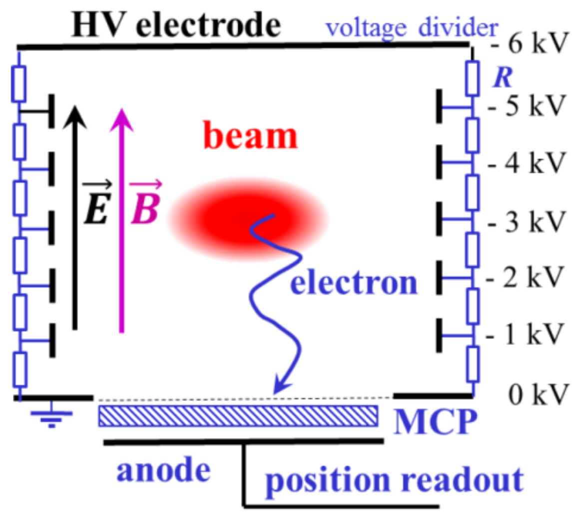

⇒ broadening by beam's electric field

7· 10^{10} charges per 10 m bunch

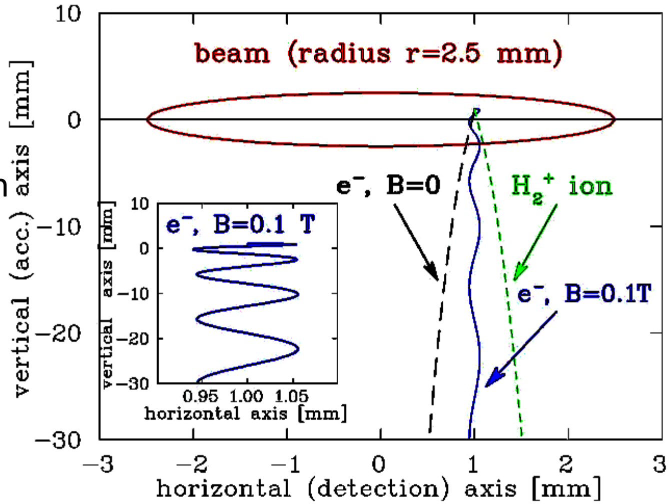

e⁻ detection in an external magnetic field

→ cyclotron radius $r_C = \frac{mv_\perp}{eB}$

for $E_{kin,\perp} = 10$ eV & $B = 0.1$ T ⇒ $r_c \approx 100$ μm

E_{kin} from atomic physics, ≈100 μm resolution of MCP

Time-of-flight: ≈1 - 2 ns ⇒ 2 - 3 cycles.

B-field: Dipole with large aperture

→ IPM is expensive & large device!

IPM: Magnet Design

Magnetic field for electron guidance:

Maximum image distortion:

5% of beam width ⇒ $\Delta B/B <$ 1 %

Challenges:

- High ***B***-field homogeneity of 1%
- Clearance up to 500 mm
- Correctors required
  to compensate beam steering
- Insertion length 2.5 m incl. correctors

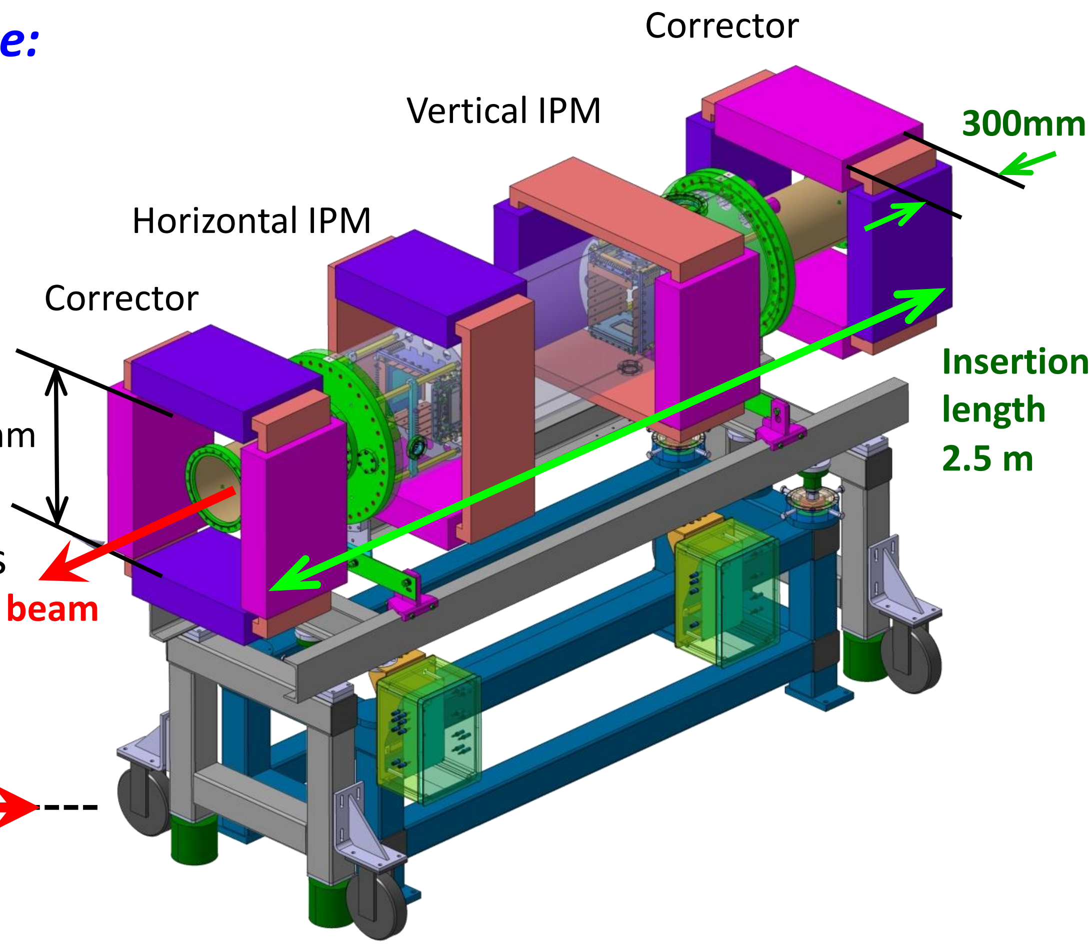

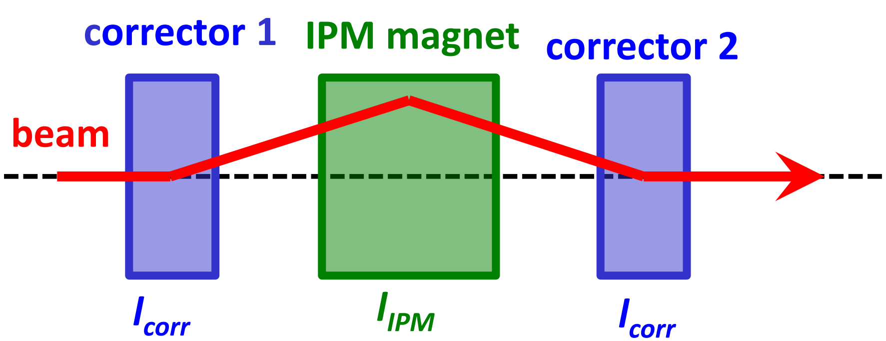

$$B_{cor} \cdot l_{corr} = - ½ \, B_{IPM} \cdot l_{IPM}$$

Remark: For MCP wire-array readoutlower clearance required

IPM: Magnet Design

Magnetic field for electron guidance:

Maximum image distortion:

5% of beam width ⇒ $\Delta B/B <$ 1 %

Challenges:

- High ***B***-field homogeneity of 1%
- Clearance up to 500 mm
- Correctors required
  to compensate beam steering
- Insertion length 2.5 m incl. correctors

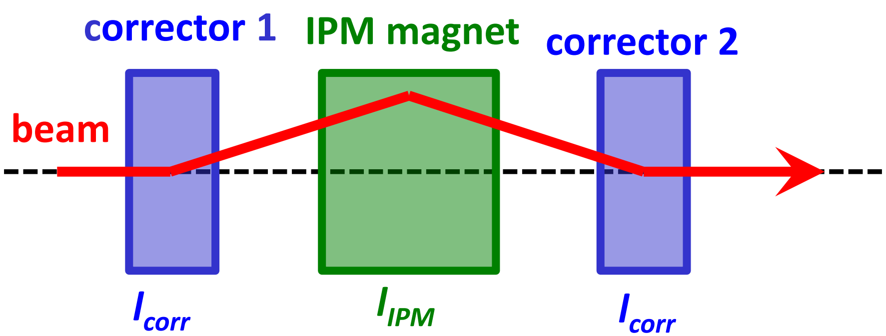

$$B_{cor} \cdot l_{corr} = -\tfrac{1}{2} B_{IPM} \cdot l_{IPM}$$

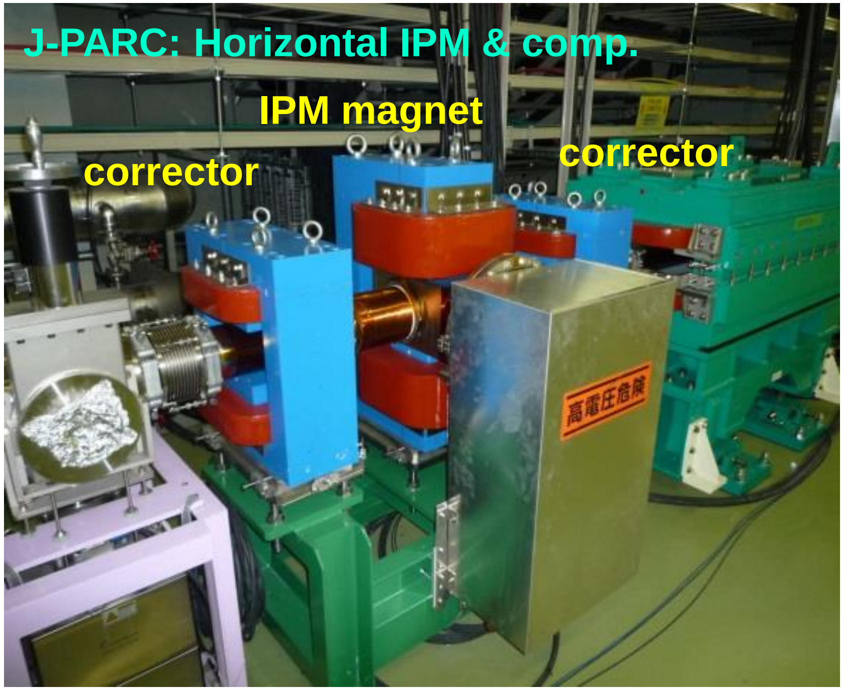

Magnet: B = 250 mT, Gap 220 mm

IPM: Profile 32 strips, 2.5 mm width

Remark for electron beams:

Resolution of 50 µm is insufficient,

but sometimes used for photon beams

Remark: For MCP wire-array readout lower clearance required

Emittance Enlargement by Injection Mis-steering

Emittance conservation requires precise injection matching

Wrong angle of injected beam:

- injection into outer phase space → large β-amplitude i.e. large beam
- might result in 'hollow' beam
- filling of acceptance i.e. loss of particles

⇒ Hadron beams: larger emittance after acceleration

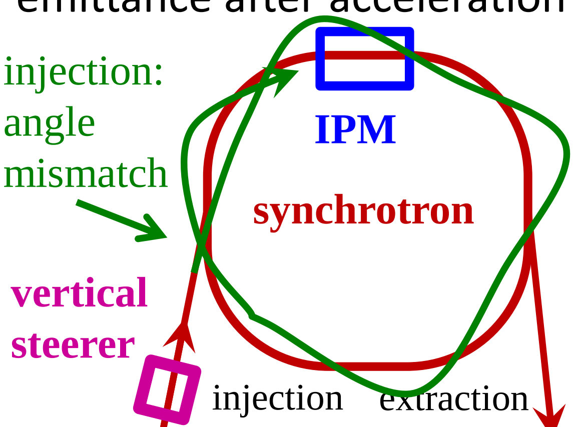

Example: Variation of vertical injection angle by magnetic steerer
Beam: C^{6+} at 6.7 MeV/u acc. to 600 MeV/u, up to $6{\cdot}10^9$ ions per fill with multi-turn injection, IPM integration 0.5 ms i.e. ≈ 100 turns

Vertical profile **at** injection:

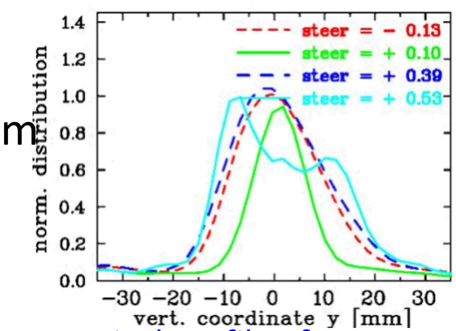

Vertical profile **after** acc.:

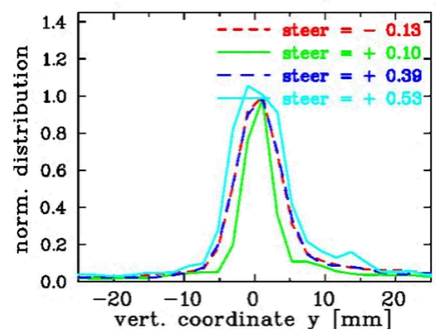

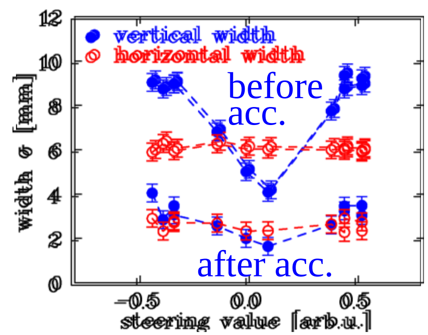

Horizontal profile **at** injection:

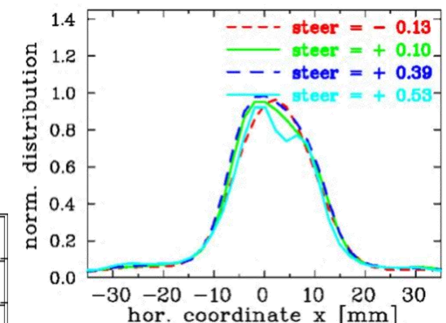

Horizontal profile **after** acc.:

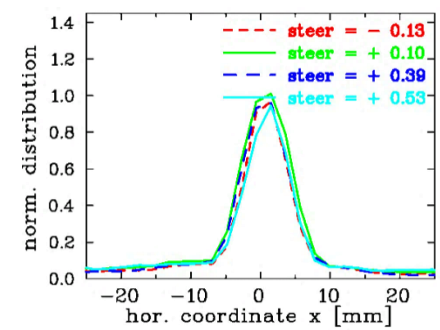

Schematic simulation:
Courtesy M. Syphers

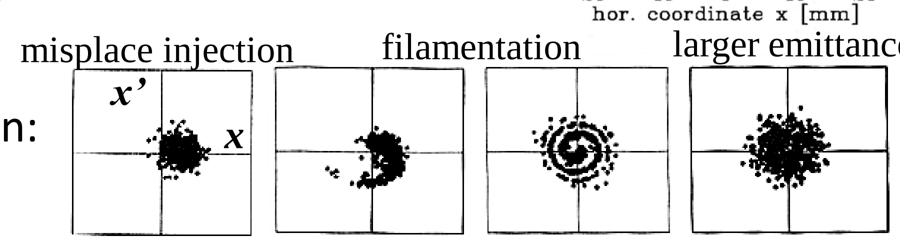

Coherent Optical Transition Radiation

Observation of coherent OTR for **compressed** bunches at LINAC based light sources

Reason: Coherent emission **if** bunch length ≈ wavelength (t_{bunch}=2 fs ⇔ l_{bunch} =600 nm)

or bunch fluctuations ≈ wavelength

Parameter reach

for most LINAC-based FELs!

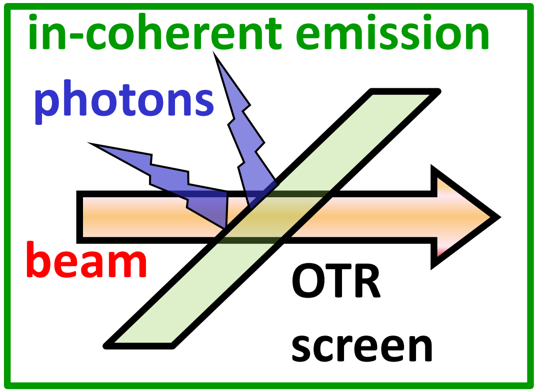

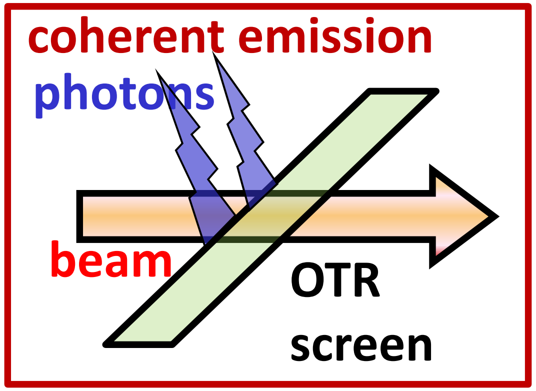

Beam parameter: FLASH, 700 MeV, 0.5 nC, with bunch compression

OTR screen *scint. screen*

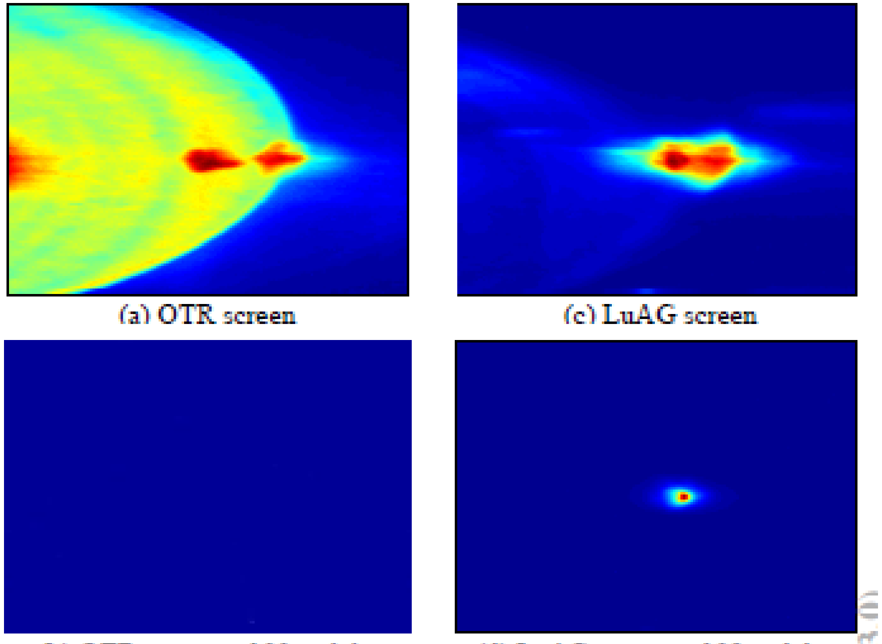

(a) OTR screen (c) LuAG screen

(b) OTR screen, +100ns delay (d) LuAG screen, +100ns delay

prompt emission for OTR and scint. screen
→ **coherent and in-coherent OTR**

100 ns delayed emission
→ no OTR as expected (classical process)
→ emission by scint. screen due to lifetime
⇔ correct profile image!

Contrary of M. Yan et al., DIPAC'11 & S. Wesch, DIPAC'11

X-ray Pin-Hole Camera

The diffraction limit is $\Rightarrow \sigma \cong 0.6 \cdot \left(\lambda^2 / \rho\right)^{1/3}$ $\Rightarrow$ ***shorter wavelength by X-rays***.

Example: PETRA III

Courtesy K. Wittenburg, DESY

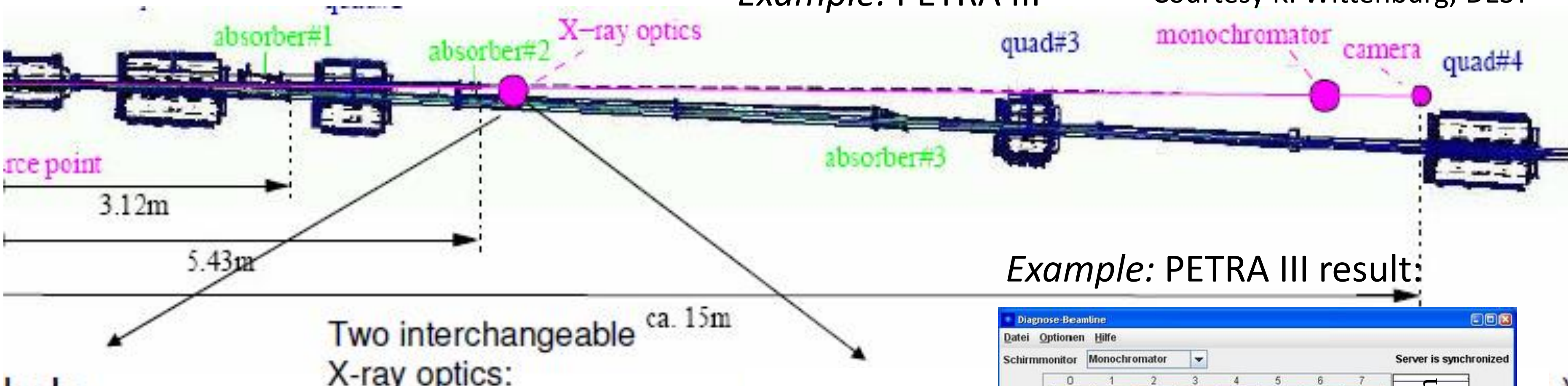

Example: PETRA III result:

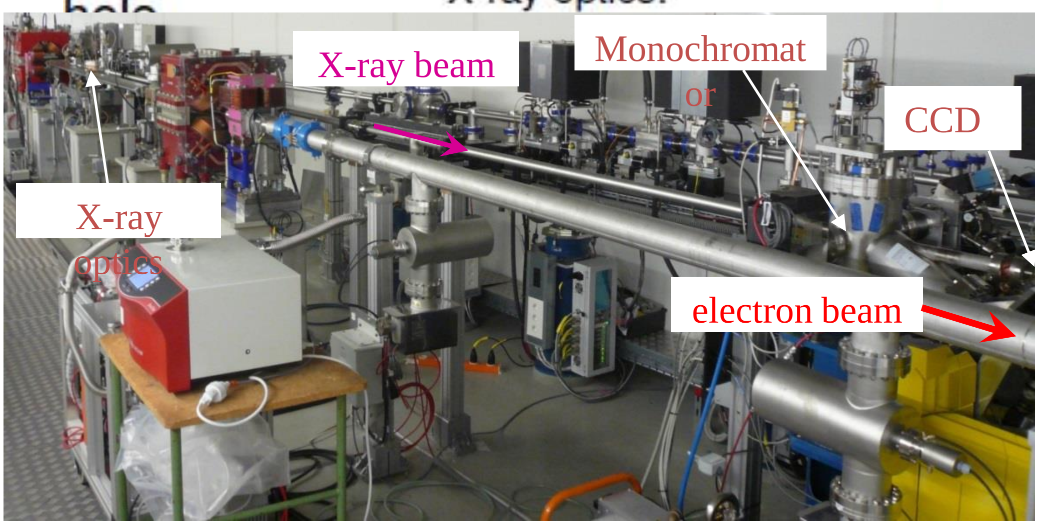

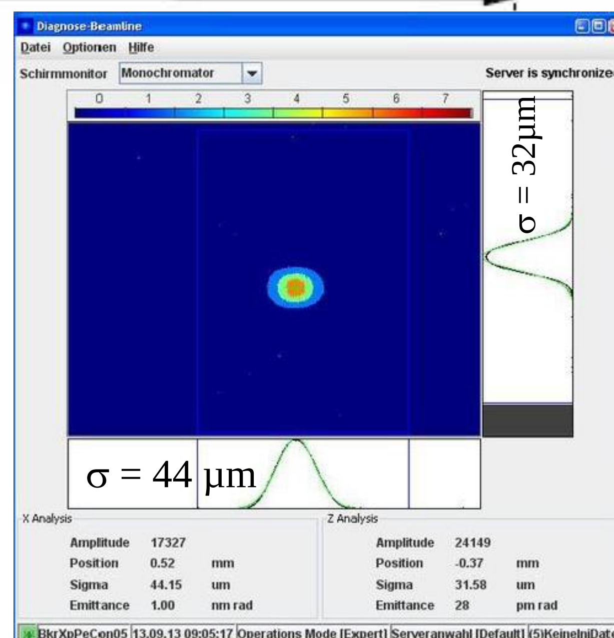

Double Slit Interference for Radiation Monitors

The **blurring of interference pattern** due to finite size of the sources

⇒spatial coherence parameter γ delivers ***rms*** beam size

i.e. 'de-convolution' of blurred image!

→ highest resolution, but complex method

Typical resolution for three methods:

- Direct optical observation: $\boldsymbol{\sigma \approx}$ **100 µm**
- Direct x-ray observation : $\boldsymbol{\sigma \approx}$ **10 µm**
- Interference optical obser: $\boldsymbol{\sigma \approx}$ **1 µm**

Ideal double slit interference pattern:

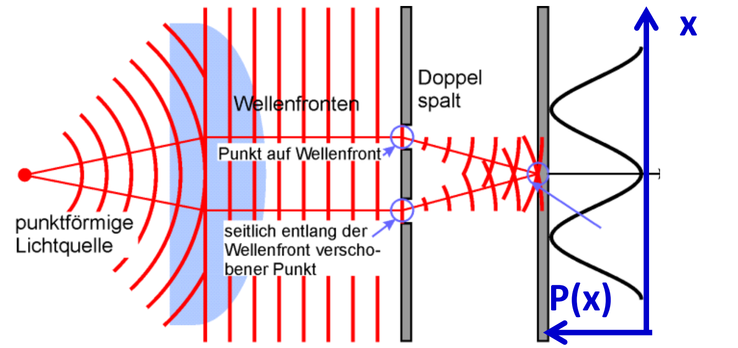

Blurring by finite source size:

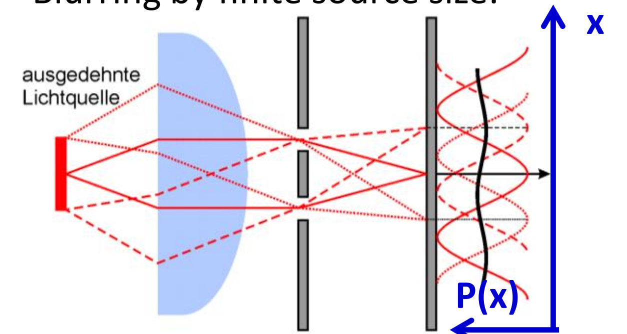

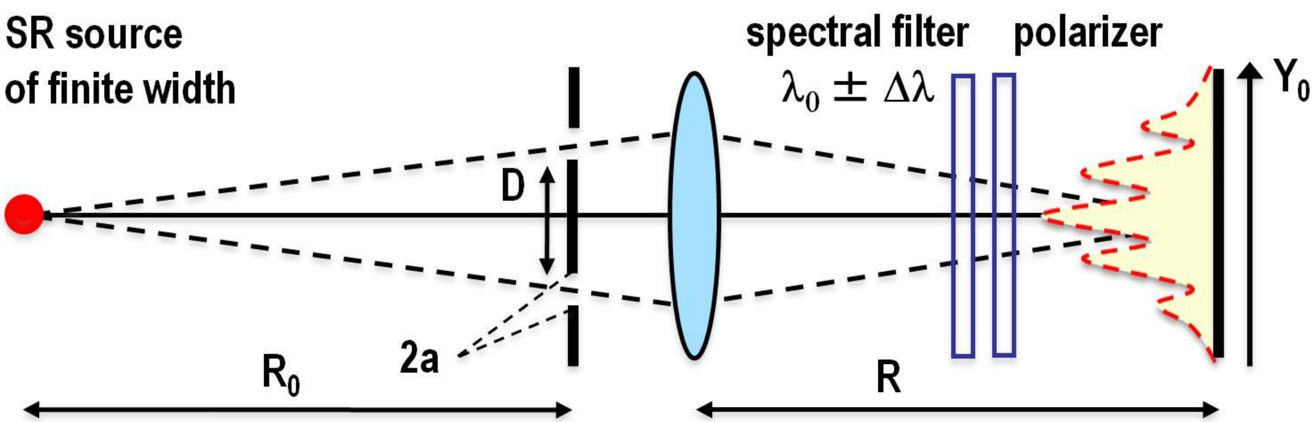

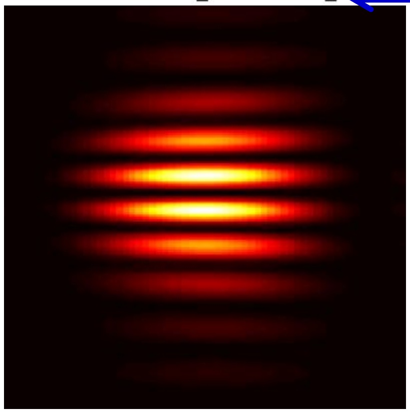

Courtesy of V. Schlott PSI

Bunch Length Measurement for relativistic Electrons

Electron bunches are too short (σ_t < 100 ps) to be covered by the bandwidth of pick-ups (f < 3 GHz $\Leftrightarrow$ t_{rise} > 100 ps) for structure determination.

$\rightarrow$ Time resolved observation of synchr. light with a streak camera: Resolution $\approx$ 1 ps.

Scheme of a streak camera

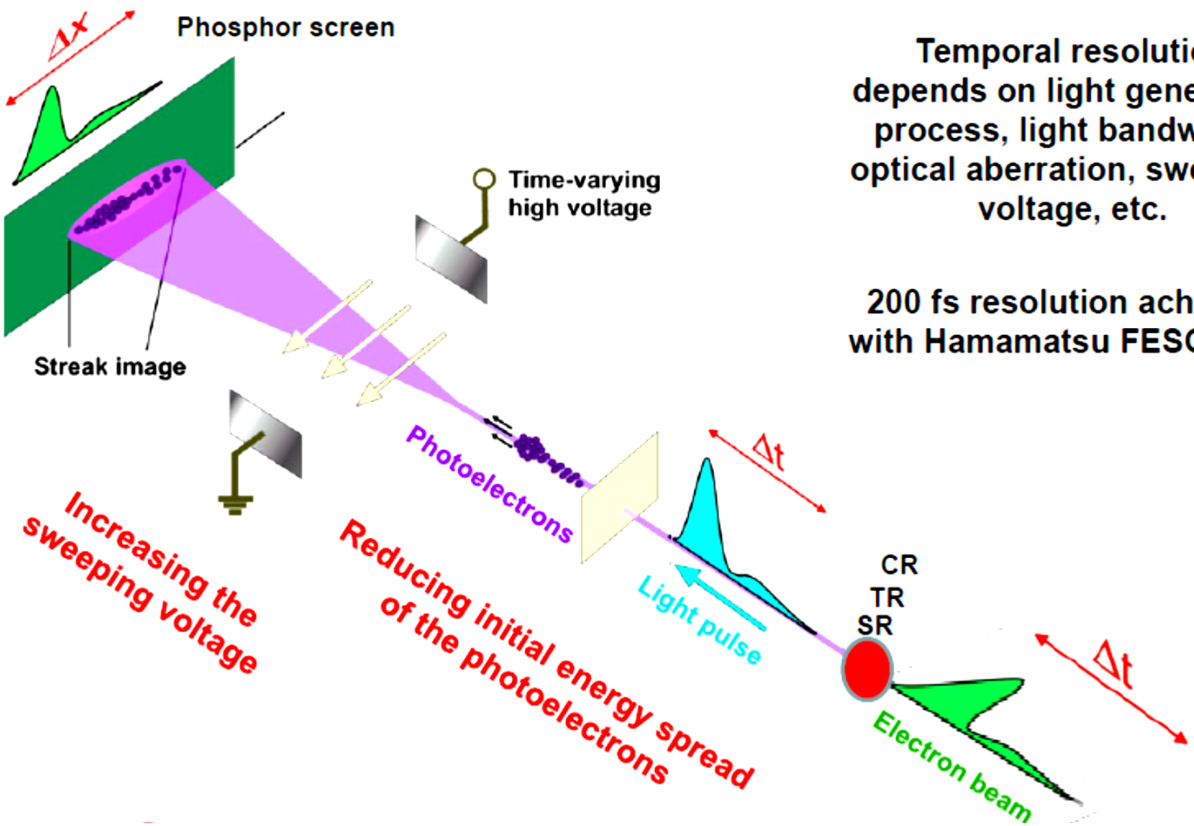

Temporal resolution depends on light generation process, light bandwidth, optical aberration, sweeping voltage, etc.

200 fs resolution achieved with Hamamatsu FESCA-200

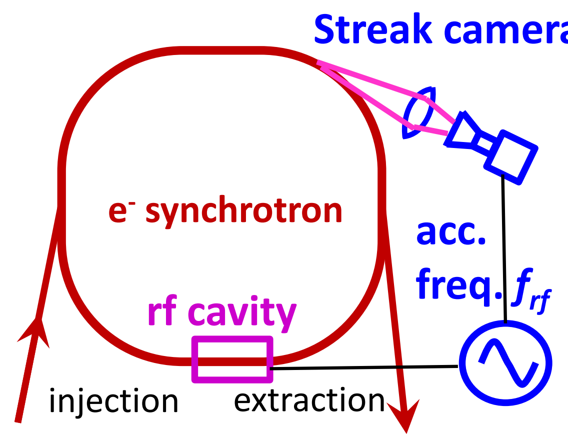

Realization of EOS Scanning

Setup of a scanning EOS method.

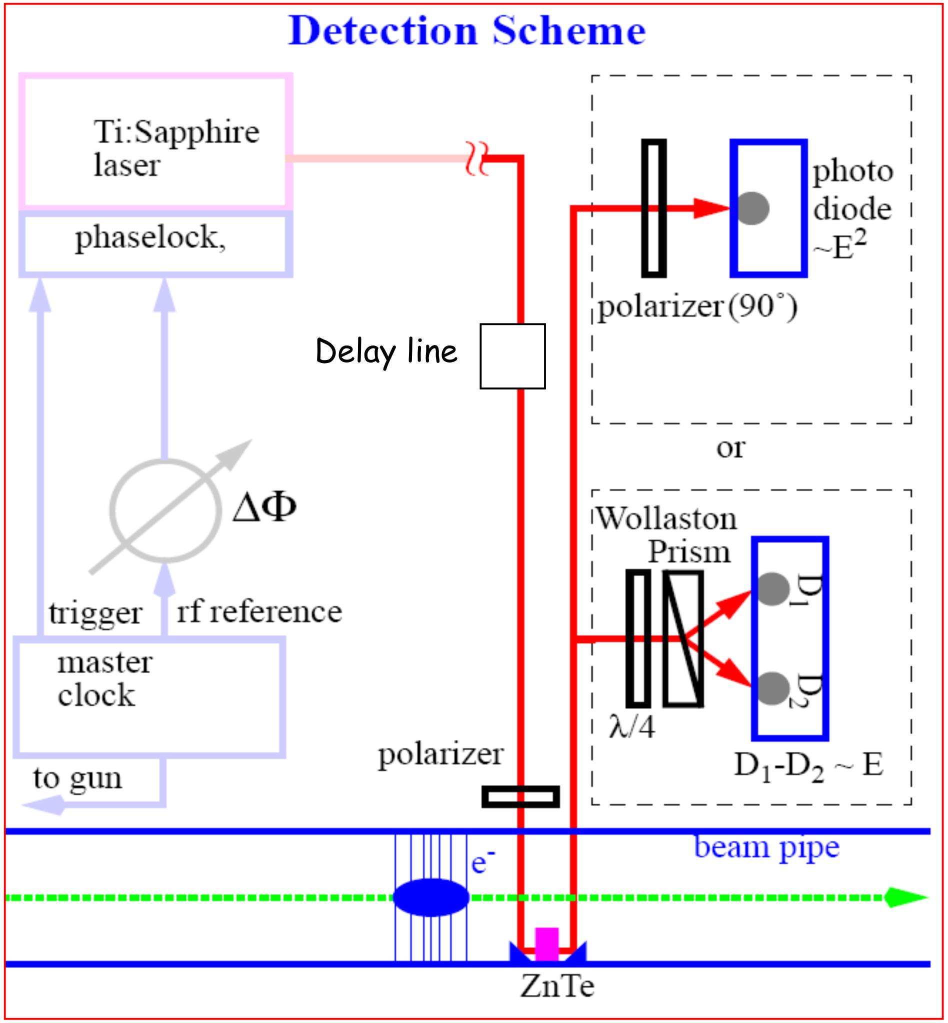

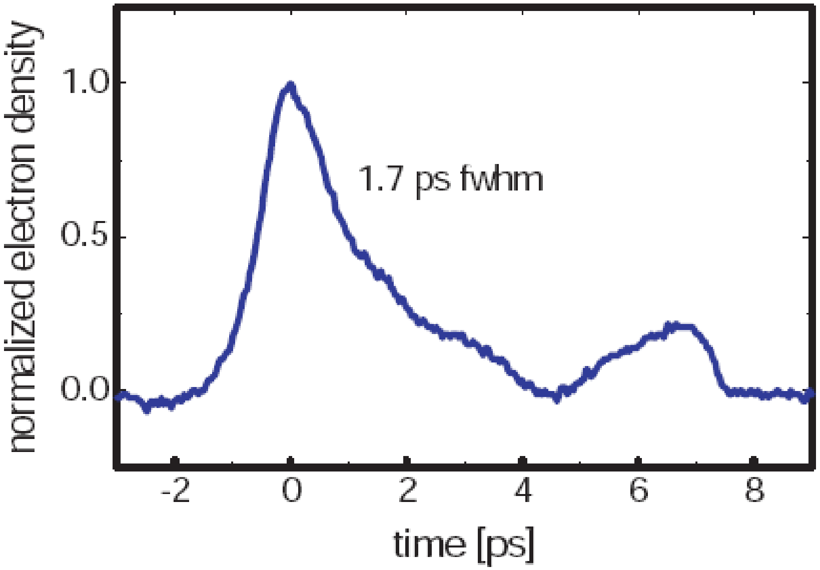

Using 12fs pulses from $Ti:Al_2O_3$ laser at 800nm and ZnTe crystal 0.5mm thick with a e^- - beam 46MeV of 200pC

X. Yan *et al*, Phys. Rev. Lett. 85, 3404 (2000)

Bunch Structure at low E_{kin}: Not possible with Pick-Ups

Pick-ups are used for:

- precise for bunch-center relative to rf
- course image of bunch shape

But:

For β << 1 → long. ***E***-field significantly modified:

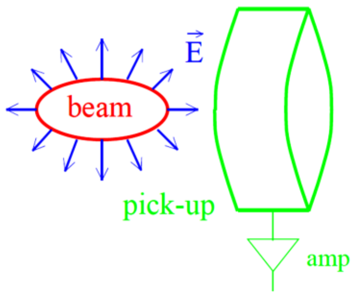

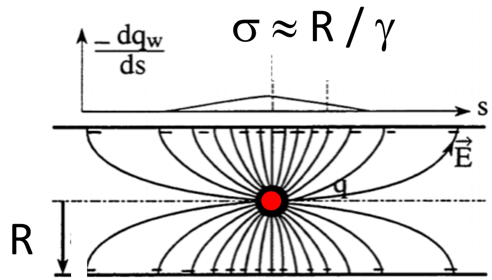

ampl.

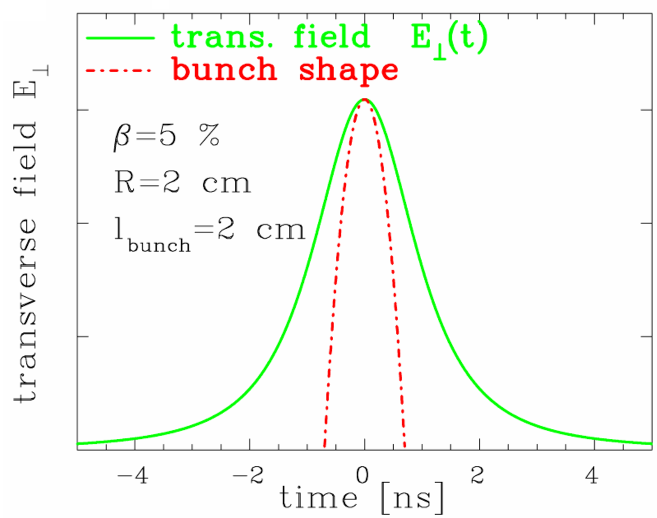

Example: Comparison pick-up – particle counter:

Ar beam of 1.4 MeV/u (***β*** = 5.5%) , ***f_{rf}*** = 108 MHz

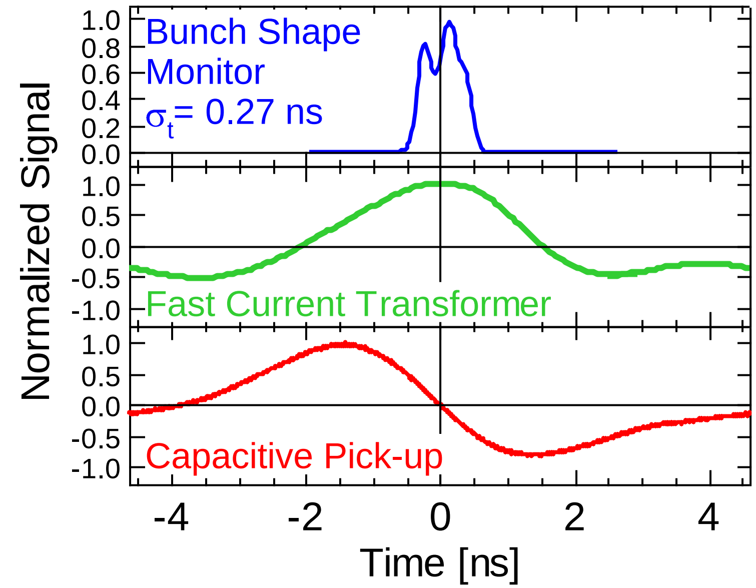

$1/f_{rf}$ = 9.2 ns

⇒ the pick-up signal is insensitive to bunch 'fine-structure'

Bunch Structure using secondary Electrons for low E_{kin} Protons

Secondary e⁻ liberated from a wire carrying the time information.

→ Bunch Shape Monitor (BSM)

Working principle:

- insertion of a 0.1 mm wire at ≈ 10 kV
- emission of secondary e⁻ within less than 10 ps
- secondary e⁻ are accelerated
- toward an rf-deflector
- rf-deflector as 'time-to-space' converter
- detector with a thin slit
- slow shift of the phase
- resolution ≈ 10 ps ≈ 1° @ 280 MHz
- Measurements are comparable

  to that obtained with particle detectors.

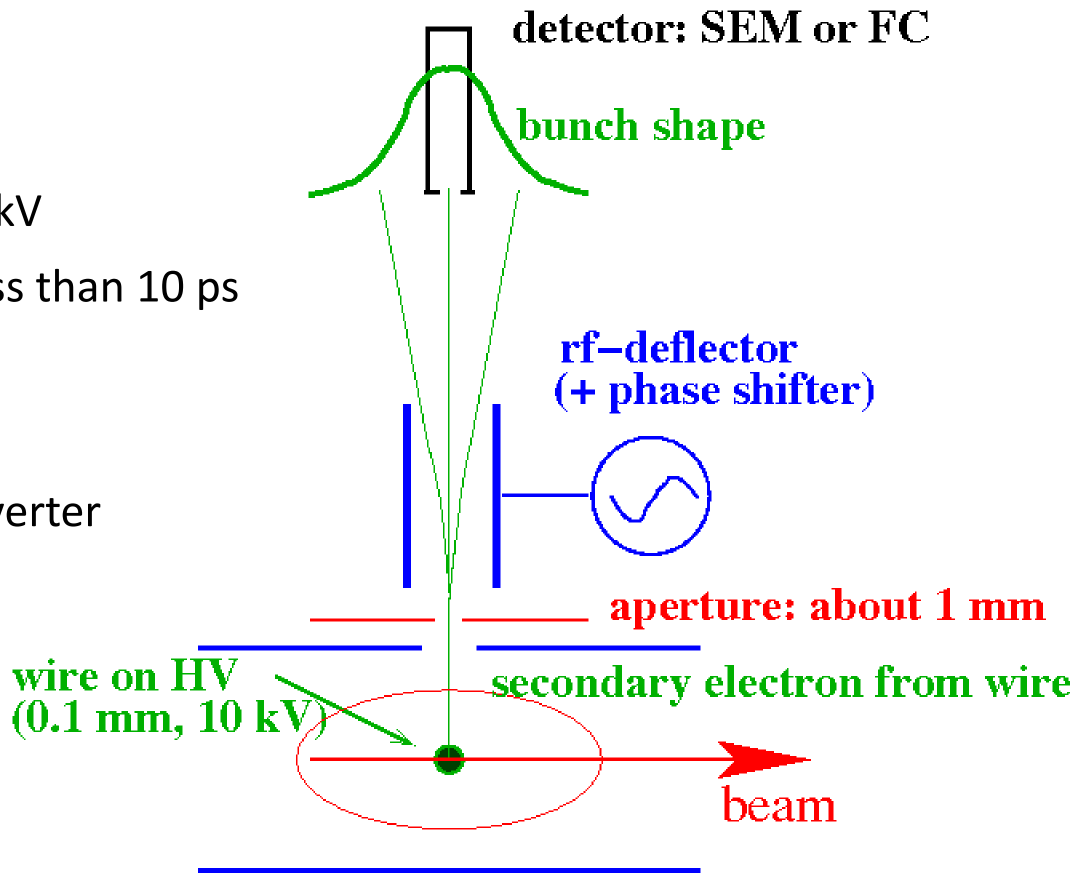

SEM: secondary electron multiplier

Realization of Bunch Shape Monitor at CERN LINAC2

Example: The bunch shape behind RFQ with120 keV/u: